CALIFORNIA INSTITUTE OF TECHNOLOGY

DYNAMICS LABORATORY

ANALYTICAL AND EXPERIMENTAL STUDIES OF RANDOM VIBRATION

by

Paul Yu-fei Hu

A report on research conducted for the National Aeronautics and Space Administration and the National Science Foundation

Pasadena, California

1965

ANALYTICAL AND EXPERIMENTAL STUDIES OF RANDOM VIBRATION

Thesis by

Paul Yu-fei Hu

In Partial Fulfillment of the Requirements

For the Degree of

Doctor of Philosophy

California Institute of Technology

Pasadena, California

1966

(Submitted August 25, 1965)

ACKNOWLEDGMENT

The author desires to gratefully acknowledge the assistance and guidance of his former advisor, the late Professor C. E. Crede, during the initial phase of this work.

The author wishes to record his deep gratitude to Professor T. K. Caughey, his present advisor, for his constant encouragement and assistance during the course of this investigation, and during the preparation of this thesis.

To Professor D. E. Hudson, many thanks are due for his suggested improvements to the manuscript.

The author is also pleased to acknowledge the interest shown by Professor W. D. Iwan.

The author is further indebted to the California Institute of Technology for the tuition scholarships and the research assistantships granted, and to the National Aeronautics and Space Administration for the support of this work under Contract No. NAS8-2451.

ABSTRACT

Analytical and experimental investigations are made of the response of linear systems subject to magnitude-limited Gaussian broadband random excitation. A mathematical analysis for determining the statistical properties of this excitation is developed. Experimental studies on the probabilistic response of linear systems with magnitude-limited input are also presented.

Secondly the peak characteristics of the response of linear systems subject to Gaussian broadband random excitation are investigated. It is shown that the number of peaks per unit time of the response of a single degree of freedom system increases as the frequency bandwidth of the excitation increases. Analytical and experimental techniques are developed to study the peak distribution characteristics of multi-degree of freedom systems and continuous systems. It is found that the normal mode random variables are statistically independent if the system damping is small, and the modal frequencies are sufficiently separated.

Finally the method of Fokker-Planck is used to obtain the statistical properties of the response of a first order Coulomb damped system. The first order probability density function of displacement of this nonlinear system is determined. A simplified method for developing the autocorrelation function, and the power spectral density is discussed and applied to the above problem. The results are further substantiated by experiment. Experimental investigations are also

carried out to determine the power spectral density of the response of a second order nonlinear system with Coulomb restoring force to white noise input. The results are compared with those given by Wolaver.

TABLE OF CONTENTS

CHAPTER I

GENERAL THEORY OF RANDOM PROCESSES

1.1. Introduction

Studies of random processes, or stochastic processes, are relatively old, yet it is only in recent years that the application of the theory of random processes to engineering problems has been exploited. The theory of random processes is generally defined as the dynamic part of probability theory. Therefore it is especially useful in the cases where one desires to know the dynamic behavior of the response of a system to random excitation.

The theory of the random process was first advanced by Einstein, who studied the Brownian motion of a free particle and obtained the mean square value of the displacement of the free particle.[1] Further investigations in the field of Brownian motion by Smoluchowski, Ornstein, Kramers, Chandrasekhar, Uhlenbeck and Wang have resulted in a general theory of random processes. In the field of electrical engineering, scientists have studied the statistical properties of noise through receivers and the theory of information, where an unique method based on the theory of Fourier integrals was developed. The principle contributions made in these areas are due to Wiener, Rice, Kolmogoroff and Khintchine. The endeavors of these scientists have proved to be fundamental to the theory of random processes. Some of the basic techniques involved in the studies of random processes are contained in the papers given by Uhlenbeck and

Wang,[2] and Rice.[3]

More recently the concept of random processes has been introduced in mechanical engineering, particularly in the field of vibration and dynamics. The engineering problems which arise in these areas are centered around the response of a mechanical system to random excitation. For example, buildings subject to ground motion during earthquakes, missiles and jets in a turbulent environment, etc., are all examples involving systems, whether linear or nonlinear, subject to random excitation. The dynamic behavior of such systems subject to random excitation have been studied extensively by Caughey,[4-9] Crandall[10-13] and others.[14-15]

All the problems treated in this thesis involve discrete dynamic systems whose input is Gaussian distributed, or sometimes derived from a Gaussian random process. Frequently the input spectrum is uniform over a frequency range extending from zero to infinity. These assumptions have proved to be important, and resulted in a great deal of simplification in the mathematical analysis of random vibration.

The objective of the present study is to extend and further the work in the area of random vibration. In the following sections, a general theory of random processes that are of interest in random vibration applications is developed and techniques indicated. A specific problem involving systems subjected to magnitude-limited random excitation is treated in Chapter II. The peak characteristics of linear systems with broadband random inputs are analyzed in

Chapter III. In Chapter IV the method of Fokker-Planck in solving a first order nonlinear system is demonstrated. In all phases of work analytical results are supported by experiments. Finally, the Summary and Conclusions drawn from the analytical and experimental investigations are presented in Chapter V. It is hoped that the results of these studies will help to further future researches in the area of random vibration.

1.2. Probability Theory and the Classification of Random Processes

Many physical phenomena in nature are characterized by unpredictable changes in time and cannot be prescribed a priori except in a statistical sense. They are in general, known as random, or stochastic processes. These statistical processes often show regularities, or stabilized properties as the time or the number of observation increases. In other words, the random processes can be described (or defined) by a set of probability functions.

The theory of probability is closely related to the concept of an ensemble, which is a collection of many physical systems. Let the members of the ensemble be denoted by $x_1(t)$, $x_2(t), \ldots x_n(t)$, which are different time dependent functions. However, they are completely described (or defined) by the following set of probability distributions:

$p_1(x, t)dx$ = probability of finding x in the amplitude range $(x, x+dx)$ at time t.

$p_2(x_1x_2;t_1t_2)\, dx_1dx_2$ = joint probability of finding x_1 in the range (x_1, x_1+dx_1) at time t_1; and x_2 in the range (x_2, x_2+dx_2) at time t_2.

$p_3(x_1x_2x_3;t_1t_2t_3)dx_1dx_2dx_3$ = joint probability of finding x_1 in the range $(x_1,\ x_1+dx_1)$ at time t_1, and x_2 in the range $(x_2,\ x_2+dx_2)$ at time t_2, and x_3 in the range $(x_3,\ x_3+dx_3)$ at time t_3.

and etc., the nth order probability density function $p_n(x_1x_2x_3\ldots x_n;\ t_1t_2\ldots t_n)$ can be defined in the same fashion.

The aforementioned set of probability functions must satisfy the following conditions:

1. $p_n(x_1x_2\ldots x_n;\ t_1t_2\ldots t_n) \geq 0$,
2. $p_n(x_1x_2\ldots x_n;\ t_1t_2\ldots t_n)$ is a symmetric function of its arguments (x_k, t_k),
3. $p_k(x_1x_2\ldots x_k;\ t_1t_2\ldots t_k) = \int\ldots\int dx_{k+1}\ldots dx_n p_n(x_1\ldots x_n;\ t_1\ldots t_n)$,
4. $\int\ldots\int dx_1\ldots dx_n p_n(x_1x_2\ldots x_n;\ t_1\ldots t_n) = 1$.

So far we have described the time dependent probability distribution function across the ensemble. In the cases where the random process is stationary in time (to be defined in next section), the probability functions will not change with a shift of time origin.

Uhlenbeck and Wang[2] attempted to classify the random processes by the order n of the probability distribution functions for a complete description.

1. Purely random process or independent process.

A random process is called a purely random process when the joint probability density functions can be defined in terms of the products of the first probability density functions, namely:

$$p_n(x_1 x_2 \cdots x_n;\ t_1 t_2 \cdots t_n) = p(x_1, t_1)p(x_2, t_2)\cdots p(x_n, t_n) \qquad (1.1)$$

In other words a small difference in time will make successive values of x completely independent. All information is then completely contained in the first probability density function.

2. Markoff process.

The concept of Markoff process has important physical application since it is a process with no memory extending before the previous instant. A simple Markoff process is defined by the following equation

$$T_n(x_n, t_n \mid x_1, x_2 \cdots x_{n-1};\ t_1, t_2 \cdots t_{n-1}) = T_2(x_n t_n \mid x_{n-1} t_{n-1}) \qquad (1.2)$$

where T(a/b) means the conditional probability (known also as the transition probability) of a given b. As the consequences of the definition given above for the simple Markoff process, the joint probability density function can be written in terms of the conditional probabilities:[16]

$$\begin{aligned} p_n(x_1, x_2 \cdots x_n; t_1, t_2 \cdots t_n) &= p(x_1 t_1)\, T(x_2 t_2 \mid x_1 t_1)\, T(x_3 t_3 \mid x_1 t_1, x_2 t_2)\cdots \\ &= p(x_1 t_1)\, T(x_2 t_2 \mid x_1 t_1)\ T(x_3 t_3 \mid x_2 t_2)\cdots \\ &= p(x_1 t_1) \prod_{k=2}^{n} T(x_k t_k \mid x_{k-1} t_{k-1}) \end{aligned} \qquad (1.3)$$

Thus it is immediately clear that a simple Markoff process is completely defined by the second probability distribution function. Many physical phenomena are found to possess Markoff properties even though very severe restrictions have been imposed on the

transition probabilities. For example, in the case of a single degree of freedom oscillator when subjected to a Gaussian distributed random external force, the response of the system is found to be a projection of the Markoff process or a vector characterization of the process.

Random processes can also be classified according to the type of their distribution functions, i. e., the probability laws involved. Some frequently encountered probability laws are the Normal (Gaussian), Poisson, Rayleigh Distributions. Nevertheless, a great number of random phenomena observed in nature possess Gaussian properties. For example, the distribution of a random variable resulting from the sum of a large number of independent random variables -- satisfying certain general conditions -- approaches asymptotically normal. This is known as the Central limit theorem,[30] one of the most important theorems in mathematical statistics.

1. 3. Stationarity and Ergodicity

To introduce the concept of stationarity and ergodicity, an ensemble of random variable $x_1(t)$, $x_2(t), \ldots x_n(t)$ of a random process is considered. Let $x_i(t)$ be a typical member of the ensemble, and let h be an arbitrary measure of time. Each function $x_i(t+h)$ may be taken as the member of a new random process with a translation of time h from the original random process. A random process is said to be stationary if the probability function of the original process is invariant under a shift of time origin. A random process, possessing this property, is sometimes called stationary in the strict sense to

distinguish it from stationary in the wide sense to be defined later. As a result of the definition given above it is not difficult to see that for a strictly stationary random process that probability distribution function (or density function) and other statistical parameters do not change for all translations in time, and depend on time instants only through their differences.

Some random processes are not stationary in the strict sense. However they are weakly stationary (or "stationary in the wide sense", "covariance stationary", and "second order stationary" used by some other authors). If the random process is weakly stationary then its second moment exists and is a function only of the absolute value of the time difference (see Eq. 1.8 and 1.9), i.e.,

$$E\left[x(t)\, x(t+\tau)\right] = R_x(\tau) \tag{1.4}$$

Obviously, any random process, which is stationary in the strict sense, is also stationary in the wide sense but not vice versa. Random processes are known as nonstationary, if the properties mentioned above are not satisfied.

In many physical applications one is often required to measure, from the observation of a random process, certain statistical quantities from a single record. It is natural to ask the question: Under what conditions is one able to estimate the ensemble average from the temporal average. The condition or the property, which is often assumed in the analysis of stationary random process, is called the Ergodic property. Before entering into the formal definition for an ergodic process, let the temporal average for a random process be

$$\langle V\left[x(t)\right]\rangle = \lim_{T\to\infty} \frac{1}{T}\int_0^T V\left[x(t)\right]\,dt \qquad (1.5)$$

where x(t) is a random process, $V\left[x(t)\right]$ represents a function (with zero memory) of the random process, and T is the averaging time. Likewise, the ensemble average can be defined as

$$E\left(V\left[x(t)\right]\right) = \int_{-\infty}^{\infty} V\left[x(t)\right] p(x)dx \qquad (1.6)$$

A stationary random process is said to be ergodic if the temporal average from a single record can ultimately be identified with the average computed across the ensemble. The following equality must exist:

$$E\left(V\left[x(t)\right]\right) = \langle V\left[x(t)\right]\rangle \qquad (1.7)$$

The ergodicity condition, in effect, shows that, each sample function must eventually take on all modes of behavior of each other sample functions in order to be ergodic. Imagine a sample record of an ergodic process be cut into a sequence of strips each of length T, where T is large. Then this sequence of samples drawn from a single record can be considered as an ensemble. This new ensemble, according to the Ergodic Hypothesis, possesses the same probabilistic characteristics as the original ensemble. In general the ergodic property is not a consequence of the fact that the random process is stationary. Also it is not necessary for the random process to be strictly stationary in order to satisfy the ergodic theorem.

1.4. Autocorrelation, and Power Spectral Density

A more important concept in the studies of random vibration is the autocorrelation function which points out the dependence relationships of the two random variables x_1 and x_2. They are referred to as the possible values which can be assumed by the sample random variable x(t) at the time instants t_1 and t_2. The ensemble average $E(x_1, x_2)$ relating x_1 and x_2 may be defined as

$$E\left[x_1, x_2\right] = \int_{-\infty}^{\infty} \int_{-\infty}^{\infty} x_1 x_2 \, p(x_1, t_1; x_2, t_2) dx_1 dx_2 \qquad (1.8)$$

The above equation reveals the specific correlation properties of x(t) with itself at the time t_1 and t_2. It is generally known as the autocorrelation function to distinguish it from the crosscorrelation functions between two different random variables x(t) and y(t). The time autocorrelation function for the sample random function x(t) is given by

$$R_x(\tau) = \lim_{T \to \infty} \frac{1}{T} \int_0^T x(t)x(t+\tau)dt \qquad (1.9)$$

The autocorrelation function $E\left[x_1, x_2\right]$ may depend on both time instants if the random process is nonstationary. In the event that the random process is weakly stationary or covariance stationary, the autocorrelation function depends only on the absolute value of the difference of two time instants. The equality given by Eq. (1.4) exists.

In the analysis of a signal, the harmonic components are often determined through a simple Fourier analysis. In the case of a

periodic function of period T the energy over a period is finite, then by Parsval's theorem the time average of its energy, or the power, is equal to the sum of the squares of the coefficients in its Fourier series expansion. If the signal is not periodic it cannot, of course, be decomposed into discrete harmonic components as in the case of a periodic wave; however if it has a Fourier transform or is square integrable,[31] then it will have a continuous spectrum which can be treated in very much the same way as that for a periodic signal. The technique of Fourier analysis can also be applied to a stationary random process. The study of spectral density, the autocorrelation and their relations are known as the Generalized Harmonic analysis.[17] The term "Generalized" implies obviously a larger class of functions including those not possessing a Fourier transform, in other words the class of random variables which are not square integrable.

Under the condition that the autocorrelation function is absolutely integrable and finite, the power spectral density and the autocorrelation function will form a Fourier transform pair

$$S(f) = 4\int_0^\infty R(\tau)\cos 2\pi f\tau \, d\tau$$

$$R(\tau) = \int_0^\infty S(f)\cos 2\pi f\tau \, df \qquad (1.10)$$

where S(f) is the power spectral density and $R(\tau)$ is the auto-correlation function. These equations are known as the Wiener-

Khintchine relations.

For the most part one will be primarily concerned with the power spectral density of a stationary (not necessarily strictly stationary) random process. For a stationary random process the autocorrelation defined by Eq. (1. 8) does not change with a shift of time origin, and the results derived from it, namely the power spectral density, will not be expected to be dependent on an arbitrary translation of time origin. Therefore the concept of the power spectral density constitutes an important step toward a complete description of a stationary random process.

For stationary processes having ergodic properties, the power spectral densities defined by Eq. (1. 10) for the sample function are identical to the power spectral densities for the ensemble random process with probability one.

1. 5. Linear and Nonlinear Transformations of the Random Processes

With the knowledge of the basic concepts and properties of a random process, the effect of a linear or nonlinear transformation on these properties will now be investigated.

There are in general three classes of physical systems, which are most frequently encountered in nature, namely a time invariant stable linear system, a nonlinear (zero memory) device whose output is expressible in terms of the input, and a nonlinear system whose output cannot be expressed in terms of the input. We are considering a system with input and output as shown in Fig. (1. 1).

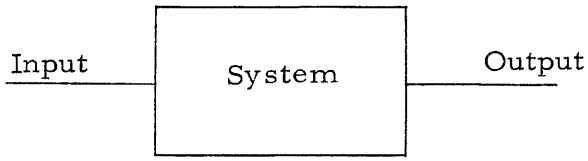

Fig. 1.1

For the first two types of systems, the method of Rice or the Fourier series method is directly applicable. For nonlinear systems, however, the method of Fokker-Planck is more appropriate. In the following, both methods will be demonstrated in obtaining the autocorrelation functions, the power spectral densities, and the probability functions.

(a) Rice's method.

The method of Rice is essentially a Fourier series method, where the attention is focused on the actual time variation of the random variable. One is usually able to develop this random variable in a Fourier series; its coefficients are likewise random variables. From the Fourier integral theorem, the power spectral density and the autocorrelation function for the random variable can be calculated. With the knowledge of these quantities, a score of other statistical properties of the random variable are easily obtained.

Consider now, for example, a time invariant stable linear system, having a system transfer function with poles located in the

left half plane, the output y(t) may be expressed in terms of the input x(t) through the convolution integral

$$y(t) = \int_0^\infty x(t-\tau)\, h(\tau)\, d\tau \tag{1.11}$$

where $h(\tau)$ is the unit-impulse-response of the system. If the input is stationary the output will also be stationary, since the output mean and the autocorrelation function are given by

$$E\left[y(t)\right] = E\left[\int_0^\infty x(t-\tau)h(\tau)\,d\tau\right] = \int_0^\infty h(\tau)E\left[x(t-\tau)\right] d\tau$$

$$= m_x \int_0^\infty h(\tau)\,d\tau$$

$$E\left[y(t)y(t+\tau)\right] = E\left[\int_0^\infty \int_0^\infty x(t-\alpha)x(t+\tau-\beta)\, h(\alpha)\, h(\beta)\, d\alpha d\beta\right]$$

$$= \int_0^\infty \int_0^\infty h(\alpha)\, h(\beta)\, R_x(\tau+\alpha-\beta)\,d\alpha d\beta$$

$$= R_y(\tau) \tag{1.12}$$

which depends only on the time differences τ . The interchanging of the order of integration and statistical averaging is allowed since the system response function $h(\tau)$ does not vary within tolerance over the ensemble. The output autocorrelation function is seen to be dependent on the time difference τ , hence the random variable is stationary.

From Eq. (1.10) and (1.12) the output power spectral density $S_y(f)$ is given by

$$S_y(f) = \left|H(j2\pi f)\right|^2 S_x(f) \tag{1.13}$$

where

$H(j2\pi f)$ = Laplace transform of $h(\tau)$

$S_x(f)$ = Power spectral density of the input.

A similar procedure can be applied to a nonlinear device, whose output is expressible in terms of the input. Therefore if

$$y(t) = f\left[x(t)\right] \tag{1.14}$$

the autocorrelation function for y(t) is given by

$$E\left[y(t)y(t+\tau)\right] = \int_{-\infty}^{\infty}\int_{-\infty}^{\infty} f(x_1)\, f(x_2)\, p(x_1, x_2)\, dx_1 dx_2 \tag{1.15}$$

In principle, other statistical properties can be derived from the known autocorrelation function given above.

Sometimes it is desired to know the probability distribution functions of the output. This is usually not a difficult problem for linear systems since it is well known from the theory of random processes that if the input random process is Gaussian distributed, the output random process is also Gaussian.

In the case of a nonlinear device such as that given by Eq. (1.14) the output probability density function can usually be written in terms of the input probability density function p(x), hence[19]

$$p(y) = p(x)\left|\frac{dx}{dy}\right| \tag{1.16}$$

if x(t) is a single-value function of y(t).

It is seen from the above discussion that the statistical properties of the output of the systems are completely characterized by using Rice's method.

(b) The method of Fokker-Planck.

In the cases of nonlinear systems, whose output is not expressible in terms of the input, Rice's method is no longer applicable, though approximation techniques have been developed to extend this method to include systems with small nonlinearity.[4, 5] The method of Fokker-Planck seems to be more appropriate to solve problems of this kind.

The behavior of many physical systems, in particular that of discrete dynamic systems, subjected to Gaussian white random excitation, are examples of continuous multidimensional Markoff processes. As it was shown earlier (Eq. 1.3), such processes are completely defined by the transition probability $T(\bar{x}, t \mid \bar{x}_o, t_o)$, where $\bar{x}$, and $\bar{x}_o$ are the position vectors of a point in n dimensional space whose components are $x_1, x_2, \ldots x_n$ and $x_{1o}, x_{2o}, \ldots x_{no}$ respectively, and n is the order of the system. The transition probability, in turn, is the fundamental solution to the appropriate Fokker-Planck equation.

$$\frac{\partial T}{\partial t} = - \sum_{i=1}^{n} \frac{\partial}{\partial x_i} \left[A_i T \right] + \frac{1}{2} \sum_{k=1}^{n} \sum_{\ell=1}^{n} \frac{\partial^2}{\partial x_k \partial x_i} \left[B_{k\ell} T \right] \qquad (1.17)$$

where the coefficients A_i and $B_{k\ell}$ are obtained from the following limiting conditions

$$A_i = \lim_{\Delta t \to 0} < \frac{\Delta x_i}{\Delta t} >$$

$$B_{k\ell} = \lim_{\Delta t \to 0} < \frac{\Delta x_k \Delta x_\ell}{\Delta t} > \qquad (1.18)$$

The required solution of Eq. (1.17) must satisfy the initial condition

$$\lim_{t \to t_o} T(\bar{x}, t \,|\, \bar{x}_o, t_o) = \prod_{i=1}^{n} \delta(x_i - x_{io})$$

as $t \to \infty$, the dependence of the transition probability on the initial condition will disappear as the system becomes stationary, hence

$$\lim_{t \to \infty} T(\bar{x}, t \,|\, \bar{x}_o, t_o) = p(\bar{x}) = p(x_1, x_2, \ldots, x_n) \qquad (1.19)$$

which is the stationary joint probability density function of the system. Since $p(x_1, x_2, \ldots, x_n)$ does not depend on time, it must satisfy the Fokker-Planck equation in the stationary form. Therefore

$$0 = -\sum_{i=1}^{n} \frac{\partial}{\partial x_i} (A_i p) + \frac{1}{2} \sum_{k=1}^{n} \sum_{\ell=1}^{n} \frac{\partial^2}{\partial x_k \partial x_\ell} (B_{k\ell} p) \qquad (1.20)$$

In addition to the stated properties for $T(\bar{x}, t \,|\, \bar{x}_o, t_o)$ and $p(\bar{x})$, they must also satisfy the basic properties for the probability density function discussed earlier. The derivation and justification of the Fokker-Planck equation, and the uniqueness of the stationary solutions are given by Uhlenbeck and Wang,[2] and Caughey.[6]

After obtaining the transition probability and the stationary probability functions for the Fokker-Planck equation, various other statistical properties of the system can be determined. The detail

procedures involved will be demonstrated in Chapter IV where the statistical properties of a nonlinear system subjected to white random excitation are completely solved.

CHAPTER II

RESPONSE OF LINEAR SYSTEMS TO MAGNITUDE-LIMITED RANDOM EXCITATION

2. 1. Introduction

In many situations, encountered both in the field and in the laboratory, the excitation produced by a broadband random source has many of the characteristics of a signal having a Gaussian distribution of instantaneous values except that the higher values predicted by the theory do not appear. Therefore, in all cases, physical systems are really excited by a magnitude-limited Gaussian random vibration rather than a strictly Gaussian random vibration. For example, the most commonly used equipment in the laboratory to generate various types of vibration conditions is the shaker, whose major components are: the vibration table, amplifier, and the servo-control unit. In the event of random wave testing or complex waves of various types, a magnitude limiting amplifier is customly provided to prevent the shaker armature from exceeding the maximum specified limit. Obviously the random wave is no longer Gaussian distributed after magnitude limiting. The clipped signal is then converted and transmitted to the vibration table. Consequently, the test specimen is, in reality, excited by a magnitude-limited Gaussian random signal rather than a true Gaussian random signal. In many other situations, such as during an earthquake, acoustic noise in the jet, etc., the vibration follows many of the properties of Gaussian distributions

with the exception that the higher values are absent. From the preceeding discussion it is not difficult to see the necessity of looking further into the response characteristics of the system when excited by a magnitude-limited broadband random vibration.

In order to investigate the statistical behavior of a physical system subject to magnitude-limited random vibration, the problem must be formulated mathematically. To simplify the problem further, only linear systems are considered. It is well known from the theory of probability that the output probability distribution of linear systems is Gaussian if the input is Gaussian. This is of course not the case for the problem we are considering. The statistical response characteristics of a linear system, when subjected to a magnitude-limited Gaussian random excitation, is not generally known. It becomes a very difficult problem analytically, since the instantaneous values of the input are magnitude-limited, and do not extend to infinity.

There are no previous works recorded in the area of magnitude-limited random vibration. However, the technique is well known in communication theories, where the problem is one of determining the statistical properties of the output of a nonlinear device and a filter, e.g., a detector. Problems of this kind have been studied by Rice,[3] Middleton,[18] Lanning and Battin,[21] Price[22] and others.[23-27] Their primary interest is directed toward the properties of correlation and the power spectral density of the response. Kac and Siegert[23] have also studied the probability distribution of the output of a square-law detector. There are few other papers available

concerning the output probability distribution of a nonlinear detector.[24-27]

In the following, an attempt will be made to set up a simple mathematical model, i. e., a single degree of freedom system, which represents an idealized mechanical structure. It is desired to know the response statistical characteristics of the system subject to a magnitude-limited external force.

In order to clarify the exact nature of the magnitude-limited Gaussian forcing function, its statistical properties are first analyzed. From there, the response characteristics of the single degree of freedom system can be easily determined. Experiments are conducted to check the correctness of the analytical results.

2. 2. A Simple Model and Assumptions

The starting point for nearly all existing theoretical investigations in random vibration has been associated with a single degree of freedom system.

$$\ddot{x} + 2\zeta\omega_n\dot{x} + \omega_n^2 x = N(t) \qquad (2.1)$$

where ζ is the critical damping ratio, ω_n is the undamped natural frequency, x(t) is the displacement of the mass with respect to the ground (Fig. 2. 1), and finally the magnitude-limited Gaussian random function N(t), which has the units of acceleration.

The original source of excitation prior to the magnitude limiting operation is assumed to have the following properties.

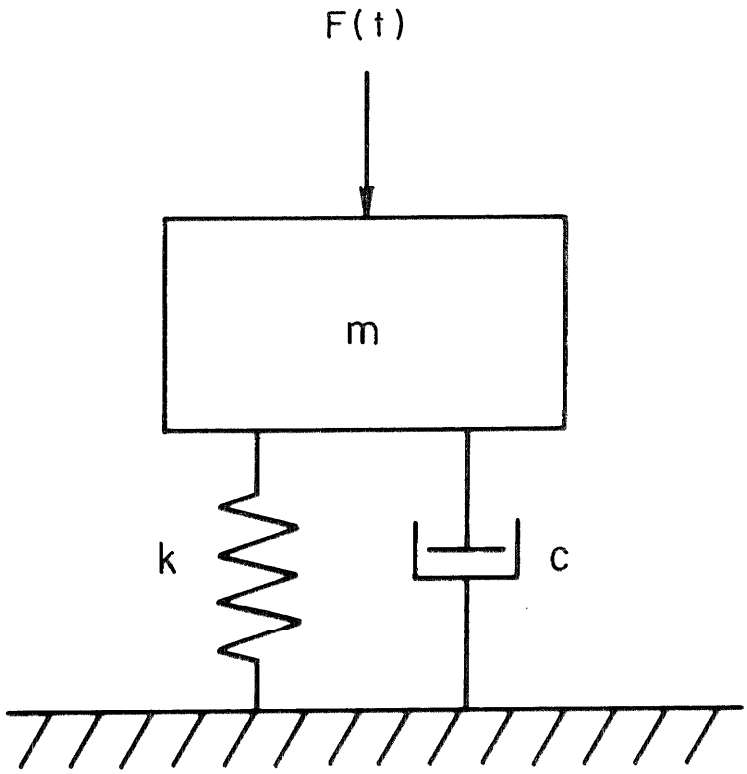

Fig. 2.1. Single Degree of Freedom System.

1. It is Gaussian distributed in probability.

2. It is stationary.

3. It possesses ergodic properties.

4. It is band limited. The nominal frequency bandwidth extends from d. c. to 10,000 cps.

This broadband random signal is then magnitude-limited through a nonlinear device, the transfer function of which is given by

$$f(x) = \begin{cases} a & x \geqslant a \\ x & a > x > -a \\ -a & x \leqslant -a \end{cases} \qquad (2.20$$

where a is the magnitude limiting level. The nonlinear operation is assumed to be symmetrical as shown in Fig. (2.2).

As it was shown in Chapter I, nonlinear magnitude limiting operation will not alter the statistical properties of stationarity and ergodicity of the random signal (see Eq. 1.7). However, the output random signal is no longer Gaussian distributed.

Various statistical properties of the magnitude-limited random function N(t) are discussed in the ensuing sections.

2.3. Statistical Properties of the Magnitude-limited Gaussian Random Process

This section is primarily concerned with the statistical properties of the magnitude-limited Gaussian random function N(t) (Eq. 2.1). The effects of magnitude limiting on the probability distribution, the auto-correlation, and the power spectral density of the broadband random signal are presented.

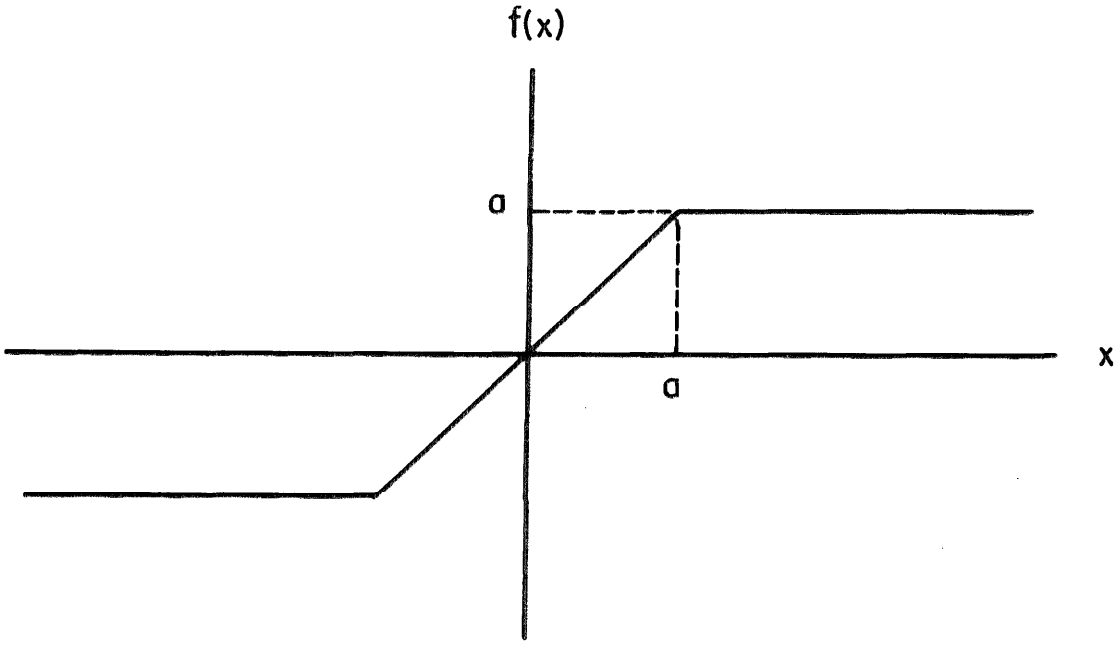

Fig. 2.2. Magnitude limiter.

2. 3. 1. Probability Density Function of the Magnitude-limited Gaussian Random Process

It is assumed from the beginning that the source of excitation prior to the magnitude limiting operation is Gaussian distributed with the probability density function given by

$$p_i(x) = \frac{1}{\sqrt{2\pi}\,\sigma_i} e^{-x^2/2\sigma_i^2} \qquad (2.3)$$

where the mean is assumed to be zero in most vibration problems, σ_i is the rms value and is constant when the random process is stationary. The output probability density function $p_o(x)$ after the nonlinear magnitude limiting operation can be defined in terms of the input probability density function $p_i(x)$ through

$$p_o(x) = \begin{cases} \delta(x+a)\int_{-\infty}^{-a} p_i(t)\,dt & x \leqslant -a \\ p_i(x) & -a < x < a \\ \delta(x-a)\int_{a}^{\infty} p_i(t)\,dt & x \geqslant a \end{cases} \qquad (2.4)$$

where $\underline{a}$ is the magnitude limiting level and is assumed to be symmetrical with respect to the d. c. level, $\delta(x+a)$ and $\delta(x-a)$ are Dirac Delta Functions at $\underline{a}$ and $-\underline{a}$ respectively. The output probability density function $p_o(x)$, as shown in (Fig. 2. 3), satisfies the basic requirements for a probability distribution, namely

$$p_o(x) \geqslant 0$$

$$\int_{-\infty}^{\infty} p_o(x)\,dx = 1$$

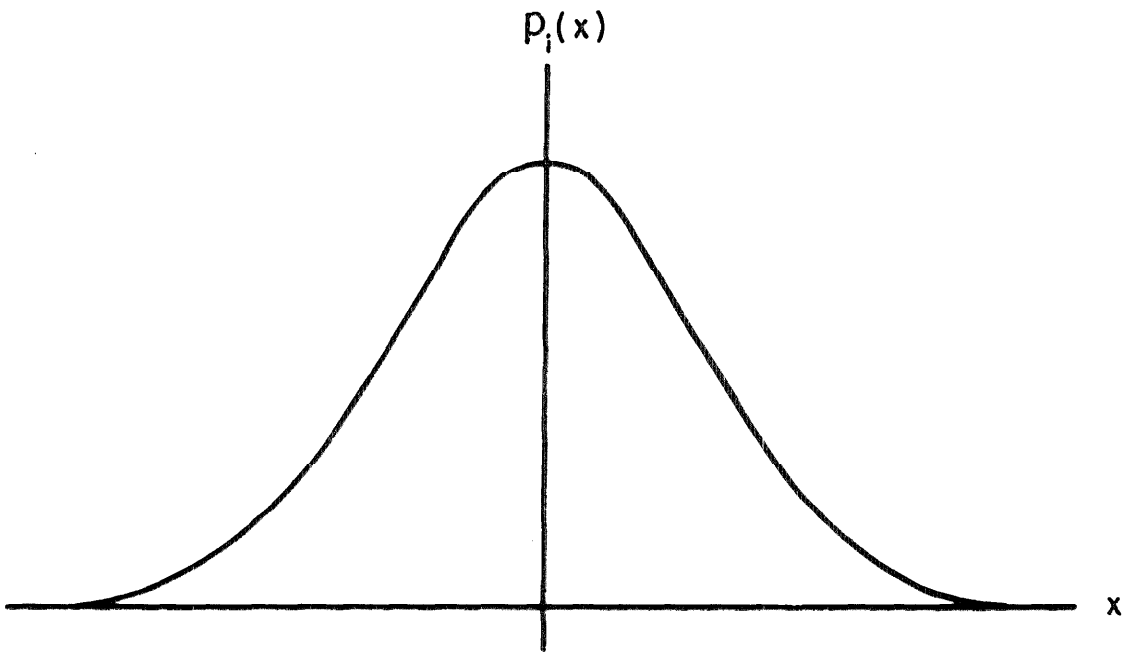

Gaussian probability density

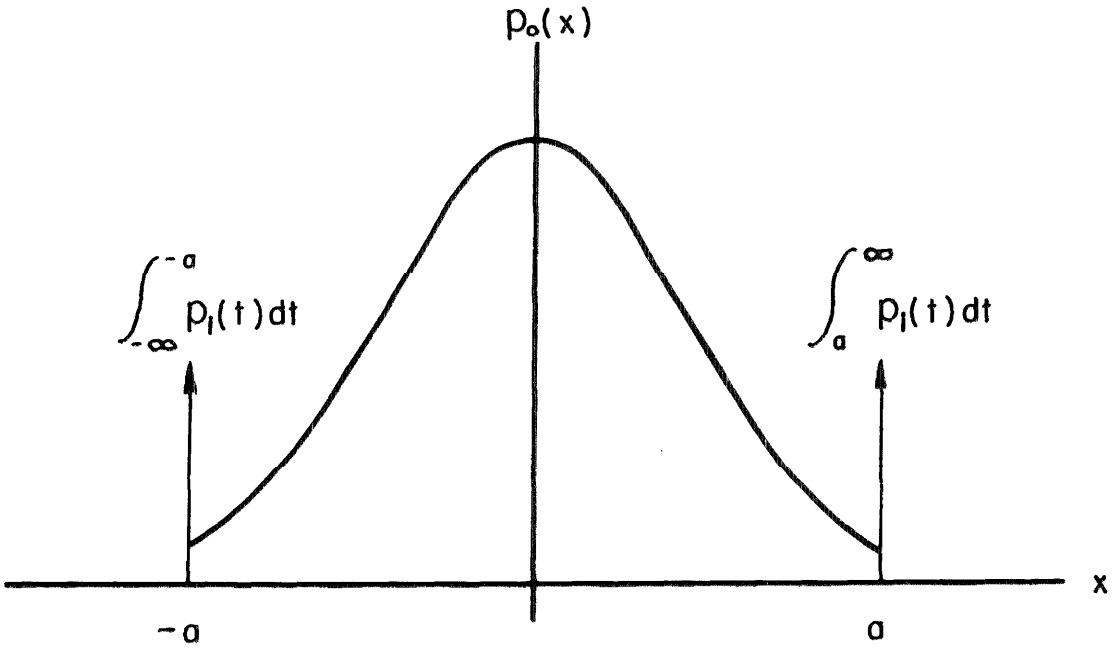

Magnitude-limited Gaussian probability density

Fig. 2.3

2. 3. 2. Autocorrelation and Power Spectral Density of the Magnitude-Limited Gaussian Random Process

The problem now is to determine the statistical characteristics of the output of the nonlinear device (Eq. 2. 4) when the statistical characteristics of its input are known. Generally, this is simply a nonlinear transformation of the random variables. Let the input to the nonlinear device be x(t), and the output be $f\left[x(t)\right]$. Then it follows from the theory of statistical averaging that the averages with respect to the output can always be obtained by averaging with respect to the input. Hence

$$E\left[f(x)\right] = \int_{-\infty}^{\infty} f(x)\, p(x)\, dx$$

the nth moment of the output is given by

$$E\left[f^n(x)\right] = \int_{-\infty}^{\infty} f^n(x)\, p(x)\, dx$$

From the known output probability density function $p_o(x)$ obtained earlier, the output ensemble moments are easily obtained. The first two moments are given by

$$E_o(x) = \int_{-\infty}^{\infty} x\, p_o(x)\, dx = 0$$

$$E_o(x^2) = \int_{-\infty}^{\infty} x^2 p_o(x)\, dx$$

$$= \int_{-\infty}^{-a} x^2 \left[\delta(x+a) \int_{-\infty}^{-a} p_i(t)\, dt\right] dx + \int_{-a}^{a} x^2 p_i(x)\, dx$$

$$+\int_a^\infty x^2\left[\delta(x-a)\int_a^\infty p_i(t)dt\right]dx$$

$$= 2a^2\left[1+P\left(\frac{a}{\sigma_i}\right)\right]+\sigma_i^2\left[2P\left(\frac{a}{\sigma_i}\right)-1\right]$$

$$+2\sigma_i^2\left[-\frac{1}{\sqrt{2\pi}}\frac{a}{\sigma_i}\exp-\frac{a^2}{2\sigma_i^2}\right]$$

where σ_i is the rms value of the input Gaussian random process, and $P(a/\sigma_i)$ is given by

$$P\left(\frac{a}{\sigma_i}\right)=\frac{1}{\sqrt{2\pi}}\int_{-\infty}^{a/\sigma_i} e^{-t^2/2}\,dt \qquad (2.5)$$

The expression given above for the second moment can alternately be written in the normalized form

$$\frac{\sigma_o^2}{\sigma_i^2}=2z_o^2\left[1-P(z_o)\right]+\left[2P(z_o)-1\right]-\frac{2z_o}{\sqrt{2\pi}}e^{-z_o^2/2} \qquad (2.6)$$

with the normalized parameter $z_o=a/\sigma_i$. The output over input rms ratio σ_o/σ_i is plotted against z_o in Fig. (2.8) along with the experimental data.

Similarly, the autocorrelation function of the output of the nonlinear device is given by

$$R_o(t_1-t_2)=\int_{-\infty}^{\infty}\int_{\infty}^{\infty} f(x_{t_1})\,f(x_{t_2})\,p(x_{t_1}x_{t_2})dx_{t_1}dx_{t_2} \qquad (2.7)$$

where the nonlinear function f(x) is defined in Eq. (2.2).

The autocorrelation function of the output of a nonlinear device can, in principle, be solved for by the direct method indicated above. Analytical difficulties may often arise in some cases in the evaluation of the integral. Indirect methods, involving Fourier transform of the nonlinear transfer functions, are often employed instead; the solutions are then presented in the transform space. The transform method of analysis will not, however, be discussed here. Following the assumptions made in Section 2.2, the output autocorrelation function given by Eq. (2.7) can be simplified.

$$R_o(t_1-t_2) = \int_{-\infty}^{\infty}\int_{-\infty}^{\infty} f(x_1)\, f(x_2)\, \frac{1}{2\pi\sigma_i\sqrt{1-\rho}^2}\, \exp-\frac{x_1^2+x_2^2-2\rho x_1 x_2}{2\sigma_i^2\ (1-\rho^2)}\, dx_1 dx_2$$

where ρ is the autocorrelation coefficient,

$$\rho = \frac{E(x_1 x_2)}{\sigma_i^2}$$

in which it is assumed that the random variable $x(t)$ has zero mean.

In order to simplify the calculation, the following normalizations are made. Let

$$\frac{x_1}{\sigma_i} = z_1 \qquad \frac{x_2}{\sigma_i} = z_2 \qquad \frac{a}{\sigma_i} = z_o$$

$$\Gamma_o(\tau) = \frac{R_o(\tau)}{\sigma_i^2} \qquad \text{where } \tau = t_1-t_2$$

thus

$$\Gamma_o(\tau) = \int_{-\infty}^{\infty}\int_{-\infty}^{\infty} f(z_1)\, f(z_2)\, \frac{1}{2\pi\sqrt{1-\rho}^2}\, \exp-\frac{z_1^2+z_2^2-2\rho z_1 z_2}{2(1-\rho^2)}\, dz_1 dz_2$$

Using Price's theorem (Appendix E), the integral can be further simplified by repeated differentiation of $\Gamma_o(\tau)$ with respect to $\rho(\tau)$

$$\frac{d^2\,\Gamma_o(\tau)}{d\rho(\tau)^2} = \int_{-\infty}^{\infty}\int_{-\infty}^{\infty} f''(z_1)\, f''(z_2)\, \frac{1}{2\pi\sqrt{1-\rho^2}}\, \exp-\frac{z_1^2+z_2^2-2\rho z_1 z_2}{2(1-\rho^2)}\, dz_1 dz_2$$

where $f''(z) = d^2 f(z)/dz^2$. From the definition for f(z), (Eq. 2.2), we have

$$\frac{d^2\Gamma_o(\tau)}{d\rho^2} = \int_{-\infty}^{\infty}\int_{-\infty}^{\infty} \left[\delta(z_1+z_o)-\delta(z_1-z_o)\right]\left[\delta(z_2+z_o)-\delta(z_2-z_o)\right]$$

$$\frac{1}{2\pi\sqrt{1-\rho^2}}\, \exp-\frac{z_1^2+z_2^2-2\rho z_1 z_2}{2(1-\rho^2)}\, dz_1 dz_2$$

$$= \frac{1}{\pi\sqrt{1-\rho^2}}\left[\exp-\frac{z_o^2}{1+\rho} - \exp-\frac{z_o^2}{1-\rho}\right]$$

where the symbol δ represents the Dirac delta function. It does not seem to be possible to recover the autocorrelation function $\Gamma_o(\tau)$ from the repeated integration due to the singularities appearing in the exponential functions. However, $\Gamma_o(\tau)$ could be recovered from the first derivative $d\Gamma_o(\tau)/d\rho(\tau)$ by integrating term by term the series expansion of the joint probability density function. Since

$$\frac{d\Gamma_o(\tau)}{d\rho(\tau)} = \int_{-\infty}^{\infty}\int_{-\infty}^{\infty} \left[U(z_1+z_o)-U(z_1-z_o)\right]\left[U(z_2+z_o)-U(z_2-z_o)\right]$$

$$P(z_1, z_2)\,dz_1 dz_2$$

$$= \int_{-z_o}^{z_o}\int_{z_o}^{z_o} \frac{1}{2\pi\sqrt{1-\rho^2}} \exp - \frac{z_1^2 + z_2^2 - 2\rho z_1 z_2}{2(1-\rho^2)}\, dz_1 dz_2$$

where the symbol U represents the unit step function. The integrand can be expanded in terms of Hermite polynomial. Since[30]

$$\sum_{n=0}^{\infty} \frac{H_n(x)H_n(y)}{n!}\rho^n = \frac{1}{\sqrt{1-\rho^2}} \exp - \frac{\rho^2x^2 + \rho^2y^2 - 2\rho xy}{2(1-\rho^2)} \qquad (2.8)$$

where

$$H_n(x) = (-1)^n e^{x^2/2}\left(\frac{d}{dx}\right)^n e^{-x^2/2}$$

Hence the series expansion for the joint probability density function is given by

$$\frac{1}{\sqrt{1-\rho^2}} \exp - \frac{x^2 + y^2 - 2\rho xy}{2(1-\rho^2)} = \sum_{n=0}^{\infty} \frac{\rho^n}{n!}\left[\left(\frac{d}{dz_1}\right)^n e^{-z_1^2/2}\right]$$

$$\left[\left(\frac{d}{dz_2}\right)^n e^{-z_2^2/2}\right]$$

Substituting this into the integral, thus

$$\frac{d\Gamma_o(\tau)}{d\rho(\tau)} = \frac{1}{2\pi}\int_{-z_o}^{z_o}\int_{-z_o}^{z_o} \sum_{n=0}^{\infty} \frac{\rho^n}{n!}\left[\left(\frac{d}{dz_1}\right)^n e^{-z_1^2/2}\right]$$

$$\left[\left(\frac{d}{dz_2}\right)^n e^{-z_2^2/2}\right] dz_1 dz_2$$

$\Gamma_o(\tau)$ could be recovered by integrating the first derivative $d\Gamma_o(\tau)/d\rho(\tau)$ with respect to $\rho(\tau)$, and by exchanging the role of integration and summation on the right hand side. This is permissible since the power series

$$\sum_{n=0}^{\infty} \frac{\rho^n}{n!}$$

is uniformly convergent for $|\rho| \leq 1$, hence

$$\Gamma_o(\tau) = \frac{1}{2\pi} \int_{-z_o}^{z_o} \int_{-z_o}^{z_o} \sum_{n=0}^{\infty} \frac{\rho^{n+1}}{(n+1)!} \left[\left(\frac{d}{dz_1} \right)^n e^{-z_1^2/2} \right] \left[\left(\frac{d}{dz_2} \right)^n e^{-z_2^2/2} \right] dz_1 dz_2$$

The above expression is further simplified by termwise integration of the orthogonal series with respect to z. This is due to the fact that Hermite polynomial (Eq. 2.8) forms a complete set and possesses the properties of mean convergence.[31] Finally

$$\Gamma_o(\tau) = \left[2P(z_o) - 1 \right]^2 + \frac{2}{\pi} \left[\frac{\rho^3}{3!} (D^1)^2 + \frac{\rho^5}{5!} (D^3)^2 + \frac{\rho^7}{7!} (D^5)^2 + \ldots \right] \tag{2.9}$$

where $P(z_o)$ is defined as in Eq. (2.5)

$$P(z_o) = \frac{1}{\sqrt{2\pi}} \int_{-\infty}^{z_o} e^{-t^2/2} \, dt$$

and the differential operator

$$D^n = \left(\frac{d}{dz_o} \right)^n$$

Four terms are used in the calculation toward the sum of the series. Selective results are shown in Fig. (2. 4), where the output autocorrelation functions are plotted against the input autocorrelation coefficients with magnitude limiting levels as the parameter.

With the knowledge of the output autocorrelation function of the nonlinear magnitude limiter, it is not difficult to calculate the power spectral density of the same. From Eq. (1. 10), autocorrelation function and power spectral density are shown to be Fourier transform pairs, in other words one can be obtained if the other is known. Hence

$$S_o(f) = 4\int_0^\infty R_o(\tau)\cos 2\pi f\tau \, d\tau \qquad (2.10)$$

where $S_o(f)$ and $R_o(\tau)$ are the output power spectral density and autocorrelation function, respectively, of the magnitude-limited random function, and since

$$R_o(\tau) = \sigma_i^2 \, \Gamma_o(\tau) \qquad \text{and} \qquad \rho(\tau) = \frac{R_i(\tau)}{\sigma_i^2}$$

Eq. (2.9) can be rewritten as

$$R_o(\tau) = \sigma_i^2 \, \Gamma_o(\tau) = \left[2P(z_o)-1\right]^2 R_i(\tau) + \frac{2}{\pi}\left[\frac{1}{3!}\frac{R_i^3(\tau)}{\sigma_i^4}(D^1)^2 + \ldots + \frac{1}{(2n+1)!}\frac{R_i^{(2n+1)}(\tau)}{\sigma_i^{4n}}(D^{2n-1})^2\right] \qquad (2.11)$$

where σ_i^2 and $R_i(\tau)$ are the mean square value and the autocorrelation function, respectively, before the magnitude limiting operation.

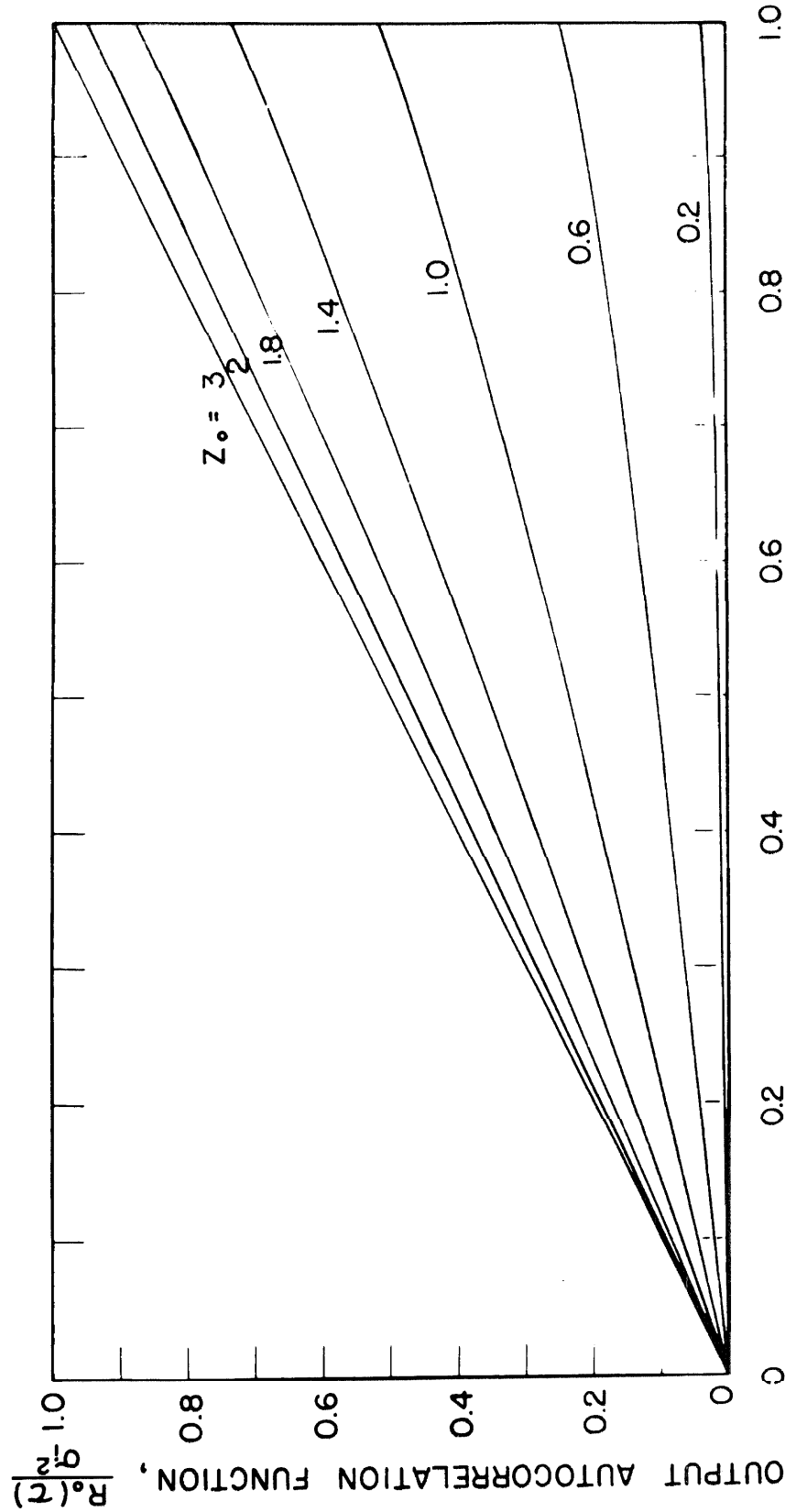

Fig. 2.4. The input and output autocorrelation function of the magnitude limiter.

As it was indicated previously that the series expansion for $d\Gamma_o(\tau)/d\rho(\tau)$ is uniformly convergent with respect to the auto-correlation coefficient $\rho(\tau)$, term by term integration is then permissible. This property can also be applied to the series expansion for $\Gamma_o(\tau)$ and $R_o(\tau)$. Therefore the power spectral density $S_o(f)$ could be calculated if the input spectrum is known.

Suppose now the input random process is band limited, and has constant power spectral densities within the frequency band and zero elsewhere, e.i.,

$$\begin{cases} S_i(f) = S_o & 0 \leq f \leq f_o \\ = 0 & \text{Elsewhere} \end{cases} \tag{2.12}$$

Hence,

$$R_i(\tau) = \int_0^\infty S_i(f)\cos 2\pi f\tau\, df = \int_0^{f_o} S_o \cos 2\pi f\tau\, df = \frac{S_o \sin 2\pi f_o \tau}{2\pi\tau} \tag{2.13}$$

The assumed spectrum is practical and can be approximated very closely by experiment.

Substituting Eq. (2.13) into Eq. (2.11), then together with Eq. (2.10) the output power spectral density could be calculated. The following integrals will be involved in the calculation. They are listed here for reference.

$$\int_0^\infty \frac{\sin^2 x}{x^2}\cos kx\,dx = \frac{\pi}{2}\left|1-\frac{k}{2}\right| \quad k < 2$$
$$= 0 \quad k > 2$$

$$\int_0^\infty \frac{\sin^3 x}{x^3}\cos kx\,dx = \frac{\pi}{8}(3-k^2) \qquad 0 < k < 1$$

$$= \frac{\pi}{16}(3-k^2) \qquad 1 \le k \le 3$$

$$= 0 \qquad 3 \le k \le \infty$$

$$\int_0^\infty \frac{\sin^5 x}{x^5} \cos kx\,dx = \frac{\pi}{384}\left[115-30k^2+3k^4\right] \qquad 0 \le k \le 1$$

$$= \frac{\pi}{192}\left[55+10k-30k^2+10k^3-k^4\right] \qquad 1 \le k \le 3$$

$$= \frac{\pi}{768}(5-k^2) \qquad 3 \le k \le 5$$

If three terms from Eq. (2.11) are used, the power spectral density of the magnitude limiter output is approximated by

$$S_o(f) = S_o\left\{\left[2P(z_o)-1\right]^2 + \frac{1}{6}\left|3-\frac{f^2}{f_o^2}\right|(D^1)^2 + \frac{1}{5760}\left(115-30\frac{f^2}{f_o^2}+3\frac{f^4}{f_o^4}\right)(D^3)^2\right\}$$

$$0 \le f \le f_o$$

$$= S_o\left\{\frac{1}{12}\left(3-\frac{f}{f_o}\right)^2(D^1)^2 + \frac{1}{2880}\left(55+10k-30k^2+10k^3-k^4\right)(D^3)^2\right\} \qquad (2.14)$$

$$f_o \le f \le 3f_o$$

$$= S_o\left\{\frac{1}{11520}\left(5-\frac{f}{f_o}\right)^4(D^3)^2\right\} \qquad 3f_o \le f \le 5f_o$$

Because of the rapid convergence of the series, the error is only of the order of 3% when a four-term approximation of the series is used. The results are shown in Table (2.1) where the power spectral densities are tabulated against the frequency and the magnitude limiting level. It is interesting to note that the power spectral densities remain essentially constant in the frequency range $0 \le f \le f_o$, and extend further beyond when the input to the limiter is heavily clipped.

A less tedious way to calculate the output power spectral density

Table 2. 1. The power spectral density S(f) given by Eq. 2. 14.

z_o \ f/f_o	0.02	0.2	0.4	0.6	0.8	1.0	1.2	1.5	2.0
0.2	.0298	.0297	.0295	.293	.0289	.0284	.0028	.00204	.0010
0.4	.112	.112	.111	.109	.108	.107	.0094	.0068	.0037
0.6	.232	.231	.230	.228	.226	.226	.01615	.0118	.0062
0.8	.367	.366	.365	.363	.36	.356	.0199	.0146	.0072
1.0	.5	.499	.498	.497	.494	.490	.0196	.0141	.0069
1.2	.625	.623	.621	.620	.616	.613	.0166	.0117	.0055
1.4	.726	.726	.725	.723	.721	.718	.01247	.0087	.0040
1.6	.809	.809	.808	.807	.806	.803	.0087	.0061	.0028
1.8	.872	.872	.871	.870	.870	.868	.0058	.0040	.0026
2.0	.917	.917	.917	.917	.916	.915	.0036	.0025	.0012
2.2	.949	.949	.948	.948	.948	.948	.0021	.0015	.0007
2.4	.969	.969	.969	.969	.969	.968	.0011	.0008	.0004
2.6	.982	.982	.982	.982	.982	.982	.0006	.0004	.0003
2.8	.999	.999	.999	.999	.999	.999	.0000	.0000	.0000
3.0	1.0	1.0	1.0	1.0	1.0	1.0	.0000	.0000	.0000

f_o = low pass filter cutoff frequency

z_o = normalized magnitude limiting level $a/\sigma_{\dot{x}}$

of the limiter is to assume the shape of the input spectrum to be the following

$$S_i(f) = S_o e^{-af^2} \qquad f \geq 0 \tag{2.15}$$

and

$$\begin{aligned} R_i(\tau) &= \int_0^\infty S_i(f)\cos 2\pi f \tau \, df \\ &= \int_0^\infty S_o e^{-af^2} \cos 2\pi f \tau \, df \\ &= \frac{S_o}{2} \sqrt{\pi/a} \; e^{-\pi^2\tau^2/a} \\ &= \sigma_i^2 \, e^{-\pi^2\tau^2/a} \end{aligned} \tag{2.16}$$

Equation (2.9) can be rewritten as

$$\frac{R_o(\tau)}{\sigma_i^2} = \left\{ \left[2P(z_o) - 1 \right]^2 e^{-\pi^2\tau^2/a} + \frac{2}{\pi} \left[\frac{(D^1)^2}{3!} \; e^{-3\pi^2\tau^2/a} + \frac{(D^3)^2}{5!} \; e^{-5\pi^2\tau^2/a} + \ldots \right] \right\} \tag{2.17}$$

The corresponding power spectral density is obtained from Fourier cosine transform, hence

$$S_o(f) = S_o \left\{ \left[2P(z_o) - 1 \right]^2 e^{-af^2} + \frac{2}{\pi} \left[\frac{(D^1)^2}{3!\sqrt{3}} e^{-af^2/3} + \frac{(D^3)^2}{5!\sqrt{5}} \; e^{-af^2/5} + \ldots \right] \right\} \tag{2.18}$$

The results are shown in Table (2.2), where the output power spectral densities are tabulated against the frequency and the magnitude limiting level. It again demonstrates the fact that the spectrum shapes remain essentially constant in the lower frequency range. A slight

Table 2.2. The power spectral density S(f) given by Eq. 2.18.

z_o \ f/f_o	0.01	0.1	0.2	0.4	0.6	0.8	1.0	1.5	2.0
0.2	.0287	.0284	.0277	.0248	.0207	.0162	.0119	.0046	.0017
0.4	.109	.108	.105	.0939	.0784	.0611	.0447	.0167	.0058
0.6	.225	.222	.217	.194	.1613	.125	.0908	.0326	.0106
0.8	.358	.355	.345	.308	.255	.197	.142	.0486	.0143
1.0	.492	.488	.474	.4225	.349	.278	.191	.0625	.0164
1.2	.616	.610	.592	.527	.434	.331	.235	.0737	.0173
1.4	.721	.714	.693	.616	.506	.385	.272	.0826	.0177
1.6	.805	.797	.774	.687	.564	.428	.300	.0895	.0179
1.8	.869	.861	.836	.742	.608	.461	.323	.0947	.0180
2.0	.916	.907	.880	.781	.640	.484	.339	.0985	.0181
2.2	.948	.939	.911	.808	.662	.501	.350	.1011	.0182
2.4	.969	.959	.931	.826	.676	.512	.357	.1028	.0182
2.6	.982	.972	.944	.837	.685	.518	.362	.104	.0182
2.8	.990	.981	.951	.844	.691	.522	.364	.105	.0183

f_o = nominal low pass filter cutoff frequency

z_o = normalized magnitude limiting level a/σ_x

increase in the magnitude of the power spectral densities at the high frequency end is noted.

2.4. Response of a Single Degree of Freedom System to Magnitude-Limited Random Excitation

It has been mentioned previously that the primary objective of the investigation is to find out the effect of magnitude-limited random input on a structure, or a test specimen, etc. A single degree of freedom oscillator will be the most representative model (Fig. 2.1) in this respect. We will study the response of this model subject to magnitude-limited Gaussian random excitation. The differential equation has already been given previously,

$$\ddot{x} + 2\zeta\omega_n\dot{x} + \omega_n^2 x = N(t) \qquad (2.1)$$

where N(t) is the magnitude-limited Gaussian random forcing function, the statistical characteristics of which have already been investigated in the preceding sections.

Now it is desired to study the statistical behavior of the displacement variable x(t). Since this involves only linear system with constant coefficients, the techniques introduced in Section (1.5) will apply. If the steady state situations alone are considered, the output random process x(t) will be stationary and ergodic if the forcing term N(t) is stationary and ergodic. Some of the results, which could be obtained analytically, are presented here. These include the power spectral density function, mean square response, and the auto-correlation function.

For a single degree of freedom system, the motion of the mass is governed by the convolution integral

$$x(t) = \int_0^\infty h(\tau)\, N(t-\tau)\, d\tau$$

where $h(\tau)$ is the impulse response of the system

$$h(\tau) = \frac{1}{\omega_n \sqrt{1-\zeta^2}}\, e^{-\zeta\omega_n\tau} \sin \omega_n \sqrt{1-\zeta^2}$$

and its Laplace transform (or the frequency response) is given by

$$H(j\omega) = \frac{1}{(\omega_n^2 - \omega^2) + j2\zeta\omega\omega_n} \tag{2.19}$$

From Eq. (1.13) the power spectral density of the oscillator is given by

$$S_x(f) = S_o(f)\, |H(j\omega)|^2 = \frac{S_o(f)}{\omega_n^4 \left\{ \left[1-\left(\frac{\omega}{\omega_n}\right)^2 \right]^2 + \left(2\zeta \frac{\omega}{\omega_n}\right)^2 \right\}} \tag{2.20}$$

where $S_o(f)$ is the power spectral density of the magnitude-limited broadband random signal (Table 2.1 or 2.2), and $S_x(f)$ is the power spectral density of the oscillator. Since the bandwidth of the input power spectral density $S_o(f)$ is usually wide compared to the natural frequency ω_n of the system, $S_o(f)$ is approximately uniform in the neighborhood of the natural frequency ω_n. The shape of the curve for $S_x(f)$ at small damping follows essentially that of $|H(j\omega)|^2$ with its magnitude modified by the magnitude of the input power spectral density $S_o(f)$ along the entire frequency range.

From Eq. (1.10), the mean square response is simply given by

$$\sigma_x^2 = \int_0^\infty S_x(f) \left| H(j2\pi f) \right|^2 df$$

$$= \int_0^\infty \frac{S_o(f)df}{\omega_n^4 \left\{ \left[1-\left(\frac{\omega}{\omega_n}\right)^2 \right]^2 + \left(2\zeta\frac{\omega}{\omega_n}\right)^2 \right\}} = \frac{S_o(f_n)}{8\zeta\omega_n^3} \qquad (2.21)$$

where $S_o(f)$ is considered to be constant (see Table 2.1, 2.2 and the experimental data in Fig. 2.11) over a frequency range which is wide in comparison with the natural frequency ω_n. The quantity $S_o(f)$ can be taken outside the integral. This can be further justified from the fact that the integral is not sensitive to the upper limit in the integration, i.e., the upper limit can be replaced by some frequency f_c. The error introduced will be less than 2% at $f_c = 10f_n$. This is estimated from the fact that the integral can be easily changed to the standard form and evaluated according to the following indefinite integral[51]

$$\int \frac{dx}{ax^4 + bx^2 + c} = \frac{1}{4aq^3 \sin\alpha} \left\{ \sin\frac{\alpha}{2} \ell n \frac{x^2 + 2qx\cos\frac{\alpha}{2} + q^2}{x^2 - 2qx\cos\frac{\alpha}{2} + q^2} + 2\cos\frac{\alpha}{2} \tan^{-1}\left(\frac{x^2 - q^2}{2qx\sin\frac{\alpha}{2}} \right) \right\}$$

where

$$q = \sqrt[4]{\frac{c}{a}}, \quad \cos\frac{\alpha}{2} = -\frac{b}{2\sqrt{ac}}, \quad \text{and} \quad b^2 - 4ac < 0$$

The ratio of the rms value output of the single degree of freedom system to the rms value of the magnitude-limited input vs the amplitude limiting levels are shown in Fig. (2.9) along with some experimental

data.

The autocorrelation function output of the single degree of freedom system can be obtained from the Fourier transform of the power spectral density

$$R_x(\tau) = 4\int_0^\infty S_x(f)\cos 2\pi f\tau\, df$$

$$= 4\int_0^\infty S_o(f)\left|H(j2\pi f)\right|^2 \cos 2\pi f\tau\, df$$

$$= \int_0^\infty \frac{4S_o(f)\cos 2\pi f\tau\, df}{\omega_n^4\left\{\left[1-\frac{\omega^2}{\omega_n^2}\right]^2 + \left(2\zeta\frac{\omega}{\omega_n}\right)^2\right\}}$$

This integral is similar to that given by Eq. (2.19), and can be evaluated in the same fashion as it was indicated earlier. Hence

$$R_x(\tau) = \frac{4S_o}{\omega_n^4}\int_0^\infty \frac{\cos 2\pi f\tau\, df}{\left\{\left[1-\left(\frac{\omega^2}{\omega_n^2}\right)^2\right]^2 + \left(2\zeta\frac{\omega}{\omega_n}\right)^2\right\}}$$

$$= 4\sigma_x^2 e^{-2\pi f_n\zeta\tau}\left[\cos 2\pi f_n\sqrt{1-\zeta^2} + \frac{\zeta}{\sqrt{1-\zeta^2}}\sin 2\pi f_n\sqrt{1-\zeta^2}\,\tau\right]$$

A schematic diagram for the power spectral density and the autocorrelation function of the single degree of freedom system is shown in Fig. (2.5).

One of the very important statistical quantities in random vibration problems is the probability function. Unfortunately, the problem, concerning the probability function of the output of the single degree of freedom system subject to magnitude-limited

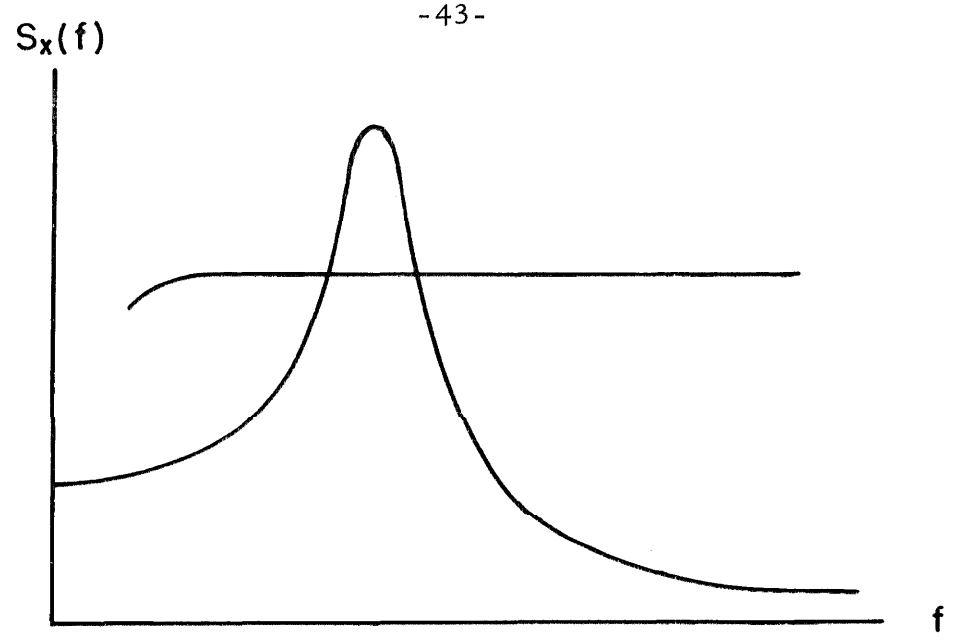

A schematic diagram for the power spectral density of a single degree of freedom system

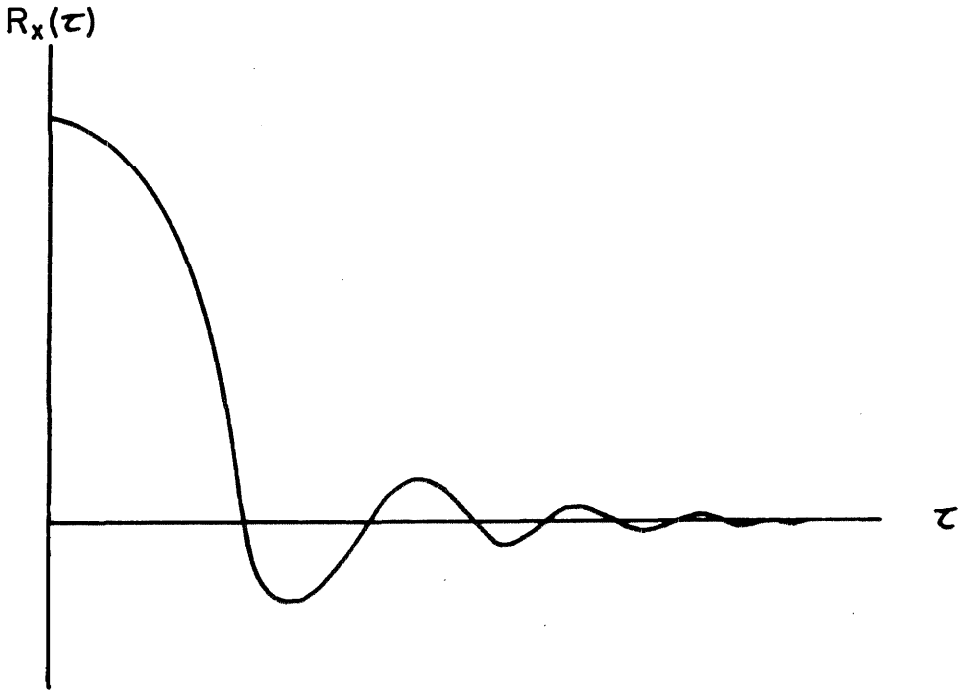

A schematic diagram for the autocorrelation function of a single degree of freedom system

Fig. 2.5

Gaussian random excitation, has not been solved. The probability function is unknown even under stationary conditions. Experimental techniques are further explored. The results are presented in the following sections.

2. 5. Experimental Investigations

This section is primarily concerned with the experimental verification of the analytic results obtained in Section (2. 3). Experiments performed on the system described in the preceding sections, and the results of these investigations are presented. An analog system is used to simulate the equation of motion for the single degree of freedom system subject to magnitude-limited random excitation (Eq. 2. 1).

The experimental results are divided into three groups: the mean square value measurements, the power spectral density measurements and the probability distribution measurements. The basic theory involved in obtaining these measurements are presented in Appendices A, B and C.

Comparisons are also made between the experimental and the analytical results whenever they are available.

2. 5. 1. Analog System

The complete analog system for a single degree of freedom system subjected to magnitude-limited broadband random excitation is shown in Fig. (2. 6). The type of instruments used are listed in Table (2. 3).

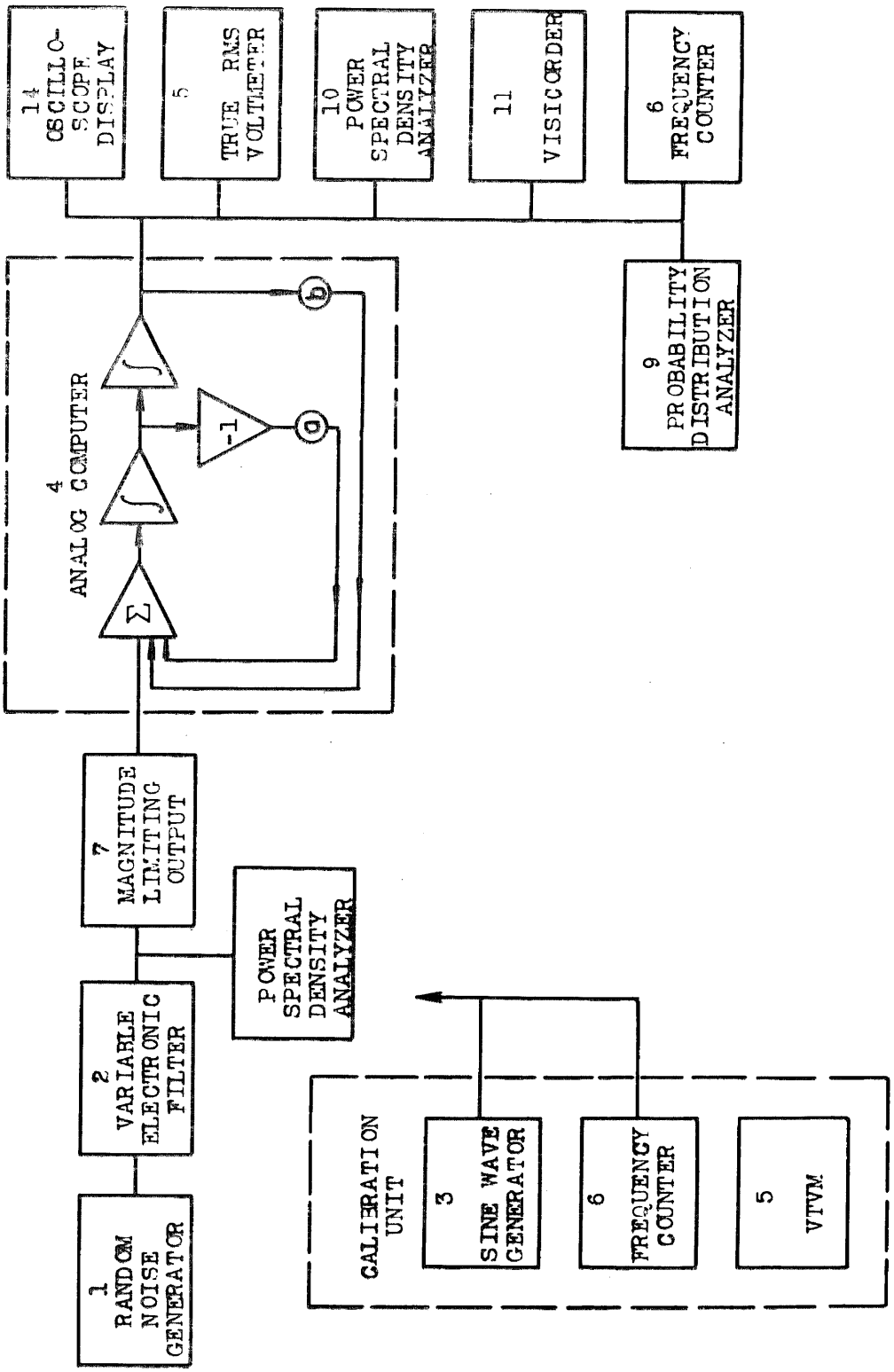

Fig. 2.6. A complete analog system.

TABLE 2. 3

Analog instruments used in the study of the response of a single degree of freedom system to magnitude-limited random excitation.

Item	Type	Manufacturer	Model Number
1	Random Noise Generator	General Radio Corp	1390B
2	Variable Filter	Krohn-Hite Corp	335
3	Sine Wave Generator	Hewlett & Packard	202B
4	Analog Manifold	Philbrick	K7-A10
5	Random Noise Voltmeter	B & K Instruments	2417
6	Frequency Counter	Beckman Instruments	7350
7	Magnitude Limiting Circuit	C. I. T. Vibration Laboratory	
8	D. C. Power Supplies	Hewlett & Packard	721A
9	*Probability Distribution Analyzer		
10	*Power Spectral Density Analyzer		
11	Visicoder	Honeywell	1508
12	Capacitors	Southern Electronics	
13	Resistors	Welwyn	
14	Oscilloscope	Tektronix	502

* Refer to Appendix (B) (C) for construction details.

To provide the analog model for the single degree of freedom system with an input, an analog voltage must be supplied to simulate the type of excitation experienced by the mechanical system. A General Radio Type 1390B Random Noise Generator is used as the source of excitation. The output voltage signal of the Noise Generator is further modified at the high frequency end by the Krohn-Hite Model 335 Variable Electronic Filter. The bandwidth of the filter can be varied in such a way as to match the frequency spectrum encountered in real situations. The filter is made up in principle by cascading 4 stages of RC filter, each of which has a 6db/octave, or a total of 24 db/octave attenuation slope at the cutoff frequency. The transfer function (the ratio of output over input) for the filter, when it is operating in low pass mode, is given by

$$\frac{1}{(1+2iA\omega\omega_o - \omega^2\omega_o{}^2)^2} \qquad (2.22)$$

when ω_o is the nominal cutoff frequency. A is the peaking factor so that the required attenuation at the cutoff frequency can be obtained. Experimental calibration (using sinusoidal input) indicates that the formula given above is correct when the peaking factor is taken to be 0.6.

Magnitude limiting of the broadband random signal obtained above is achieved by using the circuit configuration shown in Fig. (2.7). The functional relationship between the input and output of the limiter is shown in Fig. (2.2). Operational amplifiers are not included in the magnitude limiting circuit since it is found that the frequency response

characteristics are considerably improved if Zener diodes alone are used. The components involved in the magnitude limiting circuit shown in Fig. (2. 7) are two Zener diodes, a fixed input resistor and two variable d. c. power supplies. The Zener diodes are the G. E. Type (0439), having a very sharp Zener knee at -10 volts. The fixed input resistance is used to prevent loading on the preceding circuit. Two regulated variable d. c. power supplies (HP model 721A) are used primarily to allow the limiting voltage level to be set to any predetermined magnitude.

The magnitude limiting circuit is not an ideal nonlinear device. The limitations are observed to be the following.

1. An ideal sharp corner as shown in Fig. (2. 7) is impossible to achieve in practice, and it becomes worse when the signal is heavily limited.

2. The limiting level $\underline{a}$ is not in general constant, and possesses a finite but small slope.

3. Phase shifts become noticeable at higher frequencies (at about 5kc). (See the hysteretic loop shown in Fig. 2. 7.)

Even though there are some limitations in the circuitry, results obtained, as it will be shown later, have indicated that these imperfections are relatively insignificant.

The Random Noise Generator along with the Variable Filter and the magnitude limiting circuit, when connected in series, will provide the analog system with an analog voltage input which has the specified properties (see Eq. 2. 2). The analog set-up for the single degree of

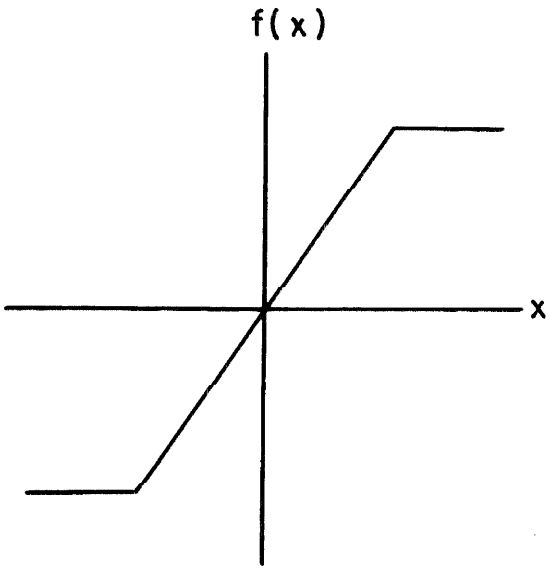

Ideal limiter

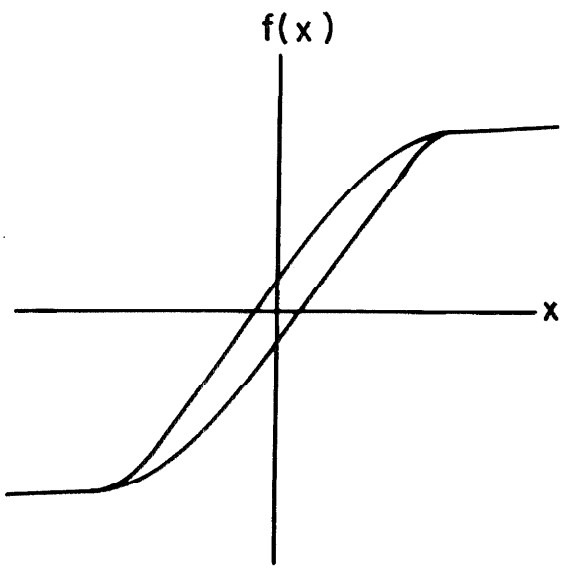

Actual limiter at high frequencies

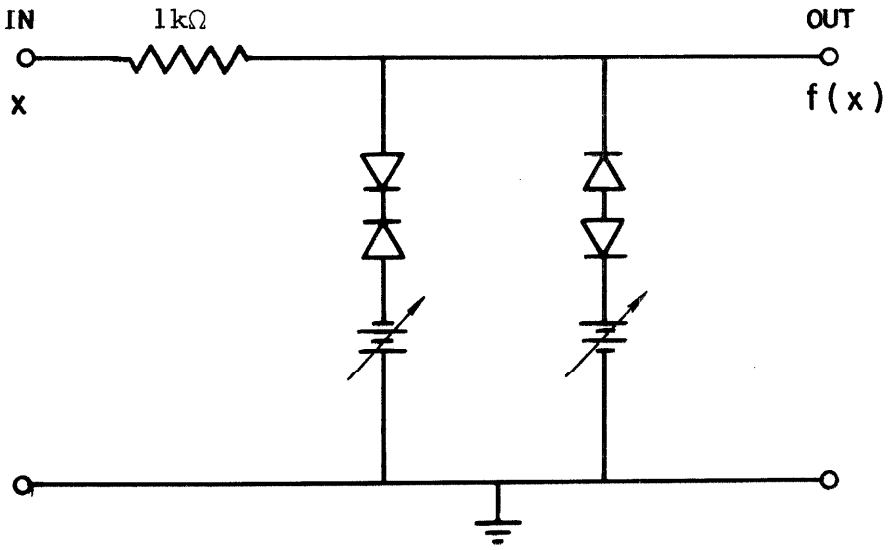

A circuit diagram for the magnitude limiter

Fig. 2.7

freedom system is discussed in Appendix A. Other specialized measuring equipment, such as the Power Spectral Density Analyzer, the Probability Distribution Analyzer, and etc., are discussed in Appendices B and C.

2. 5. 2. Experimental Procedures

The experiments are primarily designed to obtain three groups of data, namely the rms measurement, the power spectral density measurements, and finally the probability distribution measurements. With the necessary instrumentation and the calibration data, various analytical results obtained earlier can be verified. The instrument should be connected as shown in Fig. (2. 6). The operating procedures for the respective measurements are given in Appendices A, B, and C.

1. RMS value measurements.

To provide various random signals with a reference voltage, rms value measurements are made for the following types of signal:

a. The rms value σ_i of the broadband Gaussian random signal before magnitude limiting.

b. The rms value σ_o of the magnitude-limited broadband Gaussian random signal.

c. The response rms value σ_x of the single degree of freedom system (natural frequency set at 200 cps) when subjected to magnitude-limited random excitation.

2. The power spectral density measurements.

The power spectral density measurements are taken for the following types of vibration signals:

a. The Gaussian broadband random signal from the Random Noise Generator and the Variable Filter.

b. The magnitude-limited broadband random vibration signals.

3. The probability distribution measurements.

The experiments are set up to measure the probability distribution functions of

a. The broadband random signal before magnitude limiting.

b. The magnitude-limited broadband random signal.

c. The response of the single degree of freedom system subject to magnitude-limited Gaussian random excitation.

The operating mode for the Noise Generator is set at 20kc; in other words the instrument has a noise spectrum approximately uniform over a frequency range from less than 50cps to over 20kc. The signal output of the Noise Generator is not, however, symmetrically Gaussian distributed. The Krohn-Hite Variable Filter is used to reduce to effect of skewness present in the signal, and furthermore, to limit the noise signal to the desired frequency bandwidth. During the experiment, the filtered random noise signal has a nominal frequency band extending from d. c. to 10kc.

The natural frequency of the single degree of freedom system is fixed at 200cps throughout the experiment. The critical damping

ratios are set at 2%, 5%, 10%, and 20%, respectively.

2.5.3. Observations and Results

1. The quantity σ_o / σ_i, which denotes the relationship between the input and output of the nonlinear magnitude limiting circuit, is plotted against the normalized amplitude limiting level in Fig. (2.8). The agreement between the theoretical (Eq. 2.6) and the experimental results is excellent.

2. The response characteristics of the single degree of freedom system, when subjected to magnitude-limited Gaussian random excitation are shown in Fig. (2.9), where the ratio σ_x / σ_o is plotted against the normalized amplitude level a / σ_i.

It has been indicated in Section (2.4) that the response of the single degree of freedom system is closely related to the frequency spectrum of the input. The method of calculation for the response of the system was shown in Eq. (2.21). The computed results are illustrated in Fig. (2.9).

Excellent agreement between the computed and experimental data is obtained over the amplitude limiting range extending from $1\,\sigma_i$ to $3\,\sigma_i$ and beyond. The computed results show a significant departure from the experimental data when the signal is heavily limited. This is due to the fact that the series given by Eq. (2.14) is only mean convergent rather than uniformly convergent. The experimental data have shown that the ratio σ_x / σ_o is independent of the magnitude limiting level.

3. The power spectral density data for the Gaussian broadband random signal are shown in Fig. (2.10), in which the power spectral densities are normalized with respect to the value S_o, where the spectrum is approximately uniform. The hump appearing at the cutoff frequency is due to the characteristics of the Variable Filter (see Eq. 2.22).

4. The power spectral density analysis for the magnitude-limited broadband Gaussian random signal is presented in Fig. (2.11), where several power spectral density curves, representing different magnitude limiting levels, are illustrated. The actual power spectral densities are normalized with respect to the value S_o, which has already been defined in (3).

Although there are no theoretical calculations to back up the experimental data shown in Fig. (2.11) (due to the difference in the assumed theoretical and experimental spectra shapes near the cutoff frequency), the agreements between the computed results shown in Table (2.1), (2.2) and the experimental data are excellent in places where the spectrum is flat. These results are presented in Fig. (2.12), where the experimental data are compared with the theoretical power spectra having sharp cutoffs (Eq. 2.12), and Fig. (2.13), where the experimental data are compared with the exponential power spectra (Eq. 2.15).

5. No attempt has been made to analyze the spectrum of the response of a single degree of freedom system, since the power spectral densities in the vicinity of the system resonant frequency are

found to change so rapidly that it is usually impossible to measure the output of an analog filter accurately.

6. The probability distribution data for the broadband random signal are presented in Fig. (2.14) on a probability paper. The ordinates have been normalized with respect to their own rms value σ_i. It is essentially a straight line; in other words the broadband random signal is indeed Gaussian distributed in probability.

7. The probability distribution data for the magnitude-limited broadband random signal is shown in Fig. (2.15), where the results are presented for several magnitude limiting levels. The ordinates have been normalized with respect to the rms value σ_i of the broadband random signal.

8. The effects on the probability distribution of the response of the single degree of freedom system subject to magnitude-limited Gaussian broadband excitation are illustrated in Figs. (2.16) and (2.17), where the ordinates have been normalized with respect to its own rms value σ_x. It is found, within experimental capability, that magnitude limiting on the input broadband random signal has little effect on the probability distribution of the instantaneous values of the response of a single degree of freedom system if the damping present in the system is small. Experiments were carried out for the cases where the critical damping ratios of the system are 2% and 5%, respectively. The response of the system is found to be Gaussian up to $3\sigma_x$ level even though the input to the system is heavily magnitude-limited (down to $0.2\ \sigma_i$). For systems with more damping, the situation is quite

different. The probability distributions of system response have the characteristics of Gaussian distribution only at the lower amplitude levels. These results are illustrated in Figs. (2.16) and (2.17) where the system critical damping ratios are fixed at 10% and 20%, respectively.

2.5.4. Estimation of Errors

There are no appreciable statistical errors involved in the estimation of the rms values of a broadband signal. The actual errors in estimating the rms values σ_i and σ_o for the broadband random signal before and after the nonlinear magnitude limiting operation are believed to be less than 1%. In essence, this is based on the concept of the variance of the error estimator[53, 54, 55]

$$\varepsilon^2 = \frac{1}{BT}$$

where T is the total time involved in the measurement, and B is the frequency bandwidth, which has been assumed earlier to cover a range of 10kc. The product value BT in this case is 10,000 if T equals one second. The corresponding error ε is therefore 1%. The validity of this estimate is based on the assumption that the measured spectrum is relatively flat within the frequency band.

For a narrow band signal on the other hand, the situation is more complicated due to the fact that the total time T involved in the measurement must be long in order that the product value BT be large. For example, if the natural frequency f_n of a single degree of freedom system is 200cps, and the critical damping ratio c/c_c of the system is

2%, the nominal frequency bandwidth B (the distance between the half power points) is given by[37]

$$B = 2c/c_c f_n = 8\text{cps}$$

in order for the estimated error to be less than 3%, the total measurement time must be more than two minutes.

The single degree of freedom system involved in the experiment has a natural frequency fixed at 200cps, and the critical damping ratio c/c_c ranging from 2%, 5%, 10%, to 20%. Their respective measurement time periods are set according to the $\varepsilon = 3\%$ error estimate criterion.

In measuring the power spectral density of a random signal the error estimate criterion is identical to that discussed above. Here again, a narrow band filter is involved. The error estimate depends on the product value BT in places where the power spectrum is changing slowly within the narrow frequency band B.

The narrow band filters used in measuring the power spectral densities have equivalent bandwidths B_{eq} ranging from 4.53 cps, 12.43cps to 31.64cps. Their respective measurement time periods T are set according to the $\varepsilon = 3\%$ error estimate criterion. In addition to this, there are other sources of error in measuring the power spectral density, such as those involved in the data interpolation through external monitoring (see Appendix B), and those involved in the determination of the equivalent bandwidth, B_{eq}, and etc. The total accumulative errors are estimated to be around 5%.

The only uncertainty factor in measuring the probability

distribution function of a random signal is the total time T involved in the measurement (see Appendix C). In the course of the experiment, the total time T required for an accurate measurement is specified according to the repeatability of the successive data readings. It is found that the time T depends critically on the magnitude of the amplitude level, at which the measurements are taken. More time is required if the measurements are taken at a higher amplitude level, since the signal makes only infrequent passes at this level. Therefore, the data points taken in excess of the $3\sigma_x$ level are not accurate unless one is willing to wait for many hours or even days. In general, the uncertainty errors in the probability distribution measurement are found to be less than 2% within the amplitude range $|A| < 3\sigma_x$.

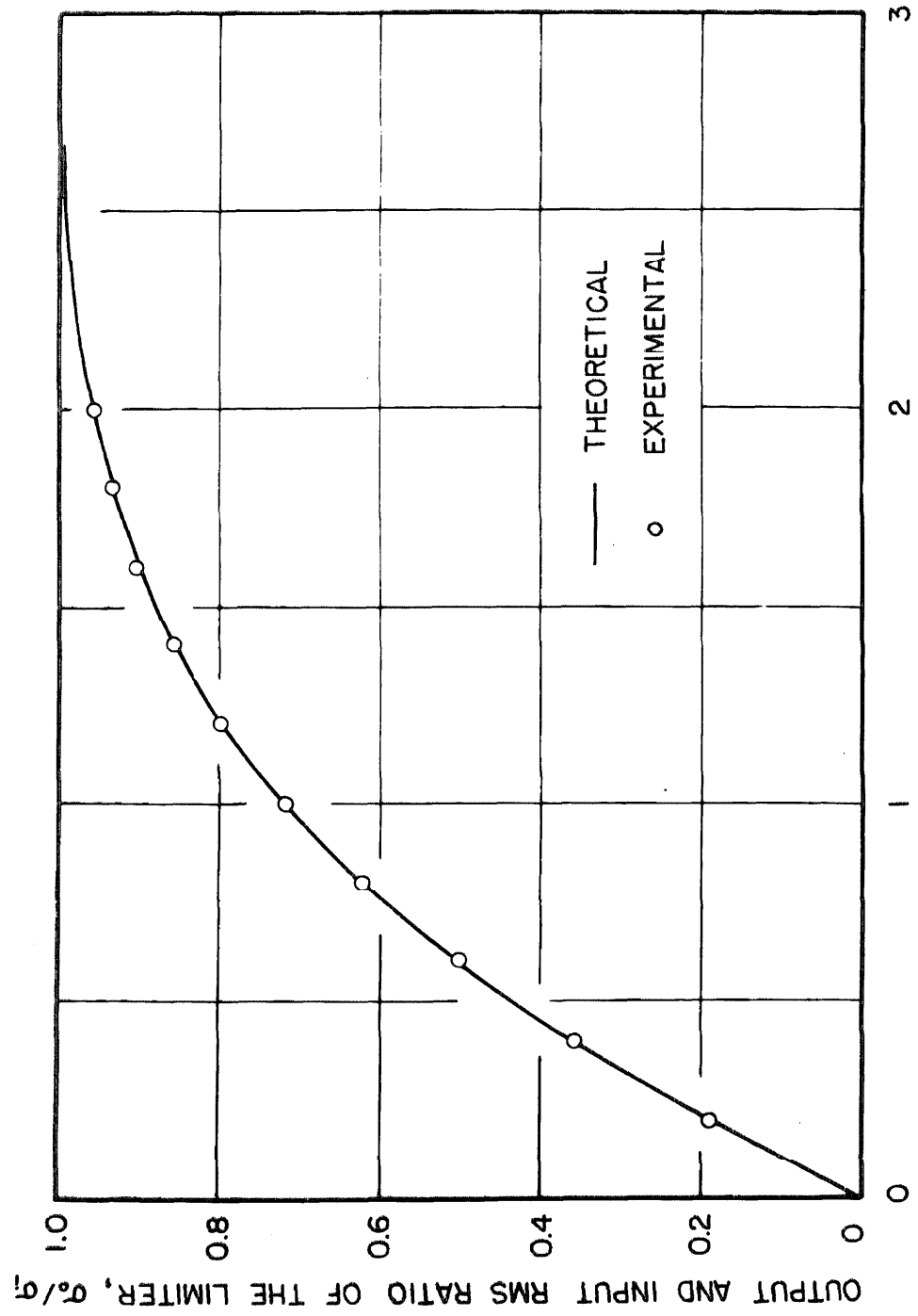

Fig. 2.8. The output and input rms values of the magnitude limiter.

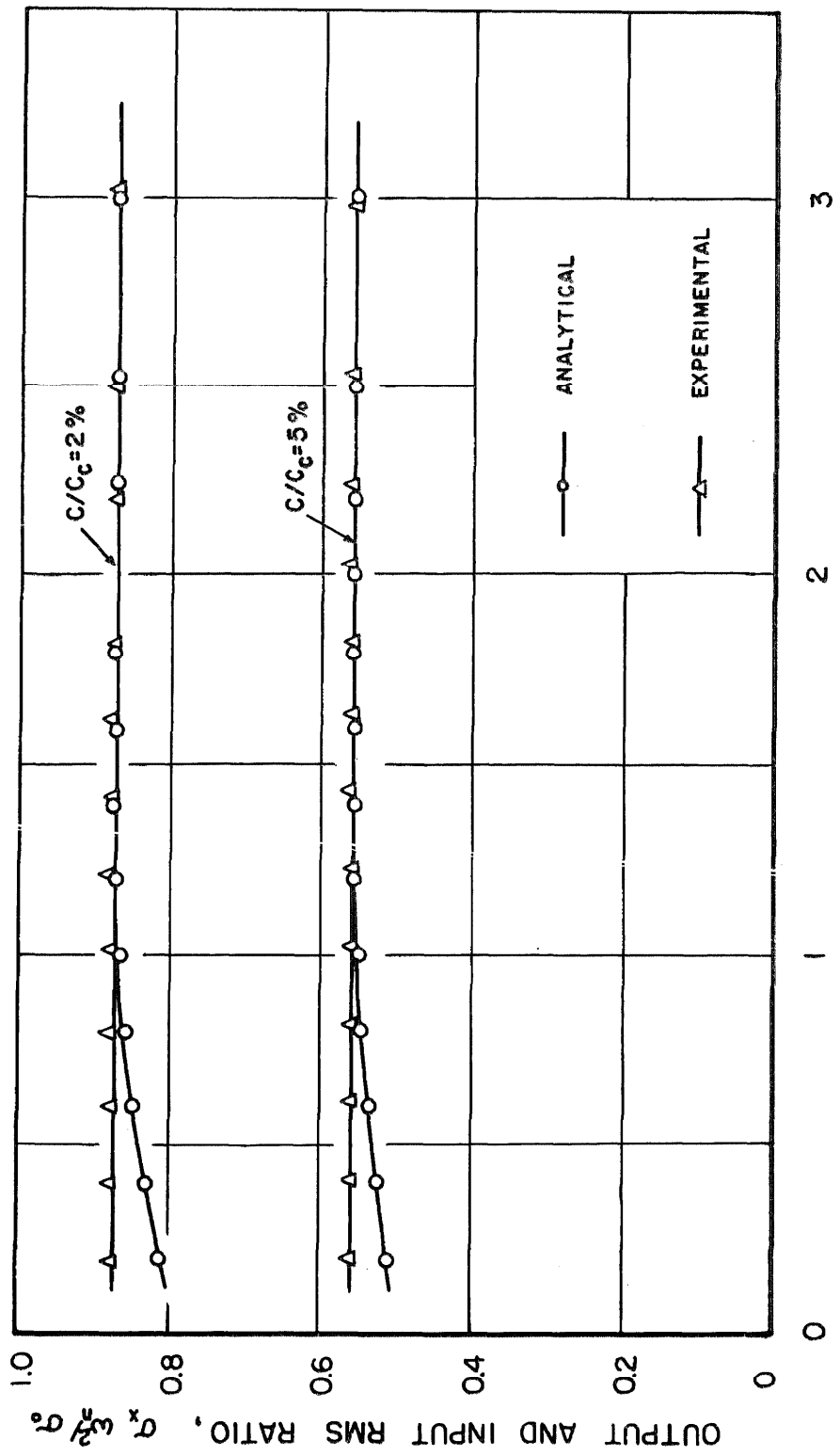

Fig. 2.9. The output and input rms ratios of single degree of freedom systems subject to magnitude-limited excitation.

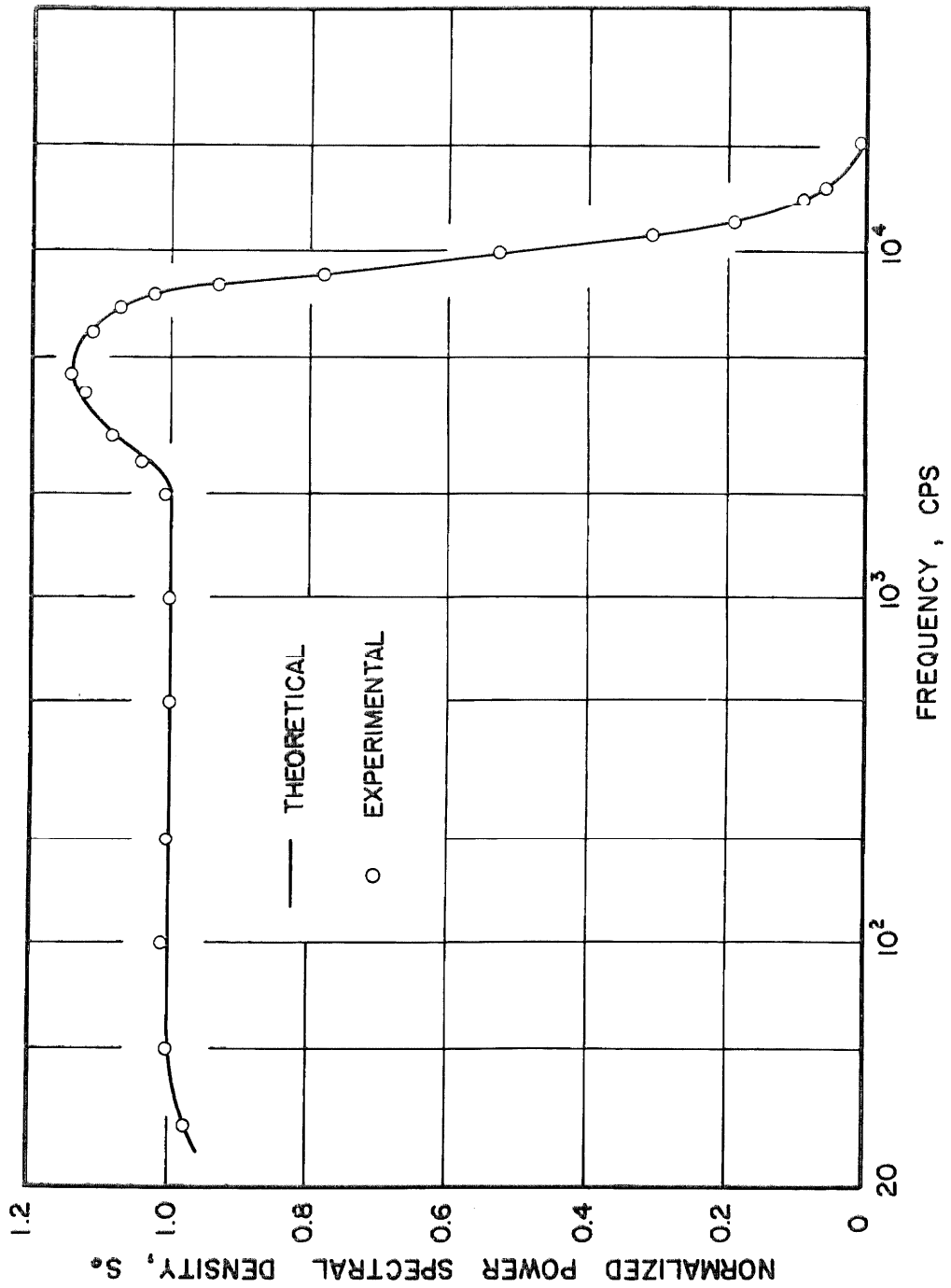

Fig. 2.10. Power spectral density of a broadband random signal.

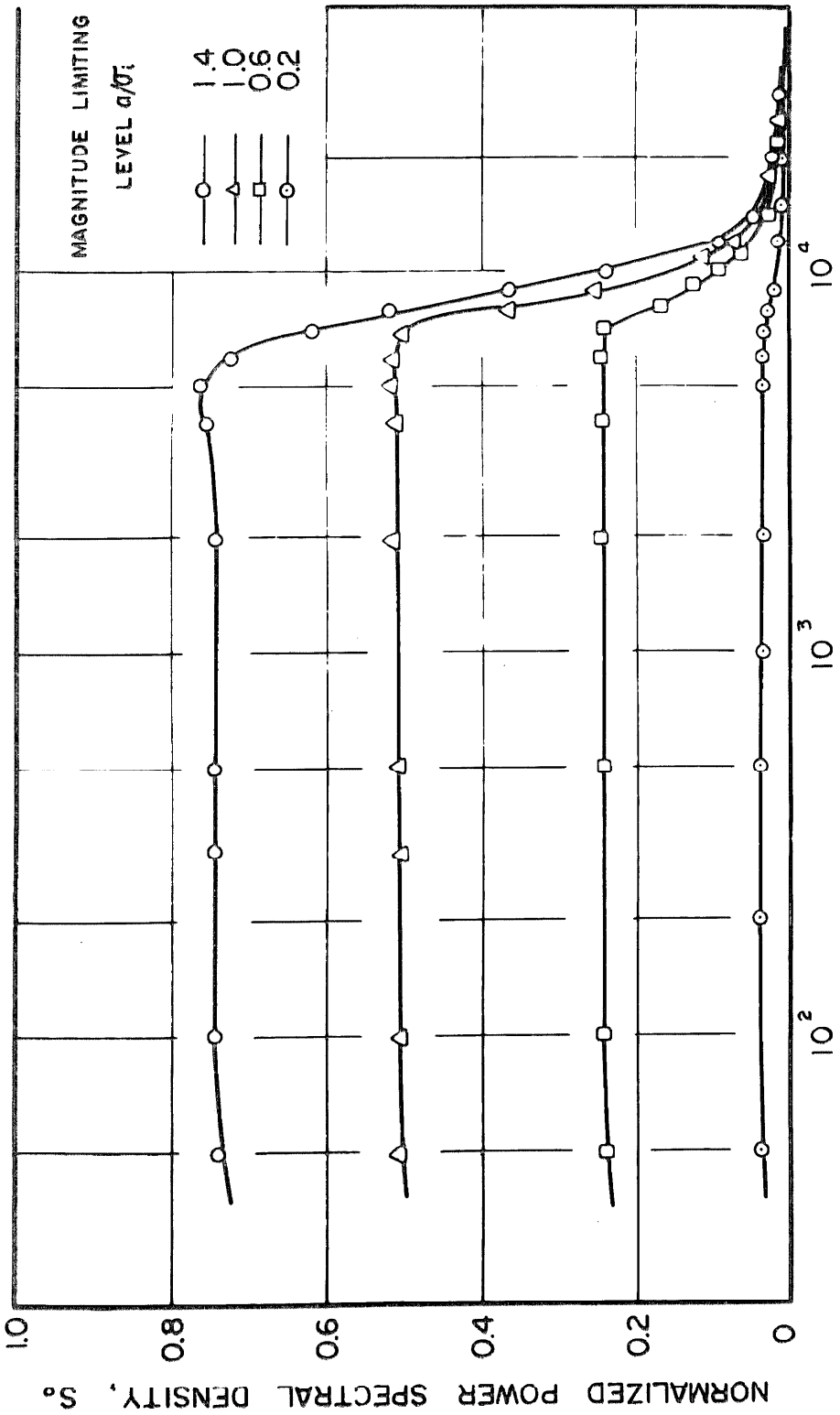

Fig. 2.11. Power spectral density of the magnitude-limited broadband random signal.

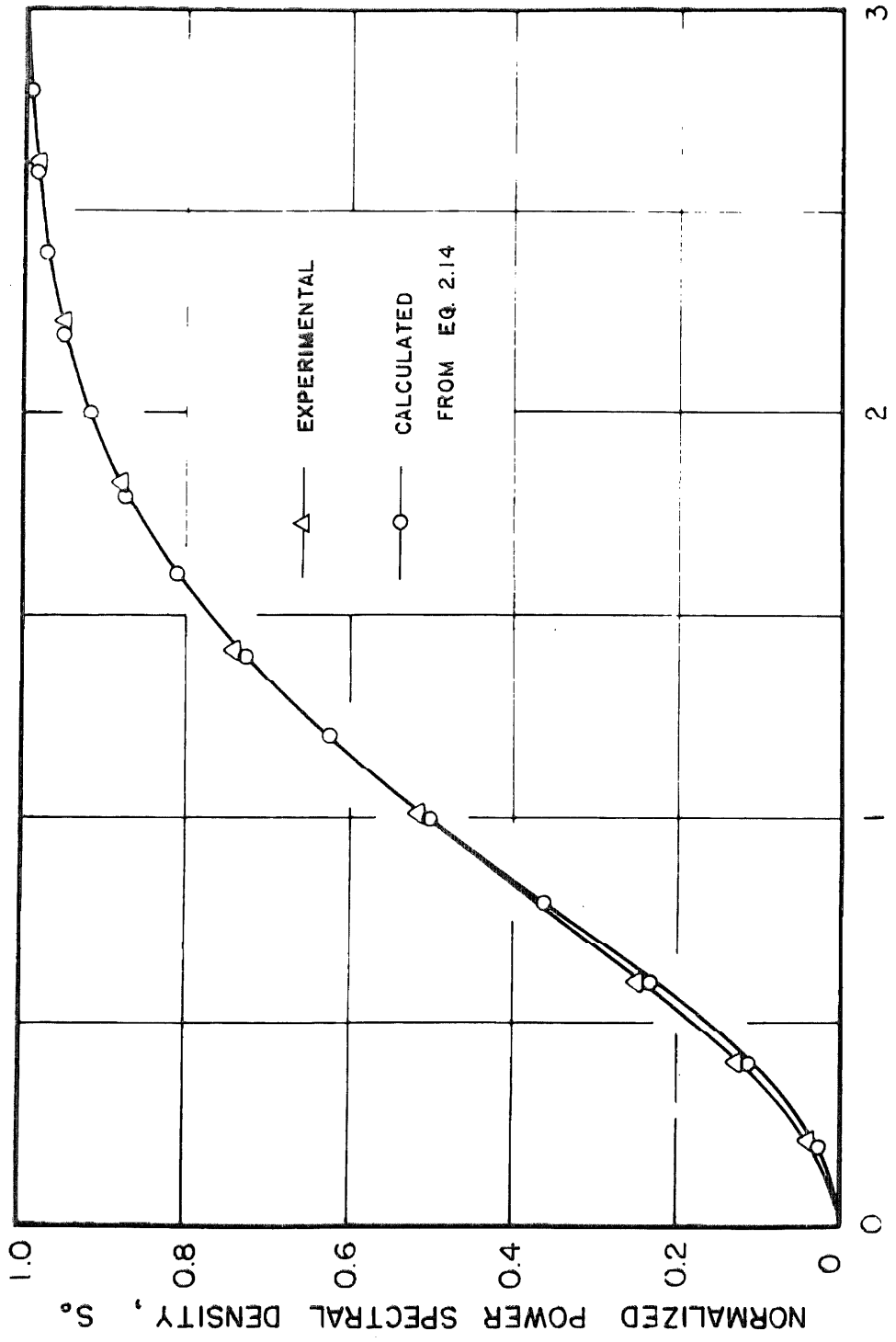

Fig. 2.12. Comparison of the theoretical and experimental power spectral density in places where the spectrum is approximately uniform.

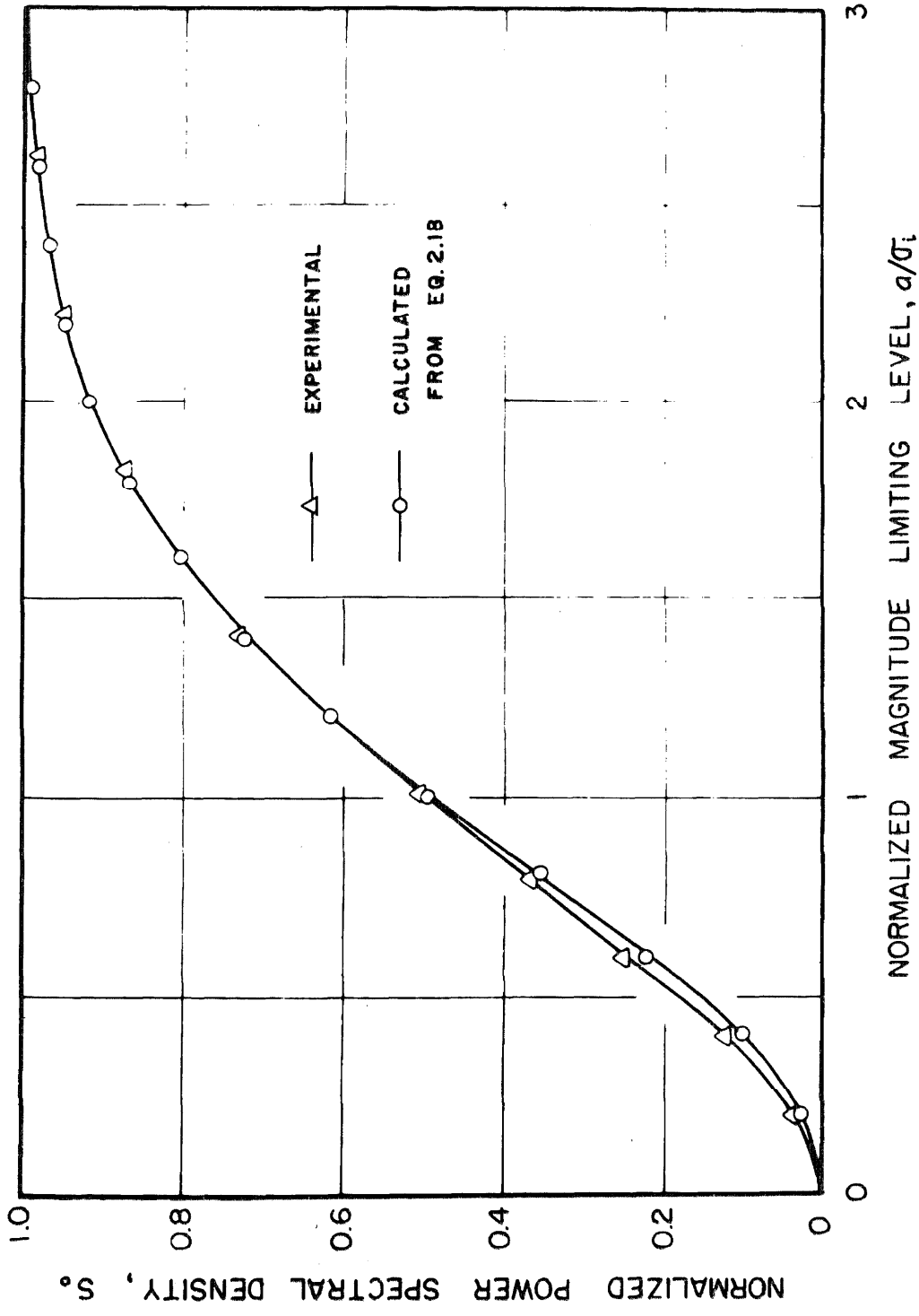

Fig. 2.13. Comparison of the theoretical and experimental power spectral density in places where the spectrum is approximately uniform.

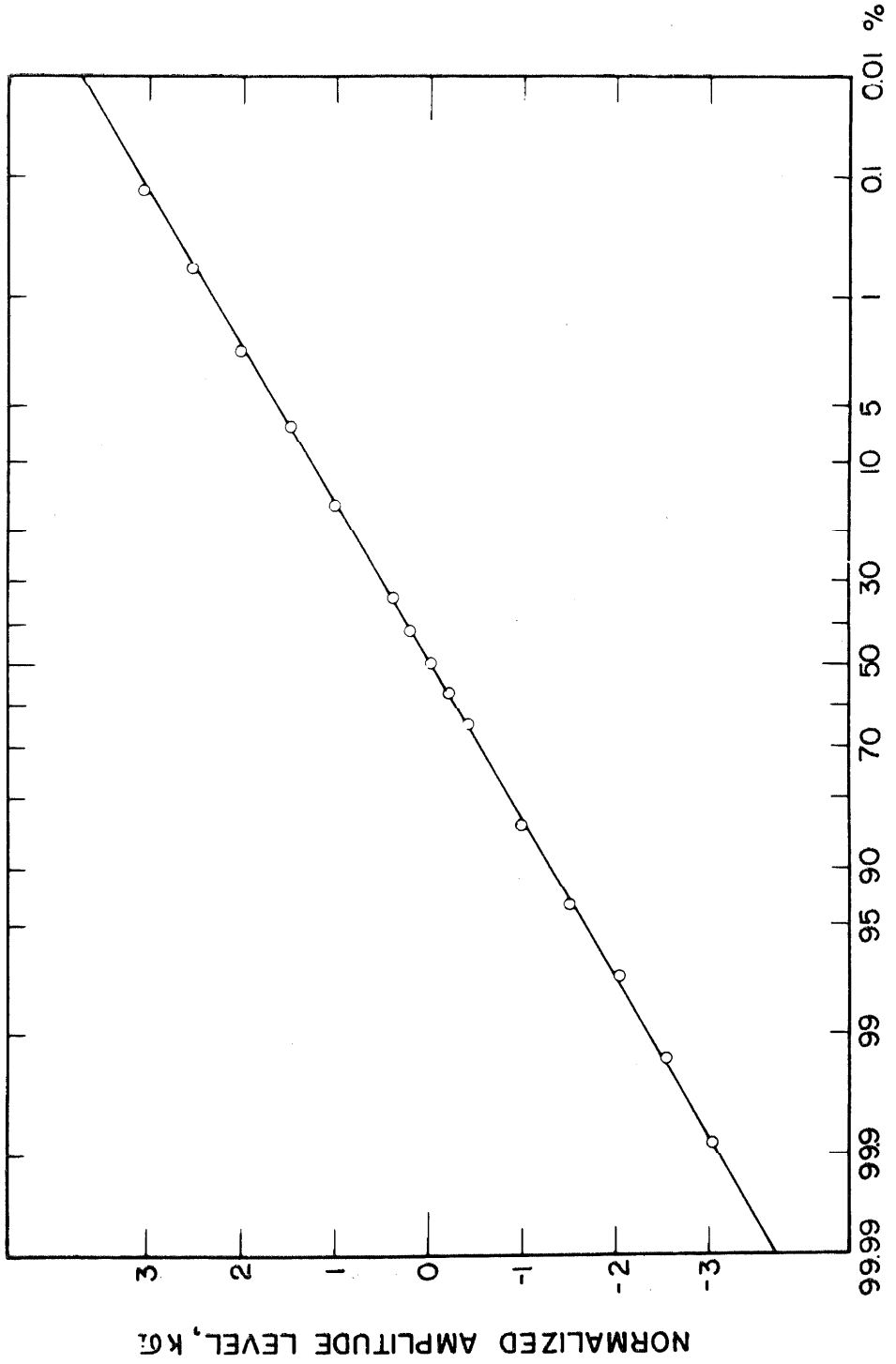

Fig. 2.14. Probability distribution of the broadband random signal.

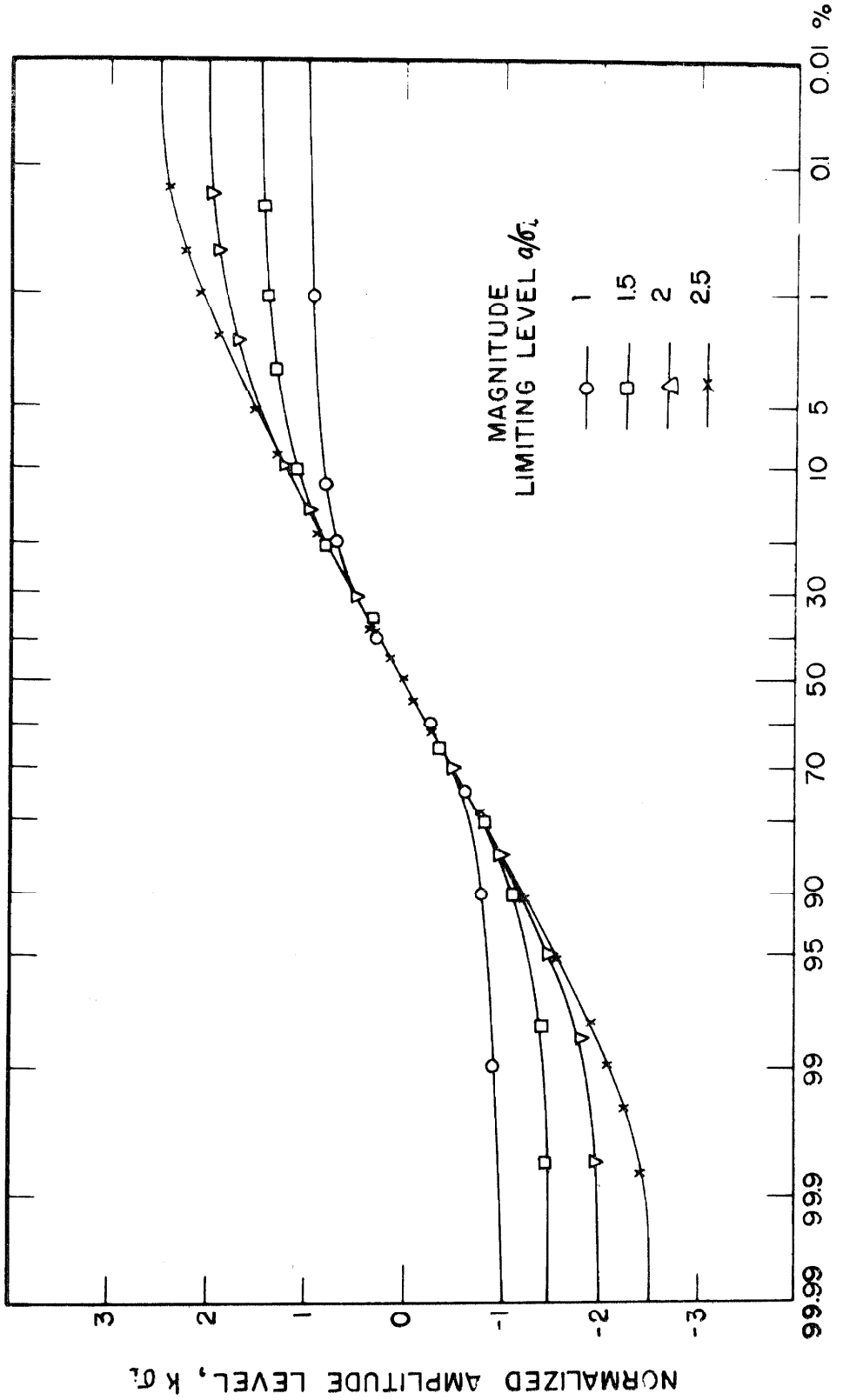

Fig. 2.15. Probability distribution of the magnitude-limited broadband random signal.

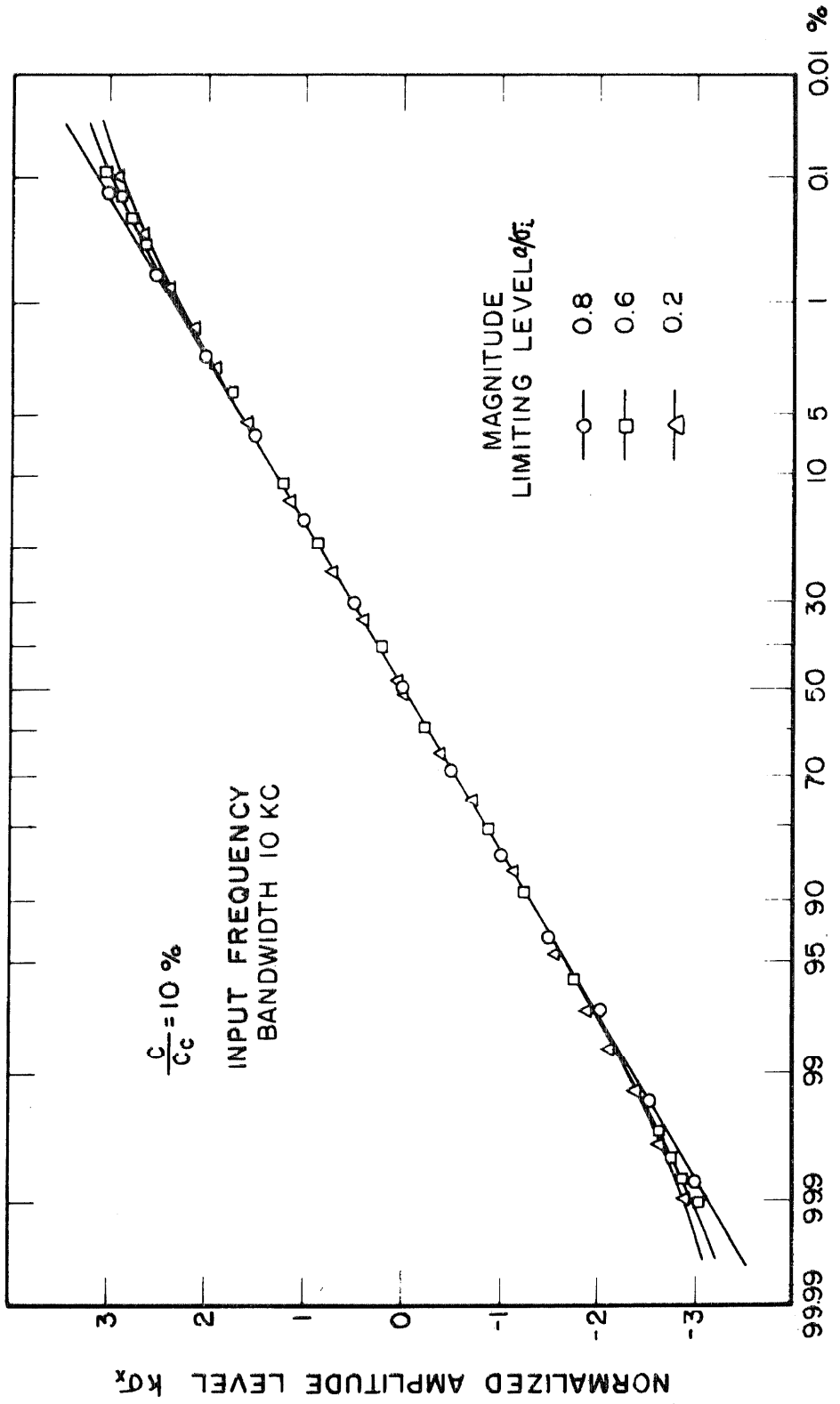

Fig. 2.16. Probability distribution of the response of single degree of freedom systems subject to magnitude-limited excitation.

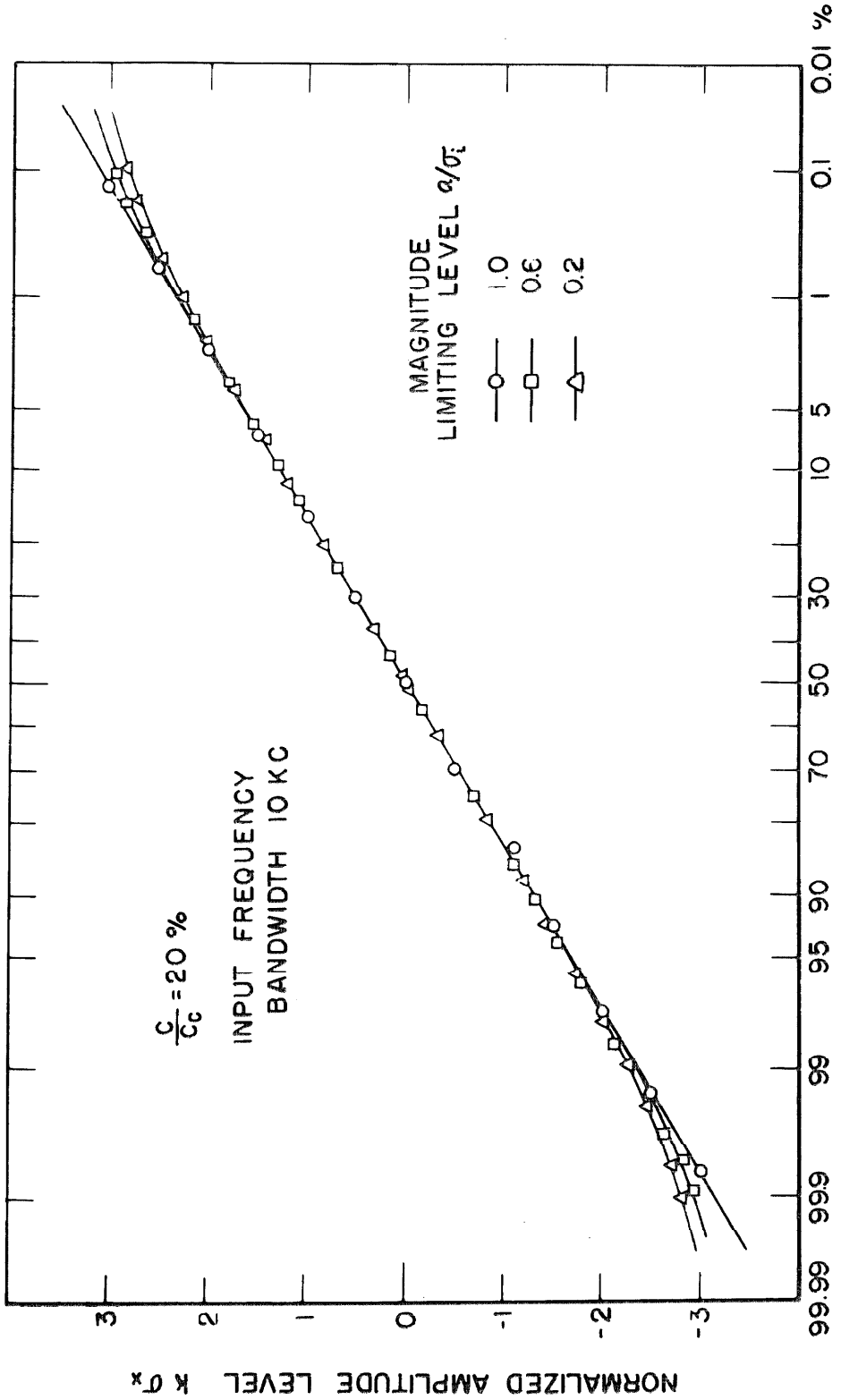

Fig. 2.17. Probability distribution of the response of single degree of freedom systems subject to magnitude-limited random excitation.

CHAPTER III

PEAK CHARACTERISTICS OF THE RESPONSE OF LINEAR SYSTEMS TO BROADBAND RANDOM EXCITATION

3. 1. Introduction

The theory of random vibration has been developed in the preceding chapters. In particular, the way in which statistical properties of a linear vibratory system depend on the source of excitation has been discussed. The response of the system may represent stresses or strains in a structure. It would be highly desirable then to know the reliability of such a structure in the randomly excited environment. In other words, a statistical quantity must be found to provide a satisfactory description of the failure mechanism. This is the primary motivation for the studies of the peak characteristics in a linear system.

There are several failure criterions commonly used by a design engineer. First of all,the well-known first passage time problem, which is mainly concerned with the probability that the random variable x(t) starting from the value $x=x_0$ reaches the value $x=x_1$ for the first time in a given time T. Many types of equipment fail the first time that x(t) reaches the fixed amplitude level x_1. The mathematical difficulties associated with this problem have been indicated by Wang and Uhlenbeck.[2] Secondly, the failure may also occur when the equipment involved stays above a certain fixed amplitude level over a prespecified fraction of the total time. Mathematically,it is a simple matter to relate the failure condition to the probability distribution of

instantaneous values. Lastly, but most important of all is the concept of cumulative damage proposed by Miner and others.[35-38] It assumes that the damage accumulates linearly, so that if a structure is subjected to n_i stress reversals at the level s_i, the partial damage is $s_i/N(s_i)$, where $N(s_i)$ is the total number of stress reversals necessary for the equipment to fail at the stress level s_i. The cumulative damage D is given by

$$D = \sum \frac{n_i}{N_i(s_i)} \tag{3.1}$$

with equipment failure occurring at D=1.

Miner's hypothesis of fatigue damage could be directly applied to the cases where random stress patterns are involved, since it does not require a knowledge of the temporal sequence of loading. In the application of Miner's rule to fatigue problems in random vibration, the knowledge of peak distribution is required in the estimate of fatigue failure in a structure. Past studies of fatigue life are restricted to a stress time history, whose peaks are distributed according to the Rayleigh distribution, and recent efforts[37, 38] have been made to study the fatigue failure for the structure with stress time histories which are more complicated. Miner's criterion can no longer be applied in such a case since some stress peaks do not experience complete stress reversals. However, it is usually found that the stress time histories can be disintegrated into several modal components in the frequency domain. It has been suggested by Schjelderup and Galef[38] that the total stress be resolved into its

mean and alternating components; the former tends to be Gaussian distributed and the latter approaches a Rayleigh distribution. By taking into account the effect of modal participation it is hoped that the fatigue life could be estimated through the alternating component of the complex stress time histories by Miner's Rule. Much experimental and theoretical work needs to be done to substantiate this hypothesis.

From the brief discussion on fatigue failure due to random loading it is not difficult to see that knowledge of peak characteristics in a randomly excited structure with complex time histories is required. This is the subject of this chapter and it is hoped that the additional studies in the probability distribution of peaks will help to rationalize the developments in the area of fatigue.

The mathematical theoreis of the distribution of peaks have been developed by Rice in his classical paper.[3] The results can be adapted directly for engineering use, since the underlying assumptions made by Rice in the studies of distribution of peaks are that the noise or the vibration signal involved be stationary and Gaussian. These, of course, have been assumed all along in the course of investigation.

In the following sections, the attention will be first focused on the analytical treatment of the distribution of peaks, peak characteristics in a linear structure as a function of input frequency bandwidth, and the peak distribution characteristics of the combination of two narrow band vibration signals in the simulation of systems with complex time histories. Experimental studies of the peak character-

istics are performed by an analog computer. Analytical and experimental results are presented in the ensuing sections.

3. 2. Analytical Investigations

We shall consider first the general theories, which are concerned with the probability distribution of peaks or maximas of a stationary Gaussian random process. The second problem is associated with the effect on the characteristics of peaks of a linear structure when subjected to a broadband random input with variable frequency bandwidth. The third problem is concerned with the peak distribution characteristics of the combination of two narrow band random vibration signals.

3. 2. 1. General Theory

It has been pointed out that Rice has given a general formula for the probability distribution of peaks. His general equation was obtained by considering the joint probability distribution function for the displacement $x(t)$, velocity $\dot{x}(t)$, and the acceleration variables $\ddot{x}(t)$. The random vibration signal is assumed to be stationary and Gaussian. The number of peaks $N(a)$ above a certain level a is given by

$$N(a) = \int_{a}^{\infty} dx \int_{-\infty}^{0} -\ddot{x}\, p(x, \dot{x}, \ddot{x})_{\dot{x}=0}\, d\ddot{x} \qquad (3.2)$$

where $p(x, \dot{x}, \ddot{x})$ is the joint probability density function mentioned above. Since the maximas occur when the first derivative $\dot{x}(t) = 0$, and $\ddot{x}(t)$ is negative, the meaning of Eq. (3. 2) is clear. Also from

the fact that the variables $x(t)$ and $\dot{x}(t)$; $\dot{x}(t)$ and $\ddot{x}(t)$ are linearly independent (correlation coefficients identically zero), the three dimensional Gaussian probability density function is then given by

$$p(x, 0, \ddot{x}) = (2\pi)^{-\frac{3}{2}} |M|^{-\frac{1}{2}} \exp\left[-\frac{1}{2}|M|^{-1}(\sigma_2^2\sigma_3^2x^2 + 2\sigma_2^4x\ddot{x} + \sigma_1^2\sigma_2^2\ddot{x}^2)\right] \tag{3.3}$$

where

$$|M| = \sigma_2^2(\sigma_1^2\sigma_3^2 - \sigma_2^4)$$

and

$$\sigma_1^2 = E(x^2) = \int_0^\infty S_x(f)df$$

$$\sigma_2^2 = E(\dot{x}^2) = -4\pi^2\int_0^\infty f^2 S_x(f)df \tag{3.4}$$

$$\sigma_3^2 = E(\ddot{x}^2) = 16\pi^4\int_0^\infty f^4 S_x(f)df$$

$S_x(f)$ = the power spectral density of the random signal

Substitute Eq. (3.3) into Eq. (3.2) and then integrate:

$$N(a) = \frac{\sigma_3}{4\pi\sigma_2}\operatorname{erfc}\frac{\sigma_3 a}{\sqrt{2(\sigma_1^2\sigma_3^2 - \sigma_2^4)}} + \frac{\sigma_2}{4\pi\sigma_1}e^{-a^2/2\sigma_1^2}\left[1 + \operatorname{erf}\frac{\sigma_2^2 a}{\sigma_1\sqrt{2(\sigma_1^2\sigma_3^2 - \sigma_2^4)}}\right] \tag{3.5}$$

In referring to Rice's paper,[3] the expected number of zero crossings per second with positive slope is given by

$$N_o = \left[\frac{\int_0^\infty f^2 S(f)\,df}{\int_0^\infty S(f)\,df}\right]^{1/2} = \frac{1}{2\pi}\left[\frac{\sigma_2^2}{\sigma_1^2}\right]^{1/2} \qquad (3.6)$$

The expected number of peaks per second can also be obtained by letting the amplitude level a in Eq. (3.2) approach $-\infty$, hence

$$N_p = \left[\frac{\int_0^\infty f^4 S(f)\,df}{\int_0^\infty f^2 S(f)\,df}\right]^{1/2} = \frac{1}{2\pi}\left[\frac{\sigma_3^2}{\sigma_2^2}\right]^{1/2} \qquad (3.7)$$

where N_p denotes the expected number of peaks per second. The complicated expression given by Eq. (3.5) can be simplified and put in terms of the quantities N_o, N_p and the normalized displacement $z = a/\sigma_1$. Hence

$$N(z) = \frac{1}{2} N_p \operatorname{erfc}\frac{z}{k\sqrt{2}} + \frac{1}{2} N_o e^{-z^2/2}\left[1 + \operatorname{erf}\frac{N_o z}{N_p k\sqrt{2}}\right] \qquad (3.8)$$

where

$$k = \sqrt{1-(N_o/N_p)^2}$$

$$\operatorname{erf} x = \frac{2}{\sqrt{\pi}}\int_0^x e^{-t^2} dt$$

$$\operatorname{erfc} x = 1 - \operatorname{erf} x$$

N(z) = Normalized peak distribution.

The ratio N_o/N_p merits special attention in the analysis of peak distribution. Since if N_o/N_p approaches unity, Eq. (3.8) becomes

$$N(z) = \begin{cases} N_p & z \leq 0 \\ N_p e^{-z^2/2} & z \geq 0 \end{cases}$$

which can be easily recognized as the peak distribution of the Rayleigh type. This result is not surprising in the sense that if the zero crossings per unit time are approximately equal to the total number of peaks per unit time, it is a narrow band process. On the other hand if N_o/N_p approaches zero, the second term in Eq. (3. 8) vanishes and the first term becomes:

$$N(z) = \frac{1}{2} N_p \operatorname{erfc}\frac{z}{\sqrt{2}}$$

$$= N_p \left[\frac{1}{\sqrt{2\pi}} \int_z^{\infty} e^{-t^2/2}\, dt\right] \qquad -\infty < z < \infty$$

This is clearly a probability distribution of the Gaussian type.

From these limiting cases the expression given by Eq. (3. 8) can, in effect, be divided into two terms the first of which is Gaussian like and the second of which is Rayleigh like. The curves for all other possible combinations of the ratio N_o/N_p, where $0 < N_o/N_p < 1$, will always lie between a Gaussian distribution and a Rayleigh distribution (Fig. 3. 1).

3. 2. 2. Peak Characteristics of a Single Degree of Freedom System

A single degree of freedom system is employed here as the structural model in the studies of peak characteristics. This is a particularly illustrative example in that the peak characteristics of

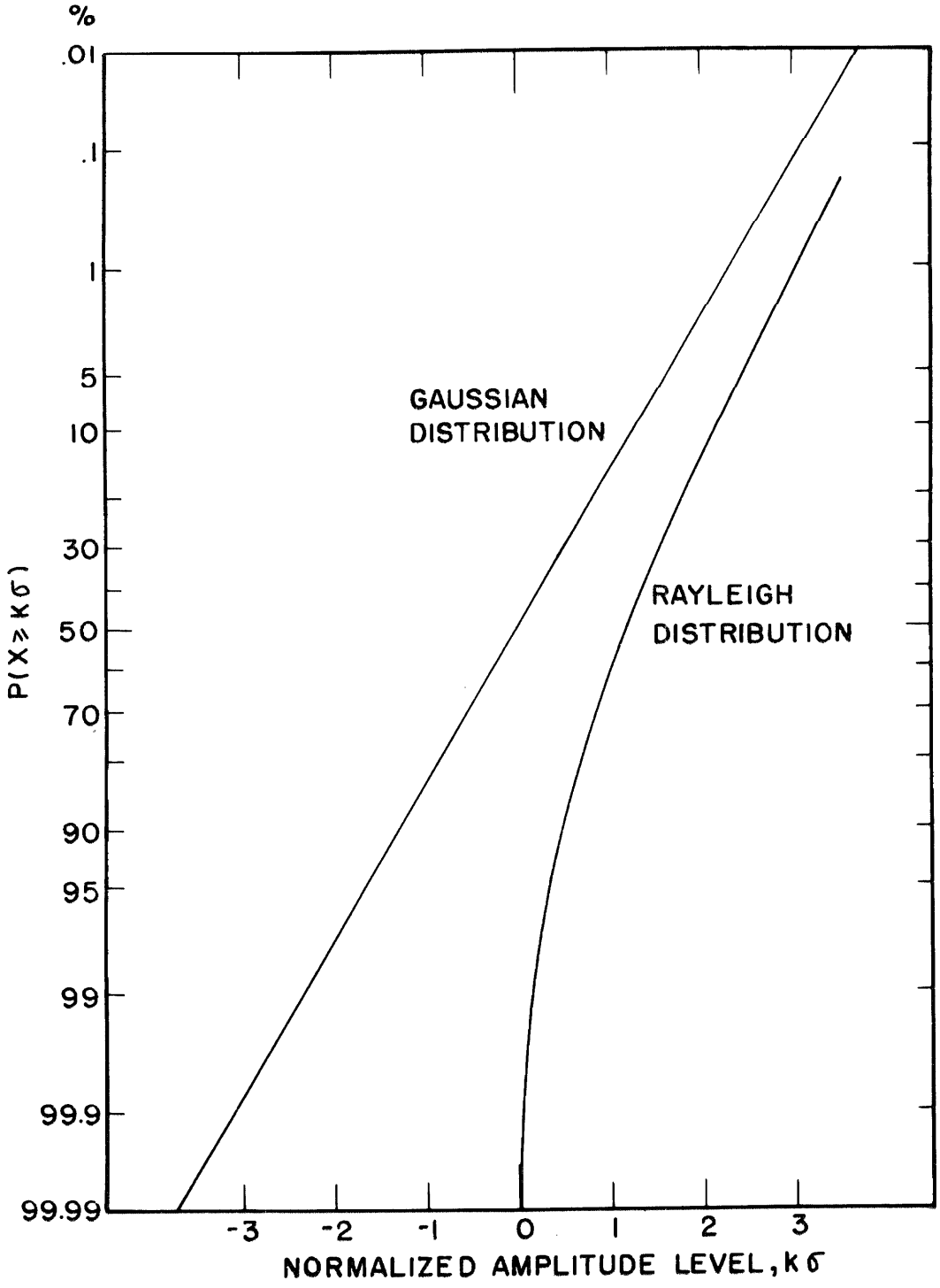

Fig. 3.1. Peak distribution of a Gaussian random signal X(t).

the single degree of freedom system show a marked change when the frequency bandwidth of the input spectrum is increased.

From Eq. (3.7) the expected number of peaks per second for the single degree of freedom system is given by

$$N_p = \frac{\int_0^\infty S_x(f)\, f^4 \left|H(j2\pi f)\right|^2 df}{\int_0^\infty S_x(f)\, f^2 \left|H(j2\pi f)\right|^2 df} \qquad (3.7)$$

where $H(j2\pi f)$ is the transfer function for the single degree of freedom system (see Eq. (2.19)), and $S_x(f)$ is the input power spectral density, which is assumed to be constant in the frequency range extending from zero to some frequencies f_o. The integral appearing in the numerator of Eq. (3.7) is divergent if f_o goes to infinity. On the other hand, however, the integral appearing in the denominator of Eq. (3.7) is well behaved and convergent.

In order to study the divergent behavior of the integral appearing in Eq. (3.7), several types of input spectrums to the single degree of freedom system are considered. First of all, let the input power spectral density be constant over the frequency range extending from zero to f_o cps and zero elsewhere, Eq. (2.12). Equation (3.7) can be reduced to

$$N_p = \left[\frac{\int_0^{f_o} f^4 S_o \left|H(j2\pi f)\right|^2 df}{\int_0^{f_o} S_o \left|H(j2\pi f)\right|^2 df}\right]^{1/2}$$

$$= f_n \left[\frac{\int_0^{f_o/f_n} \frac{x^4 dx}{x^4 - 2\cos\theta x^2 + 1}}{\int_0^{f_o/f_n} \frac{x^2 dx}{x^4 - 2\cos\theta x^2 + 1}} \right]^{1/2} = f_n \left[\frac{I_4}{I_2} \right]^{1/2} \quad (3.8)$$

where

f_n = the natural frequency of the system

x = the ratio f/f_n

$\cos\theta = 1 - 2\zeta^2$

ζ = critical damping ratio = $\sin\theta/2$

$$I_k = \int_0^{f_o/f_n} \frac{x^k dx}{x^4 - 2\cos\theta\, x^2 + 1}$$

The integral I_4 can be expressed in terms of the lower order integrals

$$I_4 = \frac{f_o}{f_n} + 2I_2 \cos\theta - I_o$$

Hence N_p is changed to

$$N_p = f_n \left[\frac{f_o/f_n + 2I_2 \cos\theta - I_o}{I_2} \right]^{1/2} \quad (3.9)$$

where I_2 and I_0 are well behaved integrals, i.e., they are convergent when the ratio f_o/f_n becomes very large, and are given respectively by

$$I_o = \int_0^{f_o/f_n} \frac{dx}{x^4 - 2\cos\theta x^2 + 1} = \frac{1}{8\cos\frac{\theta}{2}} \ln \frac{(f_o/f_n)^2 + 2\cos\frac{\theta}{2}(f_o/f_n) + 1}{(f_o/f_n)^2 - 2\cos\frac{\theta}{2}(f_o/f_n) + 1}$$

$$+ \frac{1}{4\sin\frac{\theta}{2}} \tan^{-1} \frac{2(f_o/f_n)\sin\frac{\theta}{2}}{1 - (f_o/f_n)^2}$$

$$I_2=\int_0^{f_o/f_n} \frac{x^2dx}{x^4-2\cos\theta x^2+1} = \frac{1}{8\cos\frac{\theta}{2}} \ln \frac{(f_o/f_n)^2-2\cos\frac{\theta}{2}(f_o/f_n)+1}{(f_o/f_n)^2+2\cos\frac{\theta}{2}(f_o/f_n)+1}$$

$$+ \frac{1}{4\sin\frac{\theta}{2}} \tan^{-1} \frac{2(f_o/f_n)\sin\frac{\theta}{2}}{1-(f_o/f_n)^2}$$

$$I_4=\int_0^{\infty} \frac{x^4dx}{x^4-2\cos\theta x^2+1} = \frac{f_o}{f_n} + \frac{1+2\cos\theta}{8\cos\frac{\theta}{2}} \ln \frac{(f_o/f_n)^2-2\cos\frac{\theta}{2}(f_o/f_n)+1}{(f_o/f_n)^2+2\cos\frac{\theta}{2}(f_o/f_n)+1}$$

$$+ \frac{(2\cos\frac{\theta}{2}-1)}{4\sin\frac{\theta}{2}} \tan^{-1} \frac{2(f_o/f_n)\sin\frac{\theta}{2}}{1-(f_o/f_n)^2}$$

Theoretical calculations on the expected number of peaks per second (Eq. (3.9)) with respect to the input frequency cutoff f_o are plotted in Fig. (3.6) along with some experimental data. It is readily known that the total number of peaks goes beyond bound when the ratio f_o/f_n becomes very large.

Another type of input spectrum, which is often used to approximate the power spectral density in many real situations, is given by

$$S(f) = S_o e^{-af^2} \tag{2.15}$$

where S_o is the power spectral density at d. c., and is assumed to be a constant. Equation (3.7) can be reduced to

$$N_p = \left[\frac{\int_0^\infty f^4 S_o e^{-af^2} \left| H(j2nf) \right|^2 df}{\int_0^\infty f^2 S_o e^{-af^2} \left| H(j2nf) \right|^2 df} \right]^{1/2}$$

$$= f_n \left[\frac{\int_0^\infty \frac{e^{-bx^2} x^4 dx}{x^4 - 2\cos\theta\, x^2 + 1}}{\int_0^\infty \frac{e^{-bx^2} x^2 dx}{x^4 - 2\cos\theta\, x^2 + 1}} \right]^{1/2} = f_n \left[\frac{J_4}{J_2} \right]^{1/2} \qquad (3.10)$$

where $\cos\theta = 1 - 2\zeta^2$

$$b = a f_n^2$$

$$J_k = \int_0^\infty \frac{e^{-bx^2} x^k dx}{x^4 - 2\cos\theta\, x^2 + 1}$$

Other notations are similar to those defined earlier. The integrals appearing in Eq. (3.10) can be solved by the following method. Let

$$J_0(b) = \int_0^\infty \frac{e^{-bx^2} dx}{x^4 - 2\cos\theta x^2 + 1}$$

Differentiating the integral $J_0(b)$ with respect to the variable b, we have

$$\frac{dJ_0(b)}{db} = -\int_0^\infty \frac{x^2 e^{-bx^2} dx}{x^4 - 2\cos\theta x^2 + 1}$$

$$\frac{d^2 J_0(b)}{db^2} = \int_0^\infty \frac{x^4 e^{-bx^2} dx}{x^4 - 2\cos\theta x^2 + 1}$$

Hence the integral $J_0(b)$ satisfies the following differential equation

$$\frac{d^2J_0(b)}{db^2} + 2\cos\theta\frac{dJ_0(b)}{db} + J_0(b) = \int_0^\infty e^{-bx^2}dx$$

or

$$\frac{d^2J_0(b)}{db^2} + 2\cos\theta\frac{dJ_0(b)}{db} + J_0(b) = \frac{1}{2}\sqrt{\pi/b}$$

The initial conditions are

$$J_0(0) = \int_0^\infty \frac{dx}{x^4-2\cos\theta\, x^2+1} = \frac{\pi}{4\sin\frac{\theta}{2}}$$

$$J_0'(0) = -\int_0^\infty \frac{x^2dx}{x^4-2\cos\theta\, x^2+1} = \frac{-\pi}{4\sin\frac{\theta}{2}}$$

Equation (3.10) can be solved completely in terms of the initial conditions and the convolution integral. Hence

$$J_0(b) = J_0(0)\, e^{-a\cos\theta}\cos\left[a\sin\theta\right] + \frac{J_0'(0)+ J_0(0)\cos\theta}{\sin\theta}e^{-a\cos\theta}\sin(a\sin\theta)$$

$$+ \frac{\sqrt{\pi}}{2\sin\theta}\int_0^a \frac{1}{\sqrt{a'}}\, e^{-(a-a')\cos\theta}\sin\left[(a-a')\sin\theta\right]da'$$

With the initial conditions, the following expressions are derived

$$J_0(b) = \int_0^\infty \frac{e^{-bx^2}dx}{x^4-2\cos\theta x^2+1} = \frac{\pi e^{-b\cos\theta}}{2\sin\theta}\cos\left[b\sin\theta + \frac{\theta}{2}\right]$$

$$+ \frac{\sqrt{\pi}}{\sin\theta}\, e^{-a\cos\theta}\int_0^{\sqrt{b}} e^{z^2\cos\theta}\sin\left[(b-z^2)\sin\theta\right]dz$$

$$-\frac{dJ_0(b)}{db}=\int_0^{\infty}\frac{e^{-bx^2}x^2dx}{x^4-2\cos\theta\,x^2+1}=\frac{\pi e^{-a\cos\theta}}{2\sin\theta}\cos\left[a\sin\theta-\frac{\theta}{2}\right]$$

$$+\frac{\sqrt{\pi}}{\sin\theta}e^{-a\cos\theta}\int_0^{\sqrt{b}}e^{z^2\cos\theta}\sin\left[(b-z^2)\sin\theta-\theta\right]dz$$

$$\frac{d^2J_0(b)}{db^2}=\int_0^{\infty}\frac{x^4e^{-bx^2}dx}{x^4-2\cos\theta\,x^2+1}=\frac{\pi e^{-b\cos\theta}}{2\sin\theta}\cos\left[b\sin\theta-\frac{3\theta}{2}\right]$$

$$+\frac{\sqrt{\pi}\,e^{-b\cos\theta}}{\sin\theta}\int_0^{\sqrt{b}}e^{z^2\cos\theta}\sin\left[(b-z^2)\sin\theta-2\theta\right]dz+\frac{1}{2}\sqrt{\pi/b}$$

If the above equations are substituted into Eq. (3.10) the expected number of peaks per second for the single degree of freedom system with input spectrum given by Eq. (2.15) can be computed. The results are illustrated in Fig. (3.2), where the total number of peaks is plotted against the independent variable b, which is directly related to the bandwidth of the input power spectral density. As the given quantity b decreases, the frequency bandwidth will increase correspondingly.

From the discussions made above, it is easy to see that the expected number of peaks per second is very sensitive to the bandwidth of the input spectrum. In many engineering vibration problems, however, it is often assumed that the peak distribution of a single degree of freedom system is of Rayleigh type without reference to the frequency characteristics of the input. This assumption works well

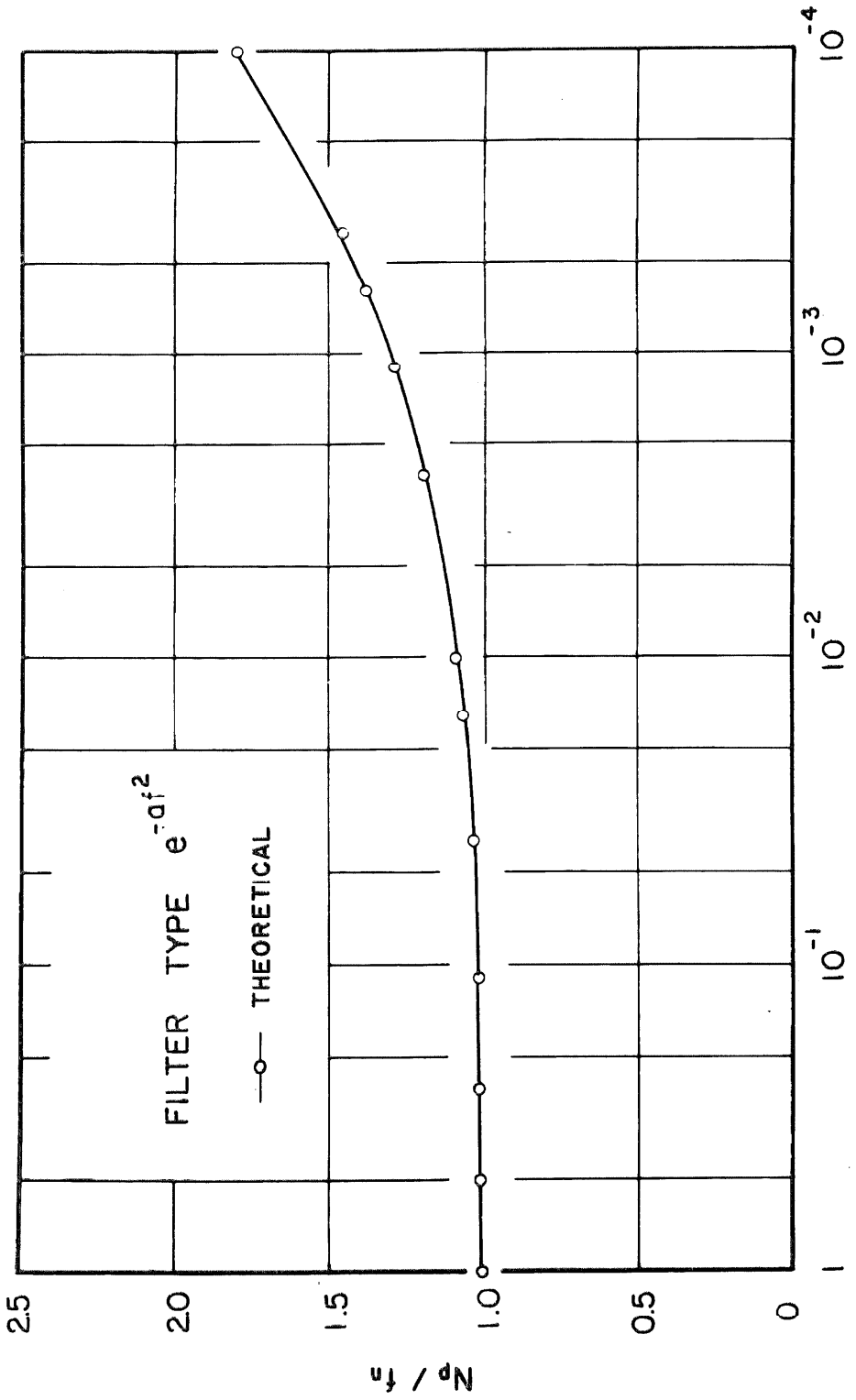

Fig. 3.2. Normalized total number of peaks per unit time of the response of a single degree of freedom system with input spectrum $\exp(-af^2)$.

as long as the bandwidth of the input spectrum is not large in comparison with the natural frequency of the system. A significant departure from the assumed Rayleigh distribution of peaks has been observed in the experiment to be described later.

3. 2. 3. Peak Characteristics for the Combination of Two Narrow Band Signals

The number of natural frequencies of vibration of a system is equal to the number of degrees of freedom. As the number of degrees of freedom increases without limit the concept of system with distributed parameters must be formed. Types of systems with infinite degrees of freedom include rods, beams, plates, and other basic structural elements. It is also common to find systems with only a finite number of degrees of freedom, for example a multi-story building where the number of structure modes equals the number of stories in the building. In any event, there are numerous examples involving system with several degrees of freedom.

In theory, a system with distributed parameters must vibrate in an infinite number of natural frequencies when subjected to a broad-band random excitation. However, this is not usually found in practice. Systems with distributed mass and elasticity usually vibrate with appreciable magnitude at only a limited number of frequencies, often at only one. For example, a simply supported beam may be found to vibrate at its lowest natural frequency (First mode), and to behave much like a single degree of freedom system.

Many other continuous systems may have two or three modal frequencies whose amplitudes at any given time are significant.

The fundamental method of solving any vibration problems for a linear system with distributed or lumped parameters is to determine the normal modes or the natural frequencies of the system. All possible vibrations of the linear system are made up of superposed vibrations in the normal modes at the respective natural frequencies. The total motion at any point of the system is the sum of the motions resulting from the vibration at each mode.

Let, for example, a two-mass system be considered as an idealized analogy of a device mounted on a chassis (Fig. 3. 3). Excitation is the broadband random vibration of the support. With regard to the failure of the device and the chassis, the relative displacements $z_1=x_1-x_o$ and $z_2=x_2-x_1$ are assumed to be significant. The differential equations of motion for the relative displacement variables $z_1=x_1-x_o$ and $z_3=x_2-x_o$ are

$$\begin{bmatrix} m_1 & 0 \\ 0 & m_2 \end{bmatrix} \begin{Bmatrix} \ddot{z}_1 \\ \ddot{z}_3 \end{Bmatrix} + \begin{bmatrix} c_1+c_2 & -c_2 \\ -c_2 & c_2 \end{bmatrix} \begin{Bmatrix} \dot{z}_1 \\ \dot{z}_3 \end{Bmatrix} + \begin{bmatrix} k_1+k_2 & -k_2 \\ -k_2 & k_2 \end{bmatrix} \begin{Bmatrix} z_1 \\ z_3 \end{Bmatrix} = -\begin{Bmatrix} m_1 \ddot{x}_o \\ m_2 \ddot{x}_o \end{Bmatrix}$$

or in a more generalized form

$$\left[M\right] \left\{\ddot{z}\right\} + \left[C\right] \left\{\dot{z}\right\} + \left[K\right] \left\{z\right\} = \left\{Q(t)\right\} \qquad (3.11)$$

where $\left[M\right]$, $\left[C\right]$, $\left[K\right]$ are the symmetrical mass matrix, damping matrix, and spring matrix, respectively, for the two degrees of freedom system. $\left\{Q(t)\right\}$ is the ground excitation applied to the system. Caughey and O'Kelly[41, 42] have shown the conditions under

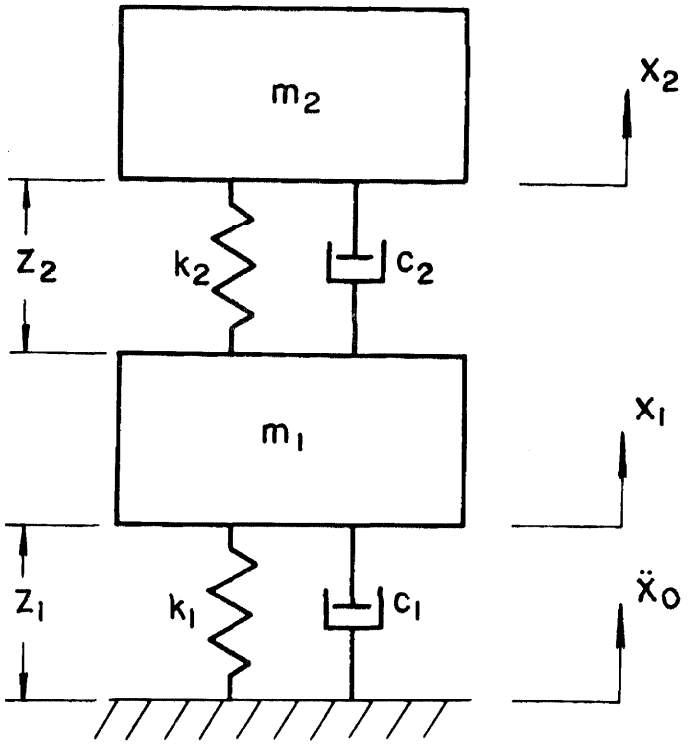

A two degrees of freedom system

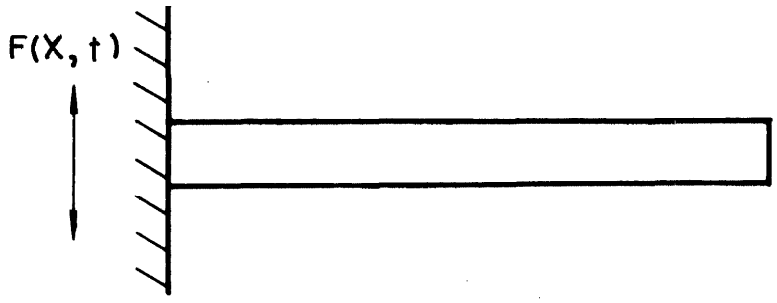

A continuous system

Fig. 3.3

which the classical normal mode solutions to Eq. (3.11) can be found. In other words, the solution is in the form

$$\{z\} = [A]\{\eta\} \tag{3.12}$$

where $\{\eta\}$ is the independent normal mode coordinate, and $[A]$ is a transformation matrix. Substituting the assumed solution into Eq. (3.11), we have

$$[M][A]\{\ddot{\eta}\} + [C][A]\{\dot{\eta}\} + [K][A]\{\eta\} = [A]\{Q(t)\}$$

Premultiply it by the transposed matrix $[A]^T$, and the following equation is obtained

$$[\bar{M}]\{\ddot{\eta}\} + [\bar{C}]\{\dot{\eta}\} + [\bar{K}]\{\eta\} = \{\bar{Q}(t)\}$$

where

$$[\bar{M}] = [A]^T[M][A] = \text{a diagonal matrix}$$
$$[\bar{C}] = [A]^T[C][A] = \text{a diagonal matrix}$$
$$[\bar{K}] = [A]^T[K][A] = \text{a diagonal matrix}$$

thus, for the two degrees of freedom system the equations of motion in normal modes are given by

$$\begin{aligned} \ddot{\eta}_1 + \beta_1 \dot{\eta}_1 + k_1 \eta_1 &= q_1(t) \\ \ddot{\eta}_2 + \beta_2 \dot{\eta}_2 + k_2 \eta_2 &= q_2(t) \end{aligned} \tag{3.13}$$

where β_1 and β_2, k_1 and k_2 are the damping and spring constants in the normal mode coordinates. The quantities $q_1(t)$, $q_2(t)$ are the random forcing functions. Hence from Eq. (3.12)

$$\begin{Bmatrix} z_1 \\ z_3 \end{Bmatrix} = \begin{bmatrix} A_1 & A_2 \\ A_3 & A_4 \end{bmatrix} \begin{Bmatrix} \eta_1 \\ \eta_2 \end{Bmatrix}$$

Since the relative displacement z_2 is given by the displacement differences $x_2-x_1= z_3-z_1$, the relative displacement variables z_1 and z_2 can be expressed in terms of the independent normal mode coordinates $\eta_1(t)$ and $\eta_2(t)$

$$\begin{cases} z_1(t) = c_1 \eta_1(t) + c_2 \eta_2(t) \\ z_2(t) = c_1 \eta_1(t) + c_2 \eta_2(t) \end{cases} \tag{3.14}$$

where $c_1 \ldots c_4$ are constants depending on system parameters.

In most cases, it is difficult to find a transformation matrix $\left[A\right]$, which will diagonalize simultaneously the symmetrical mass, spring, and damping matrices.[40, 41, 42] Nevertheless, if the damping in the system is small, the solutions to the damped system can be well approximated by the solutions to the undamped system. It is clear from Eq. (3.11) that the normal mode solutions always exist if the damping matrix $\left[C\right]$ is identically zero. Therefore Eq. (3.13) is valid for a large class of physical systems.

Similar treatments may be applied to a continuous system. Consider now an idealized beam equation

$$\frac{\partial^2 u}{\partial x^2}\left[EI \frac{\partial^2 (x,t)}{\partial x^2}\right] + \gamma\beta \frac{\partial u (x,t)}{\partial t} + \gamma \frac{\partial^2 u (x,t)}{\partial t^2} = F(x,t)$$

where

$u(x,t)$ = the displacement of the beam.

x = the distance measured along the beam.

EI = elastic properties of the beam.

β = amount damping present in the beam.

γ = mass per unit length.

The partial differential equation is solvable by separation of variables

$$u(x,t) = \sum_{i=1}^{\infty} X_i(x)\,\eta_i(t)$$

where $X_i(x)$ satisfies

$$\frac{d^2}{dx^2}\left[EI \frac{d^2 X_i(x)}{dx^2} \right] - \gamma X_i(x)\,\omega_i^{\,2} = 0$$

and $\eta_i(t)$ is the normal coordinate. Substituting the assumed solution into the beam equation, we have

$$\sum_{i=1}^{\infty} \left[\gamma X_i(x_i)\ddot{\eta}_i(t) + \gamma\beta\, X_i(x)\,\dot{\eta}_i(t) + \eta_i(t)\,\frac{d^2}{dx^2}\left(EI \frac{d^2 X_i(x)}{dx^2} \right) \right] = F(x,t)$$

with the orthogonality conditions given by

$$\int_0^L \gamma X_i(x)\, X_j(x)\,dx = 0 \qquad \text{if } i \neq j$$

$$\int_0^L \gamma X_i^{\,2}(x)\,dx = 1$$

Multiplying both sides of the equation by $X_j(x)$ and integrate along the entire length of the beam from 0 to L, the following equations are obtained

$$\ddot{\eta}_i(t) + \beta\dot{\eta}_i(t) + \omega_i^{\,2}\eta_i(t) = Q_i(t) = \int_0^L X_i(x)\,F(x,t)\,dx \qquad i=1, 2, \ldots \infty$$

Here again, the displacement variable u(x, t) is expressed in terms of an infinite number of normal coordinates $\eta_i(t)$, each of which is a solution of the single degree of freedom system.

The examples given above suggest that many complicated

physical systems, with lumped or distributed parameters, may be simulated by the combinations of a number of independent one degree of freedom systems, each of which is modified by its respective modal participation factors. The simulated approximations are good in many cases even with large damping.

Now, the response characteristics for the combination of several independent single degree of freedom systems subject to the same broadband random excitation, must be investigated. To simplify the analysis, a two degree of freedom system having two normal mode coordinates as given by Eq. (3.14) is taken as the example. The method of analysis for multi-degree of freedom systems will be essentially the same.

Let us now add $c_1 \eta_1(t)$ and $c_2 \eta_2(t)$ thereby obtaining a result corresponding to $z_1(t)$ in Eq. (3.14). Although the normal mode coordinates $\eta_1(t)$ and $\eta_2(t)$ are independent variables, they are not statistically independent in the strict sense. To study the peak characteristics of the resulting random variable $z_1(t)$, certain of its statistical properties must be investigated, namely (a) the mean square values of $z_1(t)$, (b) the autocorrelation and the power spectral densities of $z_1(t)$, (c) the probability functions and other statistical properties of $z_1(t)$.

(a) The mean square value of $z_1(t)$

Since the relative displacement $z_1(t)$ is given by

$$z_1(t) = c_1 \eta_1(t) + c_2 \eta_2(t)$$

The mean square value for the relative displacement variable is

$$E\left[z_1^2(t)\right] = c_1^2 E\left[\eta_1^2(t)\right] + 2c_1c_2E\left[\eta_1(t)\ \eta_2(t)\right] + c_2^2E\left[\eta_2^2(t)\right]$$

where from Eq. (3.13)

$$\eta_1(t) = \int_0^\infty q_1(t-u)h_1(u)du$$

$$\eta_2(t) = \int_0^\infty q_2(t-u)h_2(u)du$$

Hence

$$E\left[\eta_1^2(t)\right] = \int_0^\infty\int_0^\infty h_1(u)\ h(v)E\left[q_1(t-u)q_1(t-v)\right]dudv$$

$$= \int_0^\infty\int_0^\infty h_1(u)h(v)\ R_{11}(u-v)dudv$$

and

$$E\left[\eta_1(t)\ \eta_2(t)\right] = \int_0^\infty\int_0^\infty h_1(u)h_2(v)E\left[q_1(t-u)q_2(t-v)\right]dudv$$

$$= \int_0^\infty\int_0^\infty h_1(u)\ h_2(v)\ R_{12}(u-v)dudv$$

where

$$h_1(t) = \exp-(\tfrac{1}{2}\beta_1 t)\ \sin\ \bar{\omega}_1 t/\bar{\omega}_1, \qquad \bar{\omega}_1 = \sqrt{\omega_1^2 - \frac{\beta_1^2}{4}}$$

$$h_2(t) = \exp-(\tfrac{1}{2}\beta_2 t)\ \sin\ \bar{\omega}_2 t/\bar{\omega}_2, \qquad \bar{\omega}_2 = \sqrt{\omega_2^2 - \frac{\beta_2^2}{4}}$$

$$R_{11}(\tau) = 2DA_{11}\,\delta(\tau), \qquad R_{12}(\tau) = 2DA_{12}\,\delta(\tau)$$

and the input power spectral density is assumed to be "white" and is equal to 4D per cps. Hence

$$E\left[\eta_1^2(t)\right] = 2DA_{11}\int_0^\infty h_1^2(u)du = 4DA_{11}/(4\bar{\omega}_1^2 + \beta_1^2)\beta_1$$

$$E\left[\eta_2^2(t)\right] = 2DA_{22}\int_0^\infty h_2^2(u)du = 4DA_{22}/(4\bar{\omega}_2^2 + \beta_2^2)\beta_2$$

$$E\left[\eta_1(t)\ \eta_2(t)\right] = 2DA_{12}\int_0^\infty h_1(u)h_2(u)du$$

$$= \frac{2DA_{12}}{\bar{\omega}_1\bar{\omega}_2}\ \frac{\beta_1+\beta_2}{(\beta_1+\beta_2)^2 + 4(\bar{\omega}_1-\bar{\omega}_2)^2} - \frac{\beta_1+\beta_2}{(\beta_1+\beta_2)^2 + 4(\bar{\omega}_1+\bar{\omega}_2)^2}$$

$$\cong \frac{DA_{12}(\beta_1+\beta_2)}{2\bar{\omega}_1\bar{\omega}_2(\bar{\omega}_1-\bar{\omega}_2)^2}$$

The last approximation is made if the damping terms β_1 and β_2 are small. The cross coupling term $E\left[\eta_1(t)\ \eta_2(t)\right]$ is found to be relatively small, since

$$\frac{E\left[\eta_1(t)\ \eta_2(t)\right]}{\sqrt{E\left[\eta_1^2(t)\right]E\left[\eta_2^2(t)\right]}} = \frac{DA_{12}(\beta_1+\beta_2)}{2\bar{\omega}_1\bar{\omega}_2(\bar{\omega}_1-\bar{\omega}_2)^2}\ \frac{\omega_1\omega_2\sqrt{\beta_1\beta_2}}{D\sqrt{A_{11}A_{22}}}$$

$$= \frac{A_{12}}{2\sqrt{A_{11}A_{22}}}\ \frac{\omega_1\omega_2}{\bar{\omega}_1\bar{\omega}_2(\bar{\omega}_1-\bar{\omega}_2)^2}\ (\beta_1+\beta_2)\sqrt{\beta_1\beta_2}$$

$$= 0\left(\frac{\beta_1\beta_2}{(\bar{\omega}_1-\bar{\omega}_2)^2}\right) \qquad (3.15)$$

Thus the cross coupling terms can be neglected in the estimate of the

mean square value for the relative displacement $z_1(t)$, if the system dampings are small and the modal frequencies are well separated. Therefore

$$E\left[z_1^2(t)\right] = c_1^2\, E\left[\eta_1^2(t)\right] + c_2^2 E\left[\eta_2^2(t)\right] \tag{3.16}$$

(b) The autocorrelation and the power spectral density functions of $z_1(t)$.

The autocorrelation function for $z_1(t)$ is given by

$$E\left[z_1(t)\, z_1(t+\tau)\right] = c_1 E\left[\eta_1(t)\, \eta_1(t+\tau)\right] + c_1 c_2 E\left[\eta_1(t)\, \eta_2(t+\tau)\right]$$
$$+ c_1 c_2\, E\left[\eta_2(t)\, \eta_1(t+\tau)\right] + c_2^2 E\left[\eta_2(t)\, \eta_2(t+\tau)\right] \tag{3.17}$$

where the autocorrelation function for $z_1(t)$ is made up by the autocorrelation functions and cross correlation functions of the normal mode variables $\eta_1(t)$ and $\eta_2(t)$

$$E\left[\eta_1(t)\, \eta_1(t+\tau)\right] = \int_0^\infty \int_0^\infty E\left[q_1(t-u) q_1(t+\tau-v)\right] h_1(u) h_1(v)\, du\, dv$$

$$= \int_0^\infty \int_0^\infty R_{11}(\tau + u - v) h_1(u) h_1(v)\, du\, dv$$

$$= 2DA_{11} \int_0^\infty h_1(u+\tau) h_1(u)\, du$$

$$= \frac{DA_{11}}{\beta_1 \omega_1^2}\, e^{-\beta_1 \tau/2} \left[\cos \bar{\omega}_1 \tau + \frac{1}{2\bar{\omega}_1} \sin \bar{\omega}_1 \tau\right]$$

and

$$E\left[\eta_1(t)\ \eta_2(t+\tau)\right] = \int_0^\infty \int_0^\infty E\left[q_1(t-u)q_2(t+\tau-v)\right] h_1(u)h_2(v)\,du\,dv$$

$$= \int_0^\infty \int_0^\infty R_{12}(\tau+u-v)h_1(u)h_2(v)\,du\,dv$$

$$= 2DA_{12}\int_0^\infty h_1(u)h_2(\tau+u)\,du$$

$$= \frac{DA_{12}}{\bar{\omega}_1\bar{\omega}_2}\, e^{-\beta_1\tau/2}\left\{ \sin\bar{\omega}_2\tau\left[\frac{4(\bar{\omega}_1+\bar{\omega}_2)}{(\beta_1+\beta_2)^2+4(\omega_1+\omega_2)^2} + \frac{4(\bar{\omega}_1-\bar{\omega}_2)}{(\beta_1+\beta_2)^2+4(\bar{\omega}_1-\bar{\omega}_2)^2}\right]\right.$$

$$\left. + \cos\bar{\omega}_2\tau\left[\frac{2(\beta_1+\beta_2)}{(\beta_1+\beta_2)^2+4(\bar{\omega}_1-\bar{\omega}_2)} - \frac{2(\beta_1+\beta_2)}{(\beta_1+\beta_2)^2+4(\bar{\omega}_1+\bar{\omega}_2)^2}\right]\right\}$$

For stationary random processes the following inequality exists

$$E\left[\eta_1(t)\ \eta_2(t+\tau)\right] \leq E\left[\eta_1(t)\ \eta_2(t)\right]$$

From this inequality and Eq. (3.16), the autocorrelation coefficient ρ_{12} between the normal mode random variables $\eta_1(t)$ and $\eta_2(t)$ is given by

$$\rho_{12} = \frac{E\left[\eta_1(t)\ \eta_2(t+\tau)\right]}{\sqrt{E\left[\eta_1^2(t)\right]E\left[\eta_2^2(t)\right]}} \leq \frac{E\left[\eta_1(t)\ \eta_2(t)\right]}{\sqrt{E\left[\eta_1^2(t)\right]E\left[\eta_2^2(t)\right]}} = 0\left(\frac{\beta_1\beta_2}{(\bar{\omega}_1-\bar{\omega}_2)^2}\right) \qquad (3.18)$$

The magnitude of the cross correlation coefficient ρ_{12} is found to be very small if the system damping is small. In other words the stationary random variables $\eta_1(t)$ and $\eta_2(t)$ are only weakly correlated. For all practical purposes the cross correlation terms appearing in Eq. (3.17) can be neglected without introducing much error. Equation (3.17) is then changed to

$$E\left[z_1(t)z_1(t+\tau)\right] = c_1^2 E\left[\eta_1(t)\,\eta_1(t+\tau)\right] + c_2^2 E\left[\eta_2(t)\,\eta_2(t+\tau)\right] \quad (3.19)$$

A very important consequence resulting from neglecting the cross correlation terms is that the corresponding power spectral density function $S_{z_1}(f)$ for the relative displacement variable $z_1(t)$ can be obtained by simply adding the power spectral density functions $S_{\eta_1}(f)$ and $S_{\eta_2}(f)$ for the random variables $\eta_1(t)$ and $\eta_2(t)$, respectively. From Eq. (3.19) and the Wiener-Khintchine relationship, we have

$$S_{z_1}(f) = c_1^2 S_{\eta_1}(f) + c_2^2 S_{\eta_2}(f) \quad (3.20)$$

(c) Probability function and statistical properties of $z_1(t)$.

If the input, applied to the systems shown in Fig. (3.3), is Gaussian distributed the system output must also be Gaussian distributed. Henceforth the quantities $q_1(t)$, $q_2(t)$, $\eta_1(t)$, $\eta_2(t)$, $z_1(t)$, and $z_2(t)$ as appeared in Eq. (3.13) and Eq. (3.14) are all Gaussian distributed since they are merely linear transformations of the input random process. The probability density function for the stationary random variable $z_1(t)$ is given by

$$p(z_1) = \frac{1}{\sqrt{2\pi}\,\sigma_{z_1}} \exp - \frac{z_1^2}{2\sigma_{z_1}^2} \qquad (3.21)$$

where

$$\sigma_{z_1}^2 = c_1^2 \sigma_{\eta_1}^2 + c_2^2 \sigma_{\eta_2}^2$$

Since the random variables $\eta_1(t)$ and $\eta_2(t)$ are weakly correlated (see Eq. (3.18)), for all practical purposes they can be taken as two linearly independent random variables. Linearly independent random variables are not necessarily statistically independent. However if two Gaussian random variables are linearly independent, they are also statistically independent. Following this assumption, many simplified statistical properties for the random variables can be obtained.

Peak characteristics of the relative displacement variable $z_1(t)$, resulting from the addition of two narrow band random variables $\eta_1(t)$ and $\eta_2(t)$, are similar to those applicable to Gaussian random variables (Section 3. 2. 1). This assertion is proved by experiments, the results of which will be presented in the ensuing sections.

3. 3. Experimental Investigation

This section is primarily concerned with the experimental verification of the analytical results presented in the foregoing sections of this chapter. An analog computer is employed to simulate the system transfer function of the single degree of freedom system. Experimental techniques are also developed to measure the probability distribution of peaks of a random signal. The detailed construction of

a Peak Distribution Analyzer is presented in Appendix D.

3. 3. 1. Experimental Procedures

The main objectives of the experiments are to investigate:

1. The peak characteristics of the response of a single degree of freedom system subject to a variable band Gaussian random excitation.

2. The statistical properties of a random signal resulting from the superposition of two or more narrow band random vibration signals.

To obtain these results, a special measuring arrangement, including a General Radio Type 1390B Random Noise Generator, a Krohn-Hite Model 335 Variable Filter, a Philbrick Type K7-A10 Analog Computer, and a Peak Distribution Analyzer, is developed. The block diagram for the test set-up is shown in Figs. (3. 4) and (3. 5).

The first experiment involves the investigation of the peak characteristics of the response of a single degree of freedom system, subject to a variable band Gaussian random excitation. This is accomplished by connecting the instruments as shown in Fig. (3. 4). The natural frequency of the system is fixed at 20cps, and the critical damping ratios of the system are set at 2% and 5%, respectively. The upper cutoff frequency f_o of the random noise input can be adjusted continuously from 20cps to 20kc through the Variable Filter. This provides a convenient way to study the peak characteristics of the system as a function of the upper cutoff frequency f_o.

The second experiment involves the investigation of the

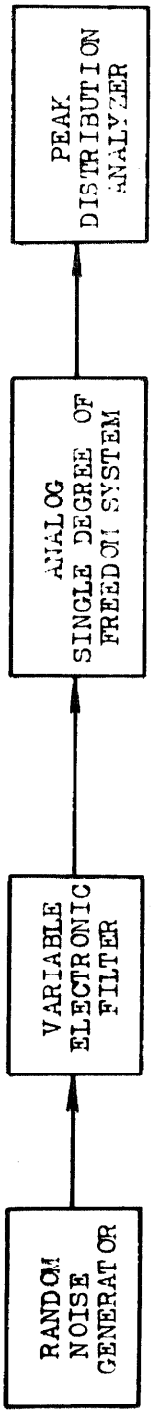

Fig. 3.4. Peak distribution measurement for a single degree of freedom system.

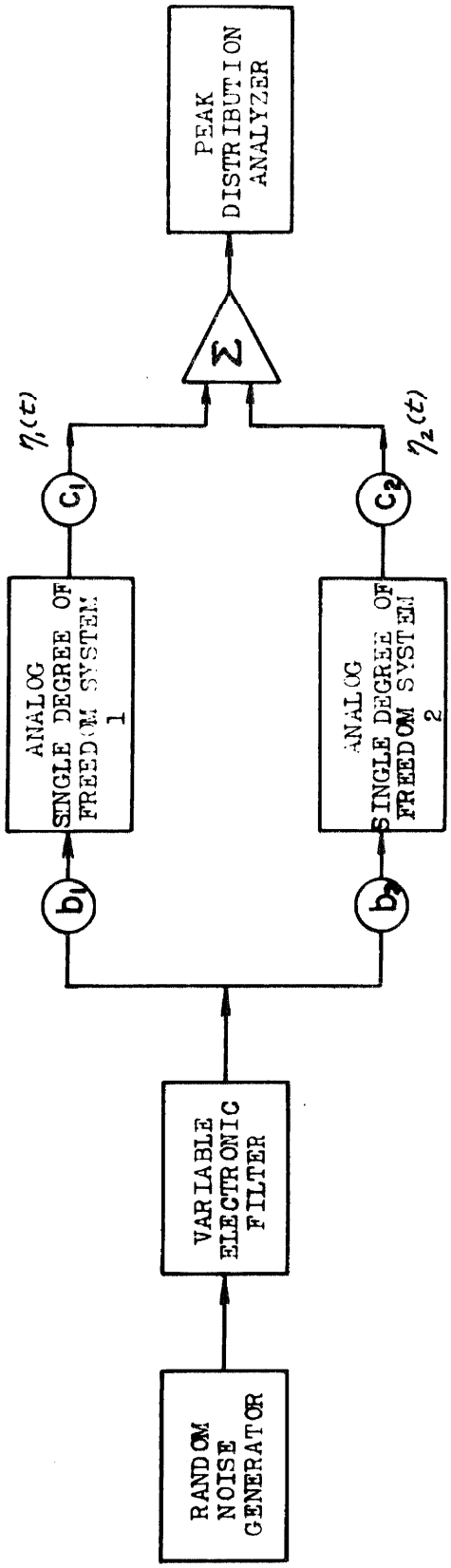

Fig. 3.5. Peak distribution measurement for two combined single degree of freedom systems.

statistical properties, in particular the peak distribution characteristics, for the combination of two narrow band random signals. The test set-up is almost identical to the previous experiment except that an additional oscillator is provided (Fig. 3.5). If the response of one oscillator is assumed to be $\eta_1(t)$ and the other one to be $\eta_2(t)$, the mathematical operations similar to that given by Eq. (3.14) can be performed through an operational amplifier (summer). In order to satisfy the condition in Eq. (3.18), only lightly damped systems, with natural frequencies sufficiently separated, are considered. The system natural frequencies used in the experiments are 80cps, 200cps, 355cps, and 500cps, respectively. The critical damping ratios for the systems are fixed at 2% and 5%.

3.3.2. Observations and Results

1. It is found, from the first experiment, that the total number of peaks per unit time N_p for the response of a single degree of freedom system depends largely on the frequency bandwidth of the input. The results are illustrated in Fig. (3.6) where the total number of peaks per second N_p, which has been normalized with respect to the system natural frequency $f_n$cps, is plotted against the ratio f_o/f_n. The frequency f_o denotes the upper cutoff frequency of the Variable Filter, operating in the low pass mode.

Excellent agreement is obtained between the analytical and the experimental results, in places where the ratio f_o/f_n is less than 100. The deviation occurs at higher values of f_o/f_n. This is because of the

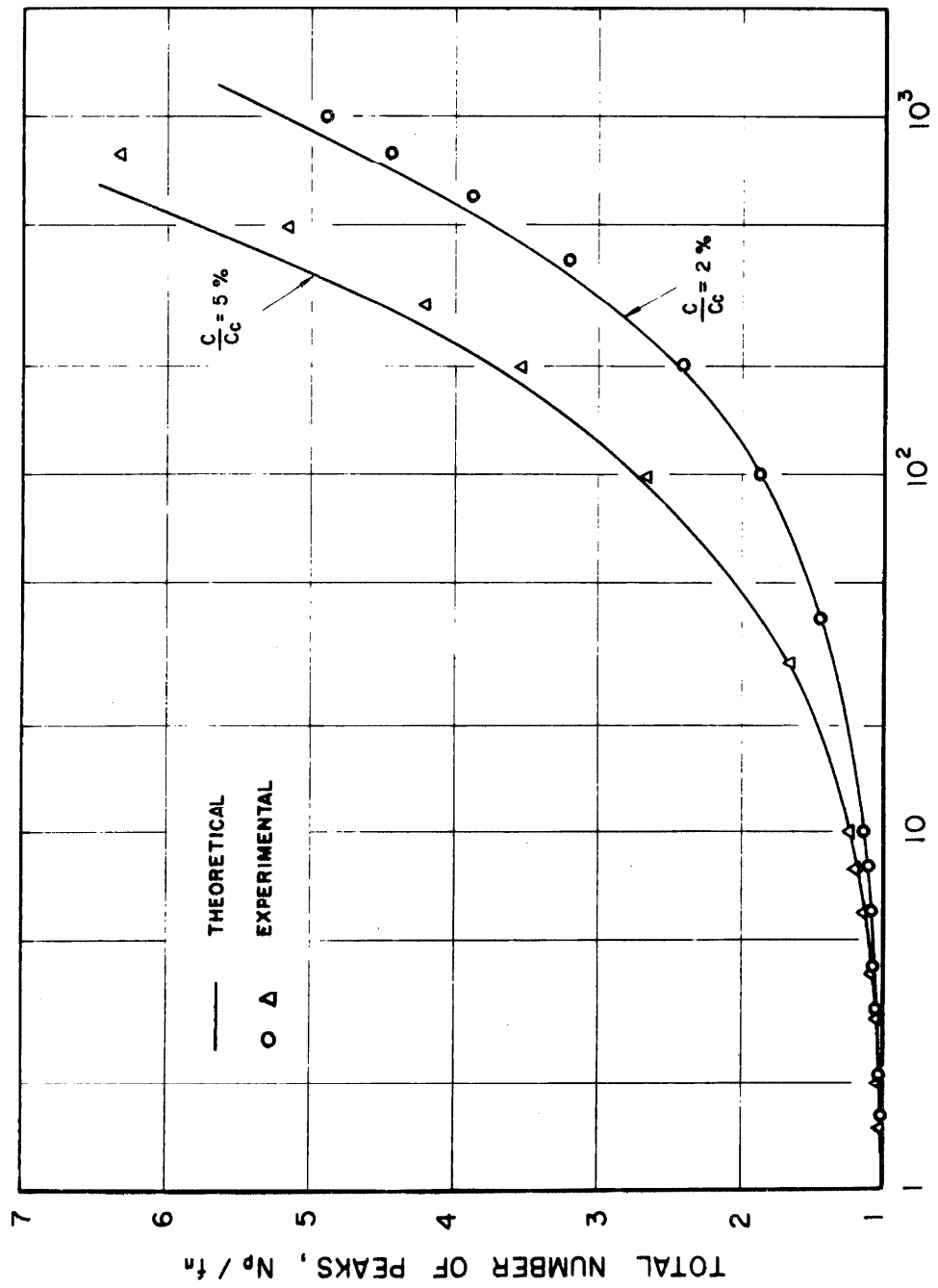

Fig. 3.6. Normalized total number of peaks per unit time of the response of single degree of freedom systems.

following reasons:

(a) The assumed theoretical spectrum (Eq. 2.12) is different from the experimental spectrum (Fig. 2.10) near the cutoff frequency f_o.

(b) The capability of the Peak Distribution Analyzer (Appendix D) in detecting the presence of small peaks is limited.

The frequency response characteristics of the differentiator (Fig. C.1) used in the Analyzer are good only for a limited range. In addition, the zero crossing detector is not sensitive to a voltage signal whose amplitude is less than 10mv. All these factors have contributed to the deviations and errors in detecting the presence of small peaks, whose number becomes increasingly large as the input frequency bandwidth increases.

Although the total number of peaks per unit time becomes a very large number when the ratio f_o/f_n increases, the response of the single degree of freedom system retains the appearance of a narrow band random signal. The excessive peaks are very small and difficult to detect. The small peaks can, however, be removed by a high pass filter. In other words the signal , in effect, consists of a mean component and an alternating component; the former is a broad-band Gaussian distributed signal and the latter is a narrow band Rayleigh distributed signal.

2. In the second experiment, the statistical characteristics of signal resulting from the superposition of two narrow band random vibration signals are investigated. The following results are obtained.

(a) It is found that the mean square values $\langle \eta_1^2(t) \rangle$, and $\langle \eta_2^2(t) \rangle$ are additive for all possible values of the constants b_1, b_2, c_1, c_2 appearing in Fig. (3. 5), if the damping present in the respective system is small and their natural frequencies are well separated (from 50cps to 100cps). Under these circumstances, Eq. (3. 20) is identically satisfied.

(b) Probability distributionsof peaks of the combined narrow band signals are found to lie in between the curves of Gaussian distribution and Rayleigh distribution. Selective results are shown in Figs. (3. 7), (3. 8) and (3. 9), where the probability distribution of peaks of the combined signal is plotted against the normalized amplitude. The combined signal is obtained by adding the properly weighted sum of the response of the respective single degree of freedom system, one of which has a natural frequency f_n=200cps, and the other f_n=355cps. The critical damping ratios are fixed at 2% and 5%. If these data are substituted into Eqs. (3. 8) and (3. 20), theoretical curves can be plotted.

The agreement between the theoretical and experimental results is good within the 3 σ_z range, outside of which it is difficult to detect the presence of peaks unless one is willing to wait for a long period of time.

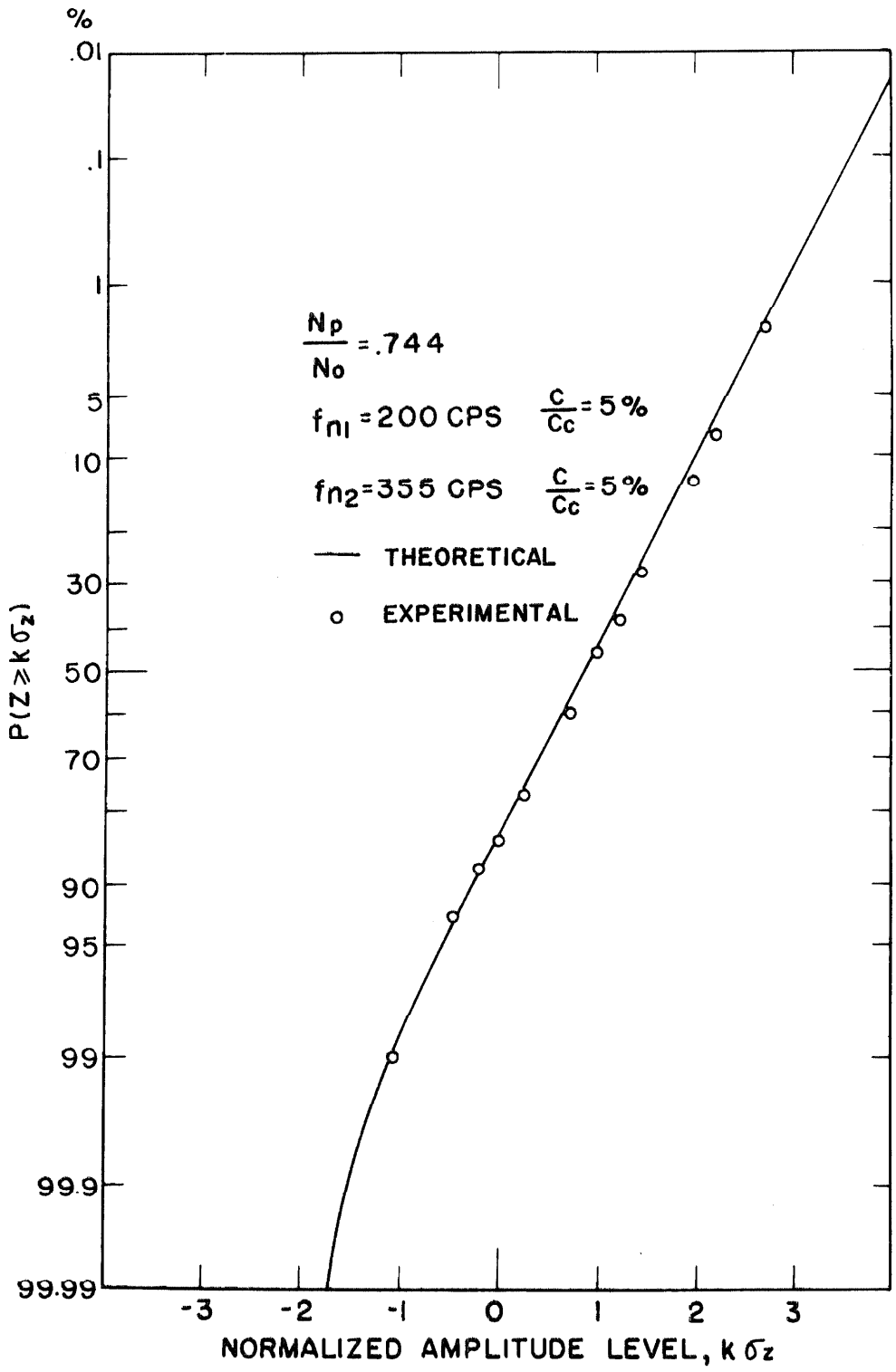

Fig. 3.7. Probability distribution of peaks of two combined narrow band signals.

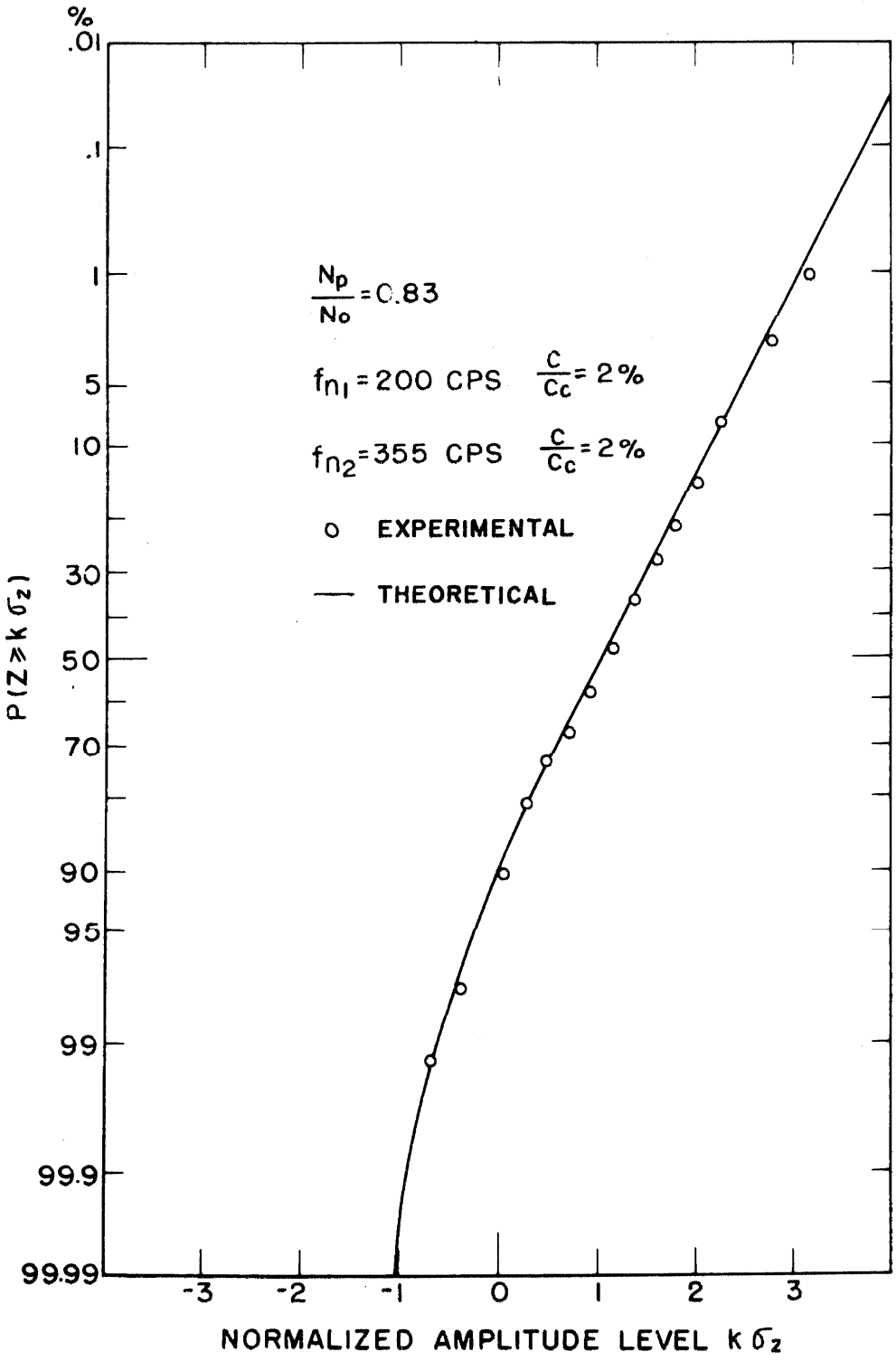

Fig. 3.8. Probability distribution of peaks of two combined narrow band signals.

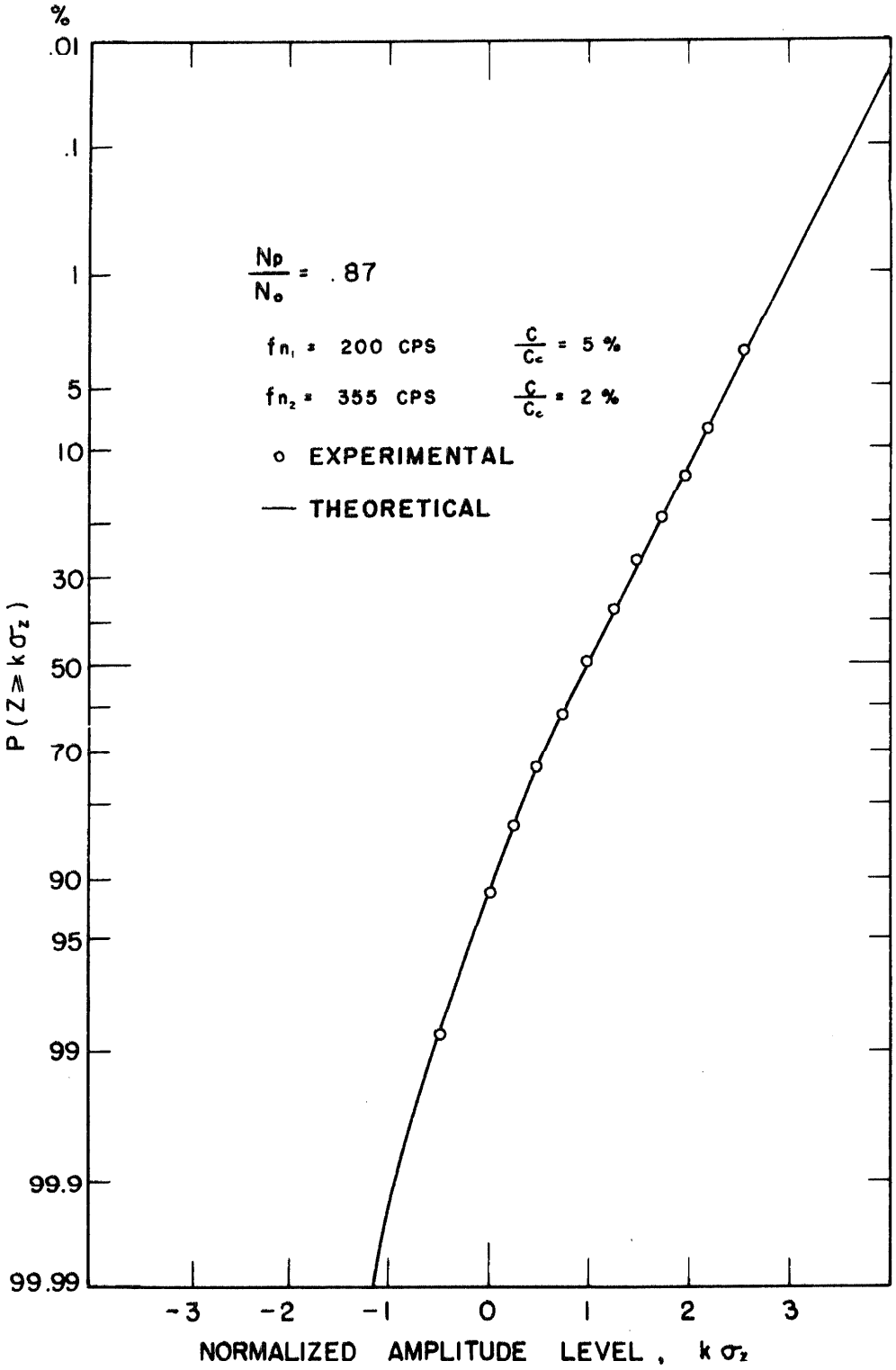

Fig. 3.9. Probability distribution of peaks of two combined narrow band signals.

CHAPTER IV

STATISTICAL PROPERTIES OF NONLINEAR SYSTEMS SUBJECT TO RANDOM EXCITATION

4. 1. Introduction

In the preceding chapters, we have considered the output statistical properties of a linear system subject to random excitation. It is not difficult to generalize the basic concepts a little further to include certain nonlinear systems as well.

For many engineering applications, especially in the field of vibration and dynamics, the probability distribution and the power spectral density function are of particular interest. In order to determine these quantities for a nonlinear system the method of Fokker-Planck or the diffusion equation method can be used, since the transition probability of a Markoff process is found to satisfy macroscopically the diffusion equation. For a nonlinear system subject to white noise excitation, the output statistical properties are completely characterized by the solutions to the Fokker-Planck partial differential equation.

A major portion of the work done in the past has been closely related to the characteristics of the stationary probability distribution functions of a nonlinear system subject to white noise excitation. This requires the solution of the Fokker-Planck equation in the stationary form. Different methods of obtaining the solution have been given by Uhlenbeck,[2] Caughey,[4-9] Crandall,[10-13] and many others. The solutions obtained are usually presented in terms of the first order

probability density function. This is, of course, no help if one is interested in the autocorrelation function and the power spectral density of the nonlinear system as well.

Caughey and Dienes[44] have derived a new method for the determination of the autocorrelation function and the power spectral density of a nonlinear system. With very little complication, they defined a generalized autocorrelation function in terms of the transition probability, which in turn is a solution of the appropriate Fokker-Planck partial differential equation. The power spectral density can then be found by means of the Wiener-Khintchine relation. This method has been demonstrated by solving a simple first order nonlinear system subject to a Gaussian white external force.

Wolaver[46] has also attempted to obtain the autocorrelation function and the power spectral density of a second order nonlinear system subject to a Gaussian white noise excitation. However, his method of analysis involves questionable boundary conditions assigned to the Fokker-Planck equation. Heretofore, the only correct solution available up to this stage remains that given by Caughey and Dienes.

A slightly different approach will be adopted in this thesis to solve the first order nonlinear system considered by Caughey and Dienes. This method is found to be very simple and can be extended to include the second order nonlinear systems as well, although the solutions are yet to be determined.

In the following sections, the analytic method of approach will

be described first. This requires the determination of the auto-correlation and the power spectral density by solving the corresponding Fokker-Planck equation for the first order nonlinear system. Experimental verifications of these results are also included.

4. 2. Relationship Between the Transition Probability and the Autocorrelation Function

It has been shown in Section (1. 4) that the autocorrelation function for a stationary random variable x(t) is given by

$$R_x(t_1-t_2) = \int_{-\infty}^{\infty}\int_{-\infty}^{\infty} x_1 x_2\, p(x_1, x_2)\, dx_1 dx_2 \qquad (4.1)$$

where

$$x_1 = x_1(t_1) \text{ and } x_2 = x_2(t_2)$$

Now, if the random process x(t) is Markoffian, the joint probability density function can be expressed in terms of the transition probability $T(x_2, t_2 \mid x_1, t_1)$ (see Eq. 1. 3). Thus

$$p(x_1, x_2) = p(x_1)\; T(x_2, t_2 \mid x_1, t_1) \qquad (4.2)$$

In physical applications there are many examples involving Markoff process. Very often if a physical process is not Markoffian, it is still possible to consider it to be a Markoff process in a higher dimensional space. In any event Eq. (4. 2) is valid for most of the physical examples of interest.

Substituting Eq. (4. 2) into the expression for the autocorrelation function, we have

$$R_x(t_2-t_1) = \int_{-\infty}^{\infty}\int_{-\infty}^{\infty} x_1 x_2\, p(x_1)\, T(x_2, t_2 \mid x_1, t_1)\, dx_1 dx_2 \qquad (4.3)$$

where $T(x_2, t_2 \mid x_1, t_1)$ is a solution to the appropriate Fokker-Planck equation, and $p(x_1)$ is the first order probability density function, which is a solution to the same Fokker-Planck equation in the stationary form.

In principle, the autocorrelation function can be determined from Eq. (4.3) once the transition probability function is known. However, to obtain the transition probability one must solve the exact Fokker-Planck equation. This is usually difficult and sometimes almost impossible for systems with nonlinearity. A generally applicable technique will now be demonstrated for a simple first order nonlinear system.

4.3. A First Order Nonlinear System

The problem to be considered here is related to the motion of a mass with idealized Coulomb damping. The differential equation involved is given by

$$\dot{x} + k \operatorname{sgn} x = N(t) \qquad (4.4)$$

where x(t) is the displacement of the mass, k sgn x is the idealized Coulomb damping, and N(t) is a Gaussian white external force, which is assumed to be stationary and ergodic, and its power spectral density is equal to 4D per cps.

The Fokker-Planck equation governing the transition probability $T(x, t \mid x_1 t_1)$ of the displacement random variable x(t) is

$$\frac{\partial T}{\partial t} = -\frac{\partial}{\partial x}\left[A(x)T\right] + \frac{1}{2}\frac{\partial^2}{\partial x^2}\left[B(x)T\right] \qquad (4.5)$$

where A(x) and B(x) can be determined from Eq. (1.18), and by integrating the system differential equation with respect to the time t, hence

$$\Delta x = -\left[k \text{ sgn } x\right]\Delta t + \int_t^{t+\Delta t} N(\eta)\,d\eta$$

therefore

$$A(x) = \lim_{\Delta t \to 0} \frac{\langle \Delta y \rangle_{Av}}{\Delta t} = -k \text{ sgn } x$$

Since

$$\langle N(t) \rangle_{Av} = 0$$

furthermore:

$$\langle \Delta x^2 \rangle = \left[-k \text{ sgn } x\right]^2 \Delta t^2 + \int_t^{t+\Delta t}\int d\zeta\, d\eta \, \langle N(\zeta)N(\eta) \rangle_{Av}$$

the double integral appearing above is $2D\Delta t$, since the external force N(t) is assumed to be white noise. Hence

$$B(x) = \lim_{\Delta t \to 0} \frac{\langle \Delta x^2 \rangle_{Av}}{\Delta t} = 2D$$

Substituting the expressions for A(x) and B(x) into Eq. (4.5), we have

$$\frac{\partial T}{\partial t} = \frac{\partial}{\partial x}(k \text{ sgn } x)T + D\frac{\partial^2 T}{\partial x^2} \qquad (4.6)$$

The initial and boundary conditions are the following.

$$\lim_{t \to t_1} T(x, t \mid x_1, t_1) = \delta(x - x_1)$$

$$\lim_{x \to \infty} T(x, t \mid x_1, t_1) = 0$$

and the normalization condition

$$\int_{-\infty}^{\infty} T(x, t \mid x_1, t_1) dx = 1$$

The first order probability density $p_1(x)$ is the solution of the stationary Fokker-Planck equation

$$0 = \frac{\partial}{\partial x}\left[(k \operatorname{sgn} x) p_1(x)\right] + D \frac{\partial^2 p_1(x)}{\partial x^2}$$

It has been shown by Caughey that the unique solution to this equation is given by

$$p_1(x) = \frac{k}{2D} e^{-k|x|/D} \tag{4.7}$$

The corresponding probability distribution function is given by

$$p_1(x \geq X) = \int_X^{\infty} p(x) dx$$

$$= \int_X^{\infty} \frac{k}{2D} e^{-k|x|/D} dx \tag{4.7a}$$

The calculated and the experimental results for the first order probability distribution function $p_1(x \geq X)$ are illustrated in Fig. (4.6).

The autocorrelation function for the random variable $x(t)$ of the nonlinear system can be determined from Eq. (4.3)

$$R_x(t - t_1) = \int_{-\infty}^{\infty} \int_{-\infty}^{\infty} x_1 x p_1(x_1) T(x, t \mid x_1, t_1) dx_1 dx$$

Now assume[43, 46, 24]

$$v(x, t) = \int_{-\infty}^{\infty} x_1 p_1(x_1) T(x, t \mid x_1 t_1) dx_1 \qquad (4.8)$$

Hence

$$R_x(\tau) = \int_{-\infty}^{\infty} x v(x, t) dx, \qquad \text{where} \quad \tau = t - t_1 \qquad (4.9)$$

The probability variable $v(x, t)$ satisfies the same Fokker-Planck equation as the transition probability $T(x, t \mid x_1 t_1)$, since the term $x_1 p(x_1)$ appearing in Eq. (4.8) does not depend on the time variable t. Hence from Eq. (4.6)

$$\frac{\partial v}{\partial t} = \frac{\partial}{\partial x} (k \operatorname{sgn} x) v + D \frac{\partial^2 v}{\partial x^2} \qquad (4.10)$$

with the initial and boundary conditions given by

$$\begin{aligned} v(x, 0) &= \int_{-\infty}^{\infty} x_1 p_1(x_1) \delta(x - x_1) dx_1 = x p_1(x) \\ v(\infty, \tau) &= 0 \\ v(x, \tau) &= -v(-x, \tau) \end{aligned} \qquad (4.11)$$

Since the function $v(x, \tau)$ is skew symmetric with respect to x for all time τ, we have the following condition at x=0.

$$v(0, \tau) = 0$$

From the known initial and boundary conditions, Eq. (4.10) may be solved. There are two methods of approach to obtain the solution to the Fokker-Planck equation. Each of them has its own merit. The detailed mathematics involved will now be demonstrated. The first approach is to take the Laplace transform of Eq. (4.10) with

respect to τ . Using the initial condition (Eq. 4.10) two ordinary differential equations are obtained

$$DV_{xx} + kV_x - sV = -xp_1(x) \qquad \text{for } x > 0$$

$$DV_{xx} - kV_x - sV = -xp_1(x) \qquad \text{for } x < 0$$

where

$$V(x, s) = \int_0^\infty v(x, \tau)e^{-s\tau}\, d\tau$$

and the subscript denotes the order of differentiations. The method of obtaining the solutions to the ordinary differential equations is standard. Thus

$$V(x, s) = A\exp(a_2 x) + B\exp(-a_1 x) - \int_0^x h_1(x-\eta)\,\eta\, p_1(\eta)\, d\eta \qquad \text{for } x > 0$$

$$V(x, s) = C\exp(-a_2 x) + E\exp(a_1 x) - \int_0^x h_2(x-\eta)\,\eta\, p_1(\eta)\, d\eta \qquad \text{for } x < 0$$

where

$$a_1 = \frac{(\lambda^2 + s)^{1/2} + \lambda}{\sqrt{D}}, \qquad a_2 = \frac{(\lambda^2 + s)^{1/2} - \lambda}{\sqrt{D}}, \qquad \lambda = \frac{k}{2\sqrt{D}}$$

the unknown constants can be determined from the fact that

$$V(0, s) = 0 \qquad \text{and} \qquad V(\pm\infty, s) = 0$$

therefore

$$V(x, s) = \frac{k}{2D}\left[\frac{x}{s} e^{-kx/D} - \frac{k}{s^2}\left(e^{-\frac{k}{D}x} - e^{-a_1 x}\right)\right] \qquad x > 0$$

$$V(x, s) = \frac{k}{2D}\left[\frac{x}{s} e^{kx/D} + \frac{k}{s^2}\left(e^{kx/D} - e^{a_1 x}\right)\right] \qquad x < 0$$

Substituting these equations into Eq. (4.9), we obtain the Laplace transform of the autocorrelation function

$$\bar{R}(s) = \int_{-\infty}^{\infty} x\, V(x, s)\, dx$$

$$= \frac{D}{2\lambda^2 s} - \frac{D}{s^2} + \frac{4\lambda^2 D}{s^4}\left[\lambda - (\lambda^2 + s)^{1/2}\right]^2 \qquad (4.12)$$

which agrees with the solution obtained by Caughey and Dienes.

The second method of obtaining the autocorrelation function is to apply the two-sided Fourier transform[47] to the Fokker-Planck equation (Eq. 4.10) with respect to the displacement variable x(t). The transforms are given by

$$F_+(\omega) = \frac{1}{\sqrt{2\pi}} \int_0^{\infty} f(x)\, e^{ix\omega}\, d\omega$$

$$F_-(\omega) = \frac{1}{\sqrt{2\pi}} \int_{-\infty}^{0} f(x)\, e^{ix\omega}\, d\omega \qquad (4.13)$$

where $\omega = a + ib$.

The inverse transform is given by

$$f(x) = \frac{1}{\sqrt{2\pi}} \int_{ia-\infty}^{ia+\infty} F_+(\omega) e^{-ix\omega}\, d\omega + \frac{1}{\sqrt{2\pi}} \int_{ib-\infty}^{ib+\infty} F_-(\omega) e^{-ix\omega}\, d\omega$$

where a is a sufficiently large positive number, and b is a sufficiently large negative number. Hence from Eq. (4.10), Eq. (4.13) and the fact that v(x,t) must vanish at x=0 for all time τ, we obtain a first order ordinary differential equation

$$\frac{dV_+(\omega,\tau)}{d\tau} + (ik\omega + D\omega^2)V_+(\omega,\tau) = -\frac{D}{\sqrt{2\pi}} f(\tau) \qquad x > 0$$

where

$$V_+(\omega,\tau) = \frac{1}{\sqrt{2\pi}} \int_0^\infty v(x,\tau) e^{i\omega x} dx$$

and

$$f(\tau) = \frac{\partial v(x,\tau)}{\partial x}\bigg|_{x=0}$$

The initial condition for $x > 0$ is given by

$$V_+(\omega,0) = \frac{1}{\sqrt{2\pi}} \int_0^\infty v(x,0) e^{i\omega x} dx$$

$$= \frac{1}{\sqrt{2\pi}} \int_0^\infty x\, p_1(x) e^{i\omega x} dx$$

$$= \frac{-k}{2D\sqrt{2\pi}\left(\omega + i\frac{k}{D}\right)^2}$$

Thus, the solution to the ordinary differential equation is

$$V_+(\omega,\tau) = V_+(\omega,0) e^{-(ik\omega + D\omega^2)\tau} - \frac{D}{\sqrt{2\pi}} \int_0^\tau f(\zeta) e^{-(ik\omega + D\omega^2)(t-\zeta)} d\zeta$$

Taking a Laplace transform of $V_+(\omega,\tau)$ with respect to the time τ, we have

$$V_+(\omega,s) = -\frac{k}{2D\sqrt{2\pi}\,(D\omega^2 + ik\omega + s)\left(\omega + i\frac{k}{D}\right)^2} - \frac{D}{\sqrt{2\pi}} f(s) \frac{1}{D\omega^2 + ik\omega + s} \tag{4.14}$$

where

$$V_+(\omega, s) = \int_0^\infty V_+(\omega, \tau) e^{-s\tau} d\tau$$

and

$$f(s) = \int_0^\infty f(\tau)\, e^{-s\tau} d\tau$$

To recover the original probability variable v(x, t) from the transform variable $V_+(\omega, s)$, we first take the inverse one-sided Fourier transform with respect to $\omega = a+ib$, where b is a sufficiently large positive number.

$$V_+(x, s) = \frac{1}{\sqrt{2\pi}} \int_{ib-\infty}^{ib+\infty} V_+(\omega, s) e^{-ix\omega} d\omega$$

Substitute Eq. (4.14) into the above expression, and evaluate the integral by residue calculus. The integral closed contour C in this case consists of an imaginary line ib and a semi-circle, which encloses all the singular poles located below the line ib. Hence

$$\begin{aligned} V_+(x, s) &= \frac{1}{\sqrt{2\pi}} \int_C V_+(\omega, s) e^{-ix\omega} d\omega \\ &= -\sqrt{2\pi}\, i \sum_{n=1}^{k} R_n \\ &= \frac{k}{2D^2}\left[\frac{e^{a_2 x}}{a_1^2(a_1+a_2)} - \frac{e^{-a_1 x}}{a_2^2(a_1+a_2)} - \frac{x e^{-\frac{k}{D}x}}{a_1 a_2} + \frac{k}{D}\,\frac{e^{-\frac{k}{D}x}}{a_1^2 a_2^2}\right] \\ &\quad -f(s)\left[\frac{e^{a_2 x} - e^{-a_1 x}}{a_1 + a_2}\right] \end{aligned}$$

where R_n denotes the residues at the respective poles, and the

negative sign is to account for the fact that the closed contour C transverses in the clockwise direction. Since the function $V_+(x, s)$ must vanish at infinity

$$V_+(\infty, s) = 0$$

the unknown function f(s) can be determined.

$$f(s) = \frac{k}{2D^2 a_1^2}$$

Substituting this back into the expression for $V_+(x, s)$, we have

$$V_+(x, s) = \frac{k}{2D} \frac{xe^{-\frac{k}{D}x}}{s} - \frac{k}{s^2}\left(e^{-\frac{k}{D}x} - e^{-a_1 x}\right)$$

Likewise, the same procedure can be applied to the transform solution of v(x, t) for the negative value of x(t). Thus

$$V_-(x, s) = \frac{k}{2D} \frac{xe^{\frac{k}{D}x}}{s} + \frac{k}{s^2}\left(e^{\frac{k}{D}x} - e^{a_1 x}\right)$$

The Laplace transform of the autocorrelation function is then given by

$$\bar{R}_x(s) = \int_{-\infty}^{0} V_-(x, s)dx + \int_{0}^{\infty} V_+(x, s)dx$$

$$= \frac{D}{2\lambda^2 s} - \frac{D}{s^2} + \frac{4\lambda^2 D}{s^4}\left[\lambda - (\lambda^2 + s)^{1/2}\right]^2 \qquad (4.12)$$

This is the same as that arrived at from the first method.

The relative advantages of the two methods are not difficult to see. The former method is considered to be simple and direct, and the solutions can be obtained easily if only ordinary differential equations in the transform space are involved. The second method is

more useful in cases where the Laplace transformed (with respect to time) differential equation is not ordinary.

From the known Laplace transform version of the autocorrelation function $\bar{R}_x(s)$, various limiting values of the time autocorrelation function can be determined. Since

$$R_x(0) = \int_0^\infty S_x(f)df = E(x^2)$$

and from Eq. (4.7)

$$E(x^2) = \int_{-\infty}^{\infty} x^2 p_1(x)dx$$

$$= \int_{-\infty}^{\infty} x^2 \frac{k}{2D} e^{-\frac{k|x|}{D}} dx = \frac{2D^2}{k^2} \qquad (4.15)$$

From the Tauberian theorem, the following relation must be true

$$E(x^2) = R_x(0) = \lim_{s \to \infty} s\bar{R}_x(s) = \frac{2D^2}{k^2}$$

then with the definition of λ, the above expression can be easily verified.

From the general theory of autocorrelation functions, it must vanish for large time. In other words the following limiting condition must be true

$$\lim_{\tau \to \infty} R_x(\tau) = \lim_{s \to 0} s\bar{R}(s) = 0$$

It can be verified by carrying out the limiting condition for the function $\bar{R}(s)$ given by Eq. (4.12). Thus

$$\lim_{s\to 0} s\bar{R}(s) = \lim_{s\to 0}\left\{\frac{D}{2\lambda^2} - \frac{D}{s} + \frac{4\lambda^2 D}{s^3}\left[\lambda-(\lambda^2+s)^{1/2}\right]^2\right\}$$

$$= \lim_{s\to 0}\left\{\frac{D}{2\lambda^2} - \frac{D}{s} + \frac{4\lambda^2 D}{s^3}\left[2\lambda^2+s-2\lambda(\lambda^2+s)^{1/2}\right]\right\}$$

$$= \lim_{s\to 0}\left\{\frac{D}{2\lambda^2} - \frac{D}{s} + \frac{4\lambda^2 D}{s^3}\left[2\lambda^2+s-2\lambda^2\left(1+\frac{s}{2\lambda^2} - \frac{1}{8}\frac{s^2}{\lambda^4} + \frac{1}{16}\frac{s^3}{\lambda^6} + o(s^4)\right)\right]\right\}$$

$$= \lim_{s\to 0} o(s) = 0$$

By carrying out the inverse Laplace transformation, the time autocorrelation function can be recovered.

$$R_x(\tau) = \frac{1}{2\pi i}\int_{c-i\omega}^{c+i\omega} e^{s\tau}\,\bar{R}_x(s)ds$$

The final expression for the autocorrelation function is given below

$$\frac{R_x(\gamma)}{\langle x^2\rangle} = \frac{(8\gamma^6+12\gamma^4-6\gamma^2+3)}{3}\,\mathrm{erfc}(\gamma) - \frac{2\gamma e^{-\gamma^2}(2\gamma^2+3)(2\gamma^2-1)}{3\sqrt{\pi}} \qquad (4.16)$$

where

$$\gamma = \frac{k}{2\sqrt{D}}\sqrt{\tau} \qquad \langle x^2\rangle = \frac{D}{2\lambda^2} = \frac{2D^2}{k^2}$$

the results are plotted in Fig. (4.1).

By means of the Wiener-Khintchine relationship, the power spectral density can be determined from the autocorrelation function.

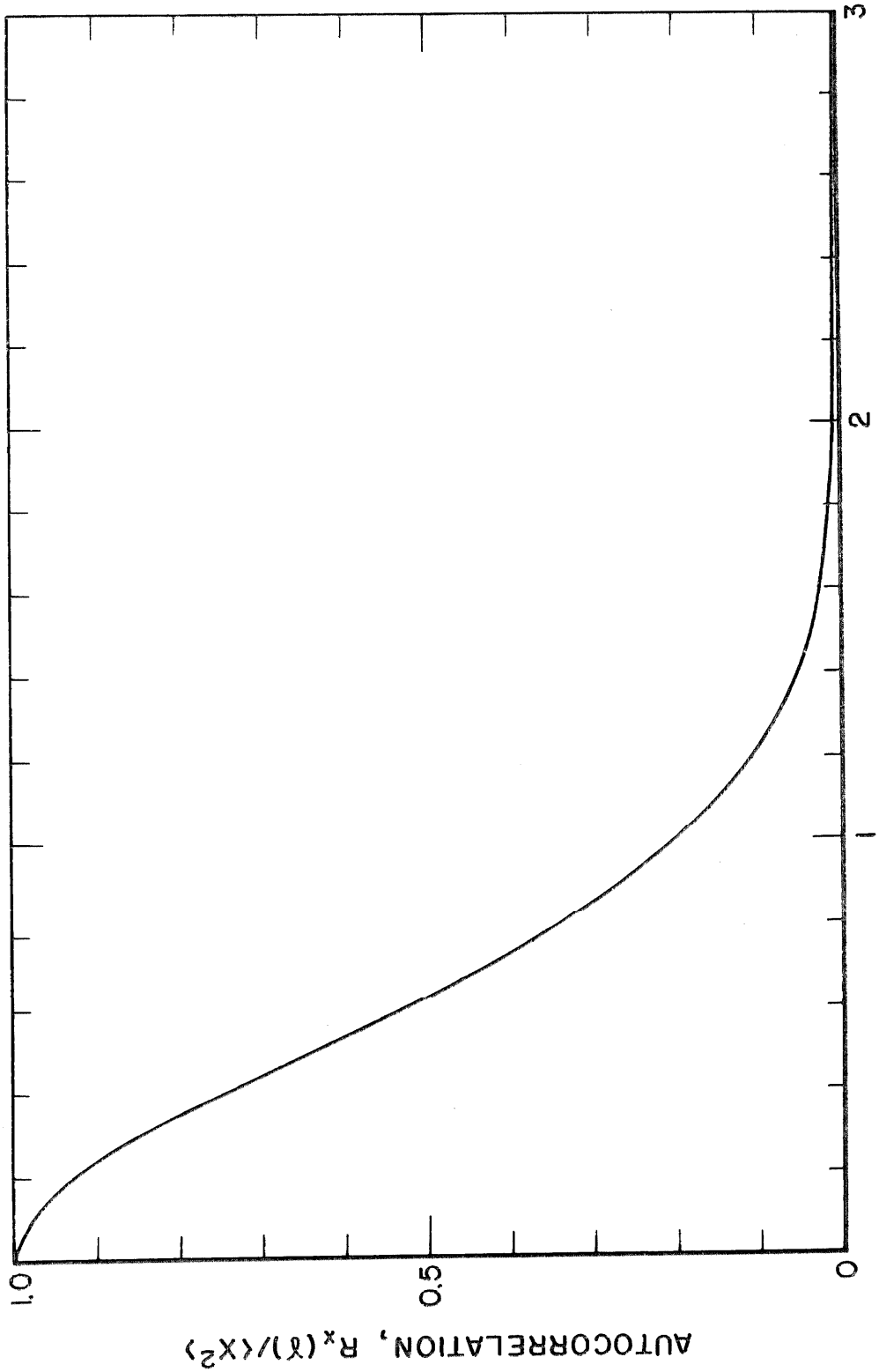

Fig. 4.1. Autocorrelation function of the first order Coulomb damped system.

Then

$$S(\omega) = \frac{2}{\pi} \mathrm{Re}\left[\bar{R}(i\omega)\right] \qquad 0 < \omega < \infty$$

$$= \frac{2D}{\pi \lambda^4}\left\{\frac{\lambda^4}{\omega^2} + \frac{8\lambda^8}{\omega^4}\left[1 - \left(\frac{1+(1+\omega^2/\lambda^4)^{1/2}}{2}\right)^{1/2}\right]\right\} \qquad (4.17)$$

where Re means the "real part of", and $S(\omega)$ has a unit of quantity square per radian per second.

The power spectral density given above can be normalized. To accomplish this a non-dimensional frequency is defined as

$$\eta = \omega/\lambda^2 = \frac{4D\omega}{k^2}$$

since

$$\int_0^\infty S(\omega)\,d\omega = \langle x^2 \rangle$$

Therefore if

$$S(\eta) = \frac{\lambda^2 S(\omega)}{\langle x^2 \rangle} \qquad 0 < \omega < \infty$$

then it follows that

$$\int_0^\infty S(\eta)\,d\eta = 1 \qquad 0 < \eta < \infty$$

The non-dimensional power spectral density is then

$$S(\eta) = \frac{4}{\pi}\left\{\frac{1}{\eta^2} + \frac{8}{\eta^4}\left[1 - \left(\frac{1+(1+\eta^2)^{1/2}}{2}\right)^{1/2}\right]\right\} \qquad (4.18)$$

The value of $S(\eta)$ at $\eta = 0$ is finite, and it can be obtained from the following limiting condition

$$S(0) = \lim_{\eta \to 0} S(\eta) = \frac{\lambda^2}{\langle x^2 \rangle} \frac{2}{\pi} \mathrm{Re}\left[\bar{R}(i\omega) \right]_{\omega=0}$$

$$= \frac{4\lambda^4}{\pi D} \lim_{s \to 0} \bar{R}(s)$$

$$= \frac{4\lambda^4}{\pi} \lim_{s \to 0} \left\{ \frac{1}{2\lambda^2 s} - \frac{1}{s^2} + \frac{4\lambda^2}{s^4} \left[2\lambda^2 + s - 2\lambda (\lambda^2 + s)^{1/2} \right] \right\}$$

$$= \frac{4\lambda^4}{\pi} \lim_{s \to 0} \left\{ \frac{1}{2\lambda^2 s} - \frac{1}{s^2} + \frac{4\lambda^2}{s^4} \left[2\lambda^2 + s - 2\lambda^2 \left(1 + \frac{s}{2\lambda^2} - \frac{s^2}{8\lambda^4} \right. \right. \right.$$

$$\left. \left. \left. + \frac{s^3}{16\lambda^6} - \frac{5s^4}{128\lambda^8} + o(s^5) \right) \right] \right\}$$

$$= \frac{5}{4\pi}$$

The normalized power spectral density is plotted in Fig. (4. 5) along with the experimental results.

4. 4. Experimental Investigation

The experiments performed on the first order nonlinear system described in the preceding section and the results of these investigation are reported in this section. In addition to this, the response characteristics of a second order nonlinear system are investigated. The objective is to check the analytical results given by Wolaver.[46]

The results are divided into two parts: the power spectral density measurements of the response of the first and second order nonlinear systems, the probability distribution measurements of the first order system.

4. 4. 1. Experimental Procedure

To study the response of the first order system with Coulomb damping, an analog computer is used to simulate the system differential equation given by Eq. (4. 4). The analog setup is shown in Fig. (4. 2) with operational amplifiers as the basic building blocks.

A very important assumption made in the theoretical investigation is that the system be driven by a Gaussian white noise. This is naturally impossible to achieve in practice. The experiment is set up such that the nonlinear system is driven instead by a broadband Gaussian random noise. The General Radio Random Noise Generator along with the Krohn-Hite Variable Filter are used to generate the broadband random noise, the nominal bandwidth of which is set at 10 kc.

The circuit parameters for the analog setup shown in Fig. (4. 2) are adjusted according to the following criterion:

1. The time constant RC of the integrator must be large so that the input frequency bandwidth appears "white" in comparison with respect to the system frequency bandwidth.

2. The time constant must not be too large so that the output voltage is operating near the amplifier noise region.

The RC constant used in the experiment to satisfy these conditions is fixed at 0. 004.

The nonlinear function generator ksgnx shown in Fig. (4. 4) is made up of a USA-3 operational amplifier, two IN271 diodes, a 24 volt battery, and a 50 kΩ potentiometer. The magnification factor k

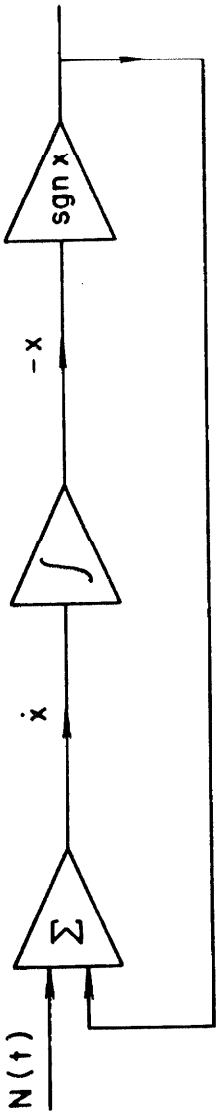

$$\dot{x} + k\,\mathrm{sgn}\,x = N(t)$$

Fig. 4.2. Analog set-up for the first order Coulomb damped system.

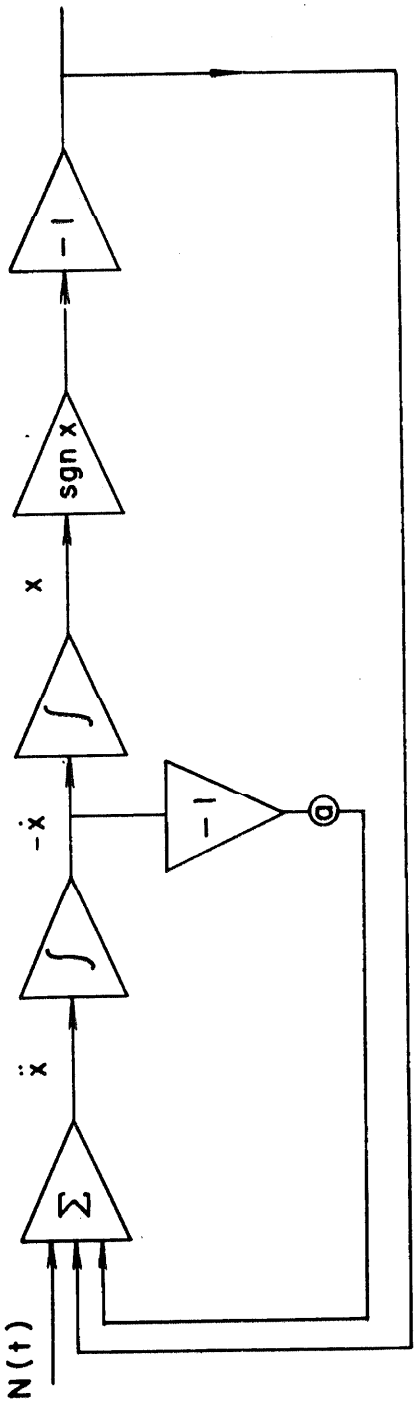

$$\ddot{x} + 2c\dot{x} + \mathrm{sgn}\,x = N(t)$$

Fig. 4.3. Analog set-up for the second order Coulomb damped system with Coulomb restoring force.

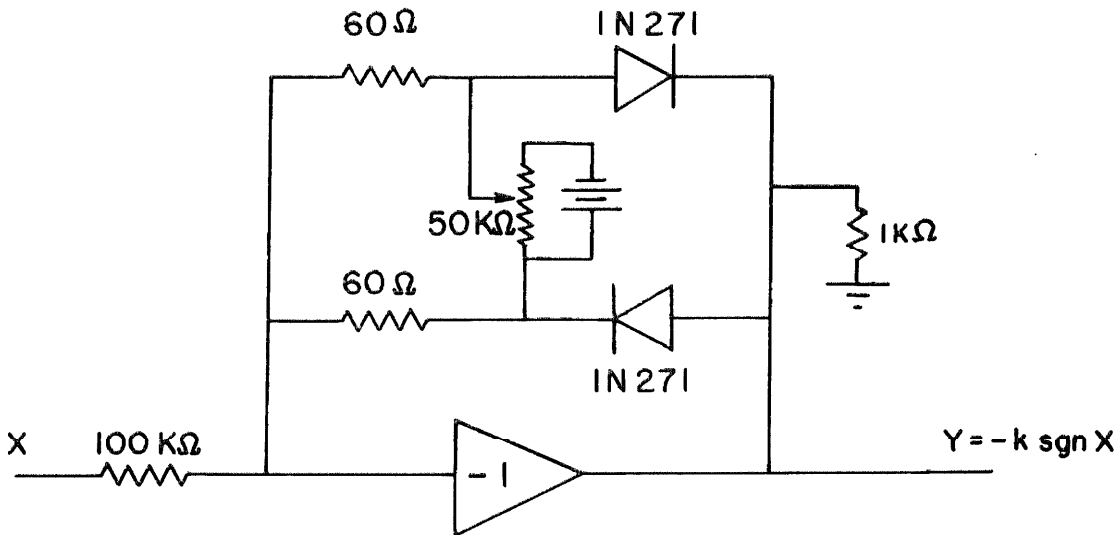

Circuit diagram for the nonlinear sgn function

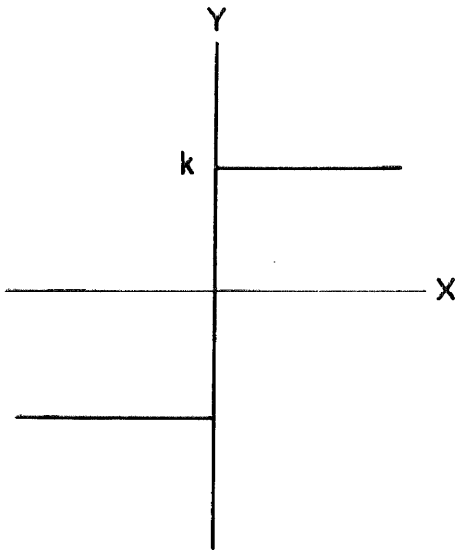

Ideal case

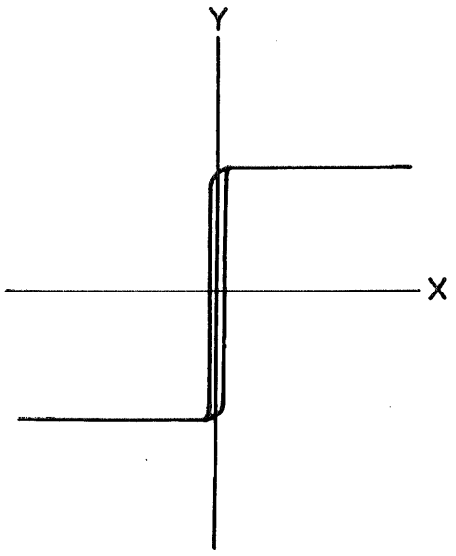

Actual case at high frequency

Fig. 4.4

can be adjusted by turning the potentiometer dial. In the course of experiment the k values are set at 1 volts, 2 volts, and 3 volts, respectively.

The basic data recorded were the power spectral density and the probability distribution function of the displacement variable x(t) of the system with Coulomb damping.

To investigate the response characteristics of a second order nonlinear system, an analog circuit is set up according to the following differential equation.

$$\ddot{x} + 2c\dot{x} + \text{sgn } x = N(t) \qquad (4.19)$$

where c is the velocity dependent damping constant, and N(t) is a Gaussian white external force. The circuit diagram is illustrated in Fig. (4.4).

The specification for the external force N(t) is similar to that given earlier for the first order system. The system parameters are fixed at R_1C_1=.001 for the first integrator, and R_2C_2=0.0004 for the second integrator. The potentiometer is used to provide fine adjustment on the damping parameter c. The primary objective of this experiment is to check the power spectral density of the output displacement variable x(t) against the theoretical results given by Wolaver.[46]

4.4.2. Observations and Results

The following results are obtained on the basis of the experimental observations and measurements. Comparisons are made

between these results and those based on the theoretical calculation.

1. It is found that the mean square value output of the displacement variable x(t) of the first order nonlinear system agrees very well with that predicted by Eq. (4.15) even though the frequency spectrum of the random noise input is not white.

2. The measured power spectral density for the first order nonlinear system agrees very well with that obtained from theoretical analysis (Eq. 4.18). The results are plotted against the frequency in Fig. (4.5). In the lower frequency range, however, the experimental values are found to be slightly less than the theoretical results, since the actual input power spectral densities are attenuated in the lower frequency range (see Fig. 2.16).

3. The experimental and theoretical probability distribution curves for the displacement variable x(t) of the first order system with Coulomb damping are presented in Fig. (4.6). It is found that the experimental values follow closely the exponential distribution curves predicted by Eq. (4.7a) up to 3σ level. The agreement is poorer at the higher amplitude levels; this is because of the magnitude limiting effect of the input.

4. For the second order system with Coulomb restoring force, (Eq. 4.19), the measured power spectral density of the output displacement variable x(t) is illustrated in Fig. (4.7), where the normalized power spectral density (total area is unity) is plotted against the frequency. The experimental results do not agree with the analytic results given by Wolaver, who theorized that the power

spectral density of the displacement variable x(t) of the second order nonlinear system (Eq. 4.19) is always monotonically decreasing regardless of the amount of damping present in the system.

5. In simulating the nonlinear function k sgn x on an operational amplifier, the phase shift present at the high frequencies (around 5kc) can be minimized, but cannot be removed completely (see Fig. 4.4). However, this exerts only a minor influence on the final experimental result.

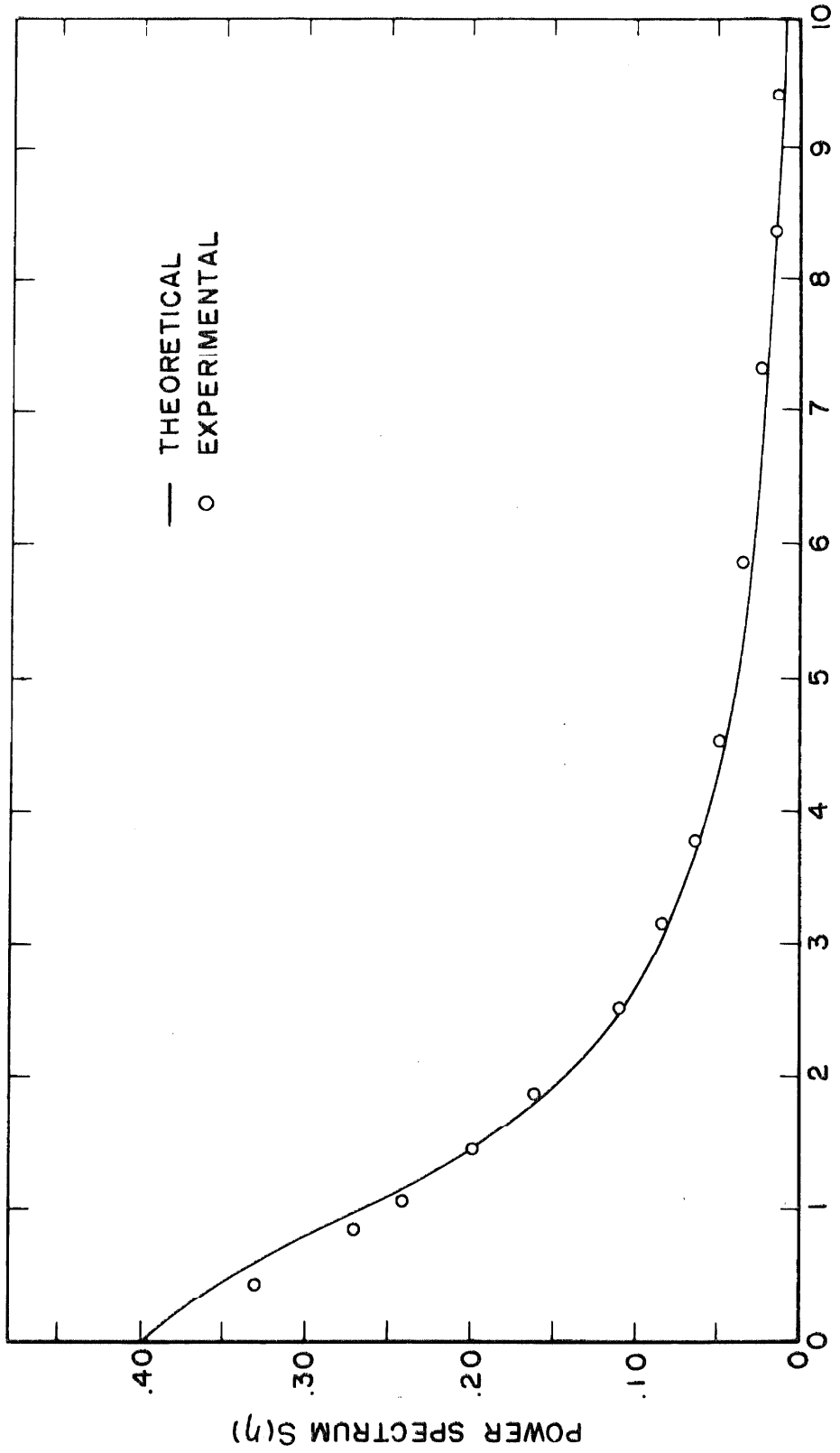

Fig. 4.5. Power spectral density of the Coulomb damped system.

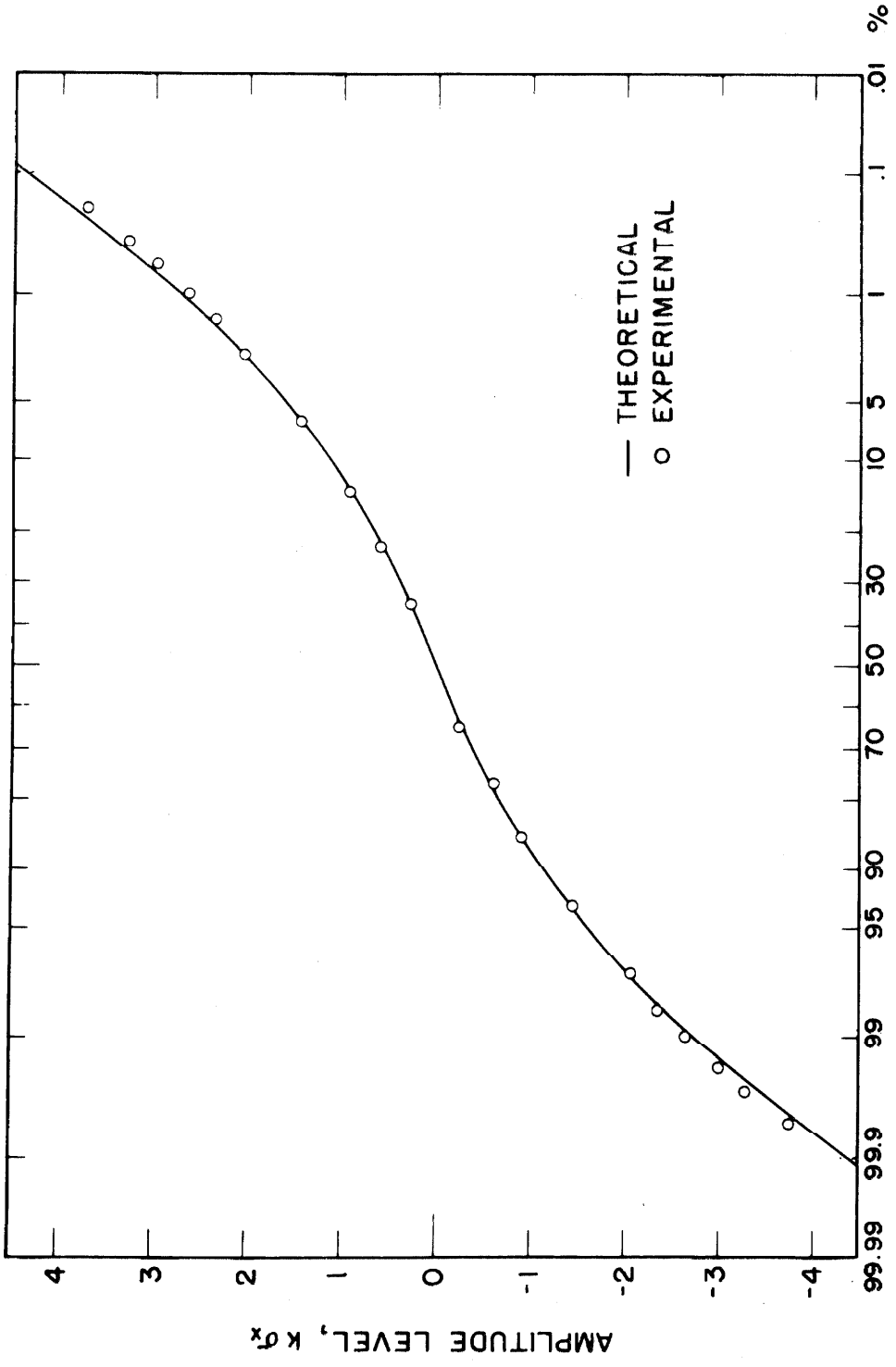

Fig. 4.6. Probability distribution of the response of the first order Coulomb damped system.

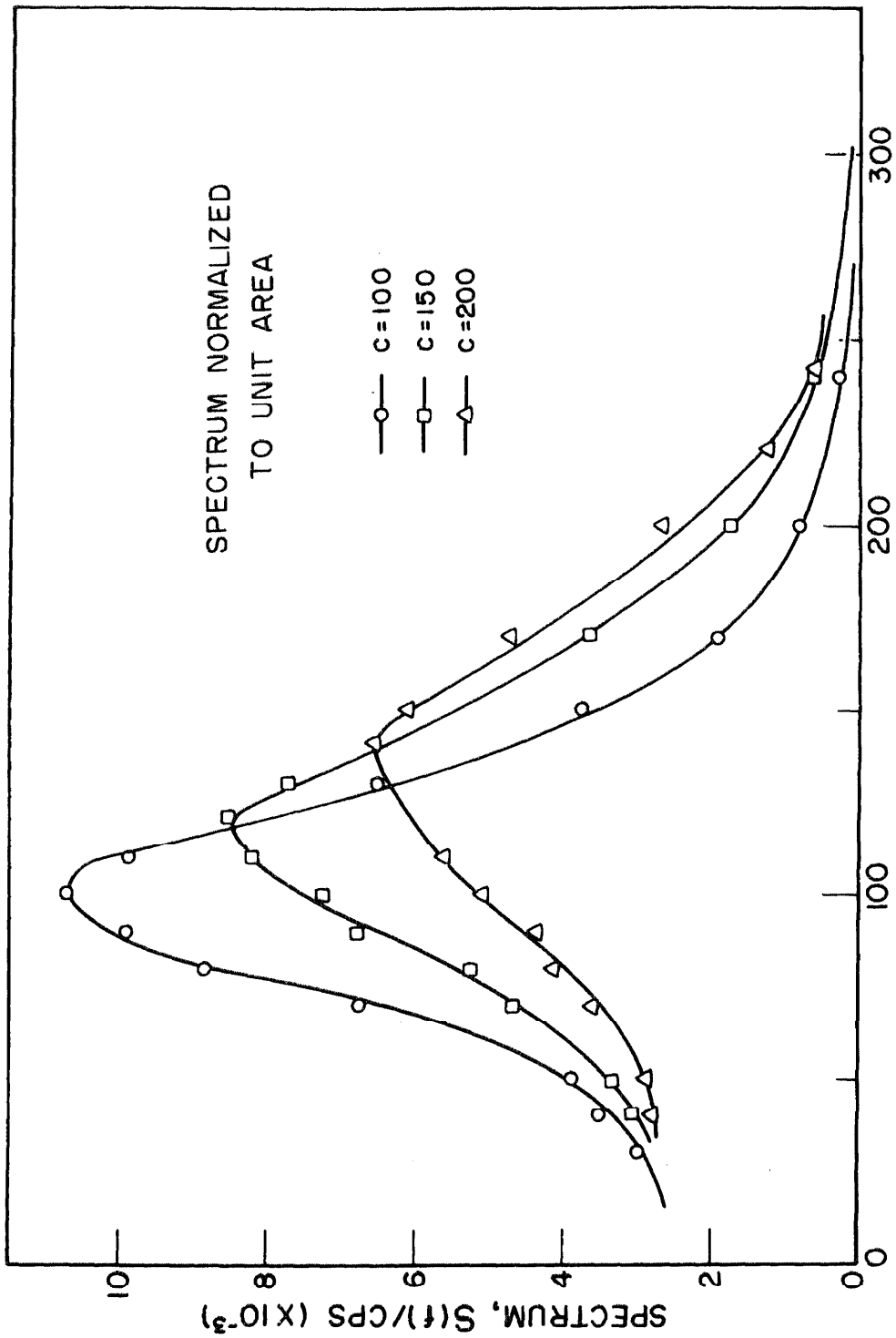

Fig. 4.7. Power spectral densities of the response of the second order with Coulomb restoring force.

CHAPTER V

SUMMARY AND CONCLUSION

The following conclusions are reached on the basis of the analytical and experimental results obtained during the course of investigation.

Chapter II describes the results of linear systems subjected to magnitude-limited random excitation; the major points of interest are:

1. If the power spectral density of the Gaussian broadband random signal is uniform in the frequency range from 0 to f_o cps, the magnitude-limited signals are found to be approximately uniform over the same frequency range. This provides a great deal of simplification in the computation of mean square values of the response of the single degree of freedom system to magnitude-limited random excitation.

2. The ratio of the rms value response (displacement) of the single degree of freedom system to the rms value input of the magnitude-limited broadband Gaussian random signal depends only on the critical damping ratio and the natural frequency of the system, and is essentially constant regardless of the magnitude-limiting level.

3. The responses (displacement) of single degree of freedom systems to magnitude-limited Gaussian random excitation are approximately Gaussian, the agreement being very good out to the $3\sigma_x$ level, if the critical damping ratio of the system is less than 10%. Within experimental capability these are found to be true even though

the input signal is heavily limited. For systems having critical damping ratio greater than 10%, the response of the system is no longer Gaussian distributed at higher amplitude levels.

4. The power spectral densities of the response (displacement) of the single degree of freedom systems to magnitude-limited random excitation are similar to $|H(j2\pi f)|^2$, the square of the system transfer function, since the power spectral densities of the magnitude-limited signal are approximately uniform over a wide frequency range.

5. Experimental studies point to the fact that many analytical results can be checked experimentally if the input spectrum is assumed to have the shape given by Eq. (2.12) or Eq. (2.15).

Chapter III describes the peak characteristics of linear systems subjected to broadband Gaussian random excitation. The main results are the following:

1. The total number of peaks per unit time in the response of a single degree of freedom system depends largely on the frequency bandwidth of the input broadband signal. The peak distribution of the response is no longer Rayleigh, if the input frequency bandwidth is wide compared to the natural frequency of the system.

2. For a multi-degree of freedom or a continuous system, it is frequently possible to obtain normal mode solutions for the system if the damping is small. Therefore the motion of the system consists essentially of a linear combination of the normal mode solutions. At a given time, such a system usually vibrates with appreciable amplitudes at only a limited number of modes. During the course of the

investigation, the statistical properties of the sum of two single degree of freedom systems are investigated. It is found that the responses of the respective system to the same source of excitation are essentially uncorrelated if the system dampings are small and the natural frequencies are sufficiently separated. Therefore the resulting signal essentially consists of the sum of two uncorrelated random variables. The peak distributions of the resulting sum lie in between the curves of Gaussian distribution and Rayleigh distribution.

Chapter IV is concerned with the statistical properties of the response of a simple first order nonlinear system to white noise excitation. The major results are:

1. The power spectral density of the response (displacement) of the first order nonlinear system with Coulomb damping is found to be monotonically decreasing with respect to frequency.

2. The autocorrelation function of the response (displacement) of the first order nonlinear system with Coulomb damping is found to be monotonically decreasing with respect to the time difference.

3. The probability distribution of the response (displacement) of the first order nonlinear system with Coulomb damping follows the exponential law.

4. Excellent agreement between the analytical and experimental results are obtained, even though the actual input spectrum is not white as it was assumed theoretically. Therefore it is justified to assume the input spectrum to be white whenever possible in the mathematical analysis of random vibration.

5. Experimental investigations have been made to check against the theoretical results given by Wolaver. It is found that the power spectral densities of the response of a second order nonlinear system with Coulomb restoring force to white noise excitation are not monotonically decreasing with respect to frequency. Therefore, the results given by Wolaver are questionable.

REFERENCES

1. Einstein, A., Investigations on the Theory of the Brownian Movement, Dover Publications, New York, (1956).

2. Wang, M. C. and Uhlenbeck, G. E., "On the Theory of Brownian Motion II", Rev. Mod. Phys. 17, (1945), pp. 323-342. (Also N. Wax et.al., Selected Papers on Noise and Stochastic Processes, Dover Publications, Inc., New York, (1945), pp. 113-132.)

3. Rice, S. O., "Mathematical Analysis of Random Noise", Bell System Tech. J., 23, (1944), pp. 282-332; 24, (1945) pp. 46-156. (Also, N. Wax et. al., Selected Papers on Noise and Stochastic Processes, Dover Publications, Inc., New York, (1954), pp. 133-294.)

4. Caughey, T. K., "Response of a Nonlinear String to Random Loading", J. Appl. Mech. 26, (1959), pp. 341-344.

5. Caughey, T. K., "Random Excitation of a Loaded Nonlinear String", J. Appl. Mech. 27, (1960), pp. 575-578.

6. Caughey, T. K., "Derivation and Application of the Fokker-Planck Equation to Discrete Nonlinear Dynamic Systems Subjected to White Random Excitation", J. Acoust. Soc. Am. 35, (1963), pp. 1683-1692.

7. Caughey, T. K., "Response of Van der Pol's Oscillator to Random Excitation", J. Appl. Mech. 26, (1959), pp. 345-348.

8. Caughey, T. K., "Equivalent Linearization Techniques", J. Acoust. Soc. Am., 35, (1963), pp. 1706-1711.

9. Caughey, T. K., "Random Excitation of a System with Bilinear Hysteresis", J. Appl. Mech., 27, (1960), pp. 649-652.

10. Crandall, S. H., et. al., Random Vibrations, Technology Press, Cambridge, Mass., and John Wiley & Sons, Inc., New York (1958).

11. Crandall, S. H., "Random Vibration of a Nonlinear System with a Set-up Spring", J. Appl. Mech., 29, (1960), pp. 477-482.

12. Crandall, S. H. and Mark, W. D., Random Vibration in Mechanical Systems, Academic Press, Inc., New York, (1963).

13. Crandall, S. H., "Perturbation Techniques for Random Vibration of Nonlinear Systems", J. Acoust. Soc. Am., 35, (1963), pp. 1700-1705.

14. Booton, R. C., "Nonlinear Control Systems with Random Inputs", IRE Trans. Circuit Theory 1, (1954), pp. 9-18.

15. Lyon, R. H., "On the Vibration Statistics of a Randomly Excited Hard-Spring Oscillator", J. Acoust. Soc. Amer., 32, (1960), pp. 716-719.

16. Barlett, M. S., Stochastic Processes, Cambridge University Press, Cambridge (1962).

17. Wiener, N., Extrapolation, Interpolation, and Smoothing of Stationary Time Series, the M. I. T. Press, Cambridge (1964).

18. Middleton, D., An Introduction to Statistical Communication Theory, McGraw-Hill Book Co., Inc., New York, (1960), pp. 343.

19. Davenport, W. B. and Root, W. L., Random Signals and Noise, McGraw-Hill Book Co., Inc., New York, (1958).

20. Bendat, J. S., Principles and Applications of Random Noise Theory, John Wiley & Sons, Inc., New York (1955).

21. Laning, J. H. and Battin, R. H., Random Processes in Automatic Control, McGraw-Hill Book Co., Inc., New York (1956).

22. Price, R., "A Useful Theorem for Nonlinear Devices Having Gaussian Inputs", IRE Transaction on Information Theory, (June, 1958), pp. 69-72.

23. Kac, M. and Siegert, A. J. F., "On the Theory of Noise in Radio Receivers with Square Law Detectors", J. Appl. Phys., vol. 18, (April, 1947), pp. 383-397. For an Improvement of this method, see Siegert, "Passage of Stationary Processes Through Linear and Nonlinear Devices", IRE Trans., vol. PGIT-3, (March, 1954) pp. 4-25.

24. Darling, D. A. and Siegert, A. J. F., "A Systematic Approach to a Class of Problems in the Theory of Noise and Other Random Phenomena - Part I and Part II", IRE Transaction on Information Theory, IT-3 (March, 1957), pp. 32-43.

25. Siegert, A. J. F., "A Systematic Approach to a Class of Problems in the Theory of Noise and Other Random Phenomena - Part III, Examples", IRE Transaction on Information Theory, IT-4 (March, 1958), pp. 4-12.

26. Doyle, W., McFadden, J. A. and Marx, I., "The Distribution of a Certain Nonlinear Functional of an Ornstein-Uhlenbeck Process", J. Soc. Indust. Appl. Math., vol. 10, No. 2, (June 1962) pp. 381-392.

27. Deutsch, R., "Piecewise Quadratic Detector", IRE Convention Record, pt. 4, (1956), pp. 15-20.

28. Parzen, E., Stochastic Processes, Holden-Day, Inc., San Francisco (1960).

29. Brunk, H. D., A Introduction to Mathematical Statistics, Ginn and Company (1960).

30. Cramer, H., Mathematical Methods of Statistics, Princeton University Press, Princeton, N. J., (1946).

31. Wiener, N., The Fourier Integral and Certain of Its Applications, Dover Publications, New York (1933).

32. Erdelyi, A., Higher Transcendental Functions, Bateman Manuscript Project, Vol. 3, McGraw-Hill Book Company, Inc., New York, (1958).

33. Kaplan, W., Advanced Calculus, Addison-Wesley Publishing Company, Inc., Reading, Mass., (1952).

34. Apostol, T. M., Mathematical Analysis, Addison-Wesley Publishing Company, Inc., Reading, Mass., (1957).

35. Miles, J. W., "On Structural Fatigue Under Random Loading", Journal of the Aeronautical Sciences, (Nov. 1954), pp. 753-762.

36. Miner, M. A., "Cumulative Damage in Fatigue", J. Appl. Mech., Vol. 12, (1945), pp. 159-164.

37. Crede, C. E., "Failure Resulting from Vibration", Random Vibration, Vol. 2, The M. I. T. Press, Cambridge (1963), pp. 103-146.

38. Schjelderup, H. C. and Galef, A. E., 'Rationalization of an Aspect of Sonic Fatigue", Aerospace Engineering, (June, 1962), pp. 44-49.

39. Harris, C. M. and Crede, C. E., Shock and Vibration Handbook, McGraw-Hill Book Company, Inc., New York (1961).

40. Bellman, R., Introduction to Matrix Analysis, McGraw-Hill Book Company, Inc., New York (1960).

41. Caughey, T. K. and O'Kelly, M. E. J., "General Theory of Vibration of Damped Linear Dynamic Systems", Dynamics Laboratory, California Institute of Technology, Pasadena, California (1961).

42. O'Kelly, M. E. J., "Normal Modes in Damped Systems", Dynamics Laboratory, California Institute of Technology, Pasadena, California (1961).

43. Caughey, T. K., "Lecture Notes and Private Communications".

44. Caughey, T. K. and Dienes, J. K., "Analysis of a Nonlinear First-Order System with a White Noise Input", Journal of Applied Physics, Vol. 12, No. 11, (Nov. 1961), pp. 2476-2479.

45. Widder, D. V., The Laplace Transform, Princeton University Press, Princeton, N. J., Ch. 6, (1946).

46. Wolaver, L. E., "Second Order Properties of Nonlinear Systems Driven by Random Noise", APL 65-61, Office of Aerospace Research, U. S. Air Force, Wright-Patterson Air Force Base, Ohio.

47. Titchmarsh, E. C., Introduction to the Theory of Fourier Integrals, Oxford University Press, Oxford, (1937).

48. Sneddon, I. N., Elements of Partial Differential Equations, McGraw-Hill Book Company, Inc., New York, (1957).

49. Garabedian, P. R., Partial Differential Equation, John Wiley & Sons, Inc., New York, (1964).

50. Erdelyi, A., Table of Integral Transforms, Bateman Manuscript Project, Vol. I, McGraw-Hill Book Company, New York, (1954).

51. Ryshik, I. M. and Gradstein, I. S., Tables of Series, Products, and Integrals, VEB Deutscher Verlag der Wissenschaften, Berlin, (1963).

52. Application Manual for Philbrick Octal Plug-in Computing Amplifiers, George A. Philbrick Researches, Inc., Boston.

53. Bendat, J. S., "Advanced Concepts of Stochastic Processes and Statistics for Flight Vehicle Vibration Estimation and Measurement", AD No. 297031, (December 1962).

54. Crandall, S. H., "Measurement of Stationary Random Processes", Random Vibration, Vol. 2, The M. I. T. Press, Cambridge, (1963) pp. 35-65.

55. Blackman, R. B. and Tukey, J. W., The Measurement of Power Spectra, Dover Publications, Inc., New York, (1958).

56. Fox, H. L., "Probability Density Analyzer - Summary Report", Report No. 895, Bolt Beranek and Newman, Inc., (January 1962).

57. Broch, J. T., "Effects of Spectrum Non-linearities Upon the Peak Distribution of Random Signals", Technical Review, B & K Instruments, Inc., (1963).

APPENDIX A

ANALOG TECHNIQUES IN RANDOM VIBRATION

It is often the case in the studies of random vibration that analytical methods are not readily available, or they are too burdensome to carry through in practice. For example, the probability density function of the output of a single degree of freedom oscillator, subjected to magnitude-limited random excitation, is not yet known analytically. The output power spectral densities of many nonlinear systems are not usually easy to find, where the calculations are lengthy and difficult even in the most simple case.[12, 44] The information concerning the probability functions and the power spectral densities are, however, often needed in the analysis of random vibration. Analog methods are extremely useful in providing the solutions to many difficult problems of this kind. In particular we shall discuss the electronic differential analyzer, an analog device which consists of a collection of electronic operational amplifiers interconnected in such a way that they are governed by the same set of equations as those describing the system to be analyzed.

The basic building block of an electronic analog computer is the d-c operational amplifier, which is the basis for adding, integrating and differentiating. Transfer functions of a linear system can be simulated faithfully by synthesizing the basic components given above. A high degree of precision could be well maintained if the system to be simulated is simple. For more complicated systems the analog

computer can only be depended upon qualitatively rather than quantitatively. Nevertheless, electronic analog computers are preferred over many other analog devices representing a given physical system. This is because:

1. It is easy to handle. The components are readily synthesized to become an electronic model for the given physical system, the parameters of which can be easily controlled.

2. The operational amplifier has such a high gain that the errors involved in the basic mathematical operations (summing, integrating, etc.) can be minimized.

3. Many system transfer functions, linear or nonlinear, can be simulated through analog circuitry.

4. Total drift--long, or short term--is very small.

5. Accuracy is well maintained over a wide frequency range.

6. The output and input of the operational amplifier are in the forms of analog voltage which can be easily monitored, measured and recorded through a variety of electronic instruments available.

The analog computer used throughout the entire experiment is the K7-A10 operational manifold made by G. A. Philbrick Researches, Inc. The function of the manifold is to provide 10 Philbrick Model USA-3 operational amplifiers, which are chopper-stabilized; high gain (10 million dc gain), wide-band dc amplifiers. Distortion, drift (less than 100 microvolts) and noise are negligible in most applications. These features are particularly important in the studies of

random vibration where stationary solutions are often needed. Since:

1. Averaging of various statistical quantities usually extends over a long period of time. The data are reliable only if the operational amplifier itself is stable, drift and noise free (at their respective minimum) during the entire period of measurement.

2. The frequency spectrum involved in many random vibration experiments are usually wide. This requires that the accuracy of the operational amplifier be well maintained over a broad frequency band.

It is not difficult to see the advantages of using the operational amplifier as a tool of research in random vibration. An example will now be illustrated in setting up the analog model for the single degree of freedom system subject to random excitation.

From the schematic diagram of the single degree of freedom system shown in Fig. (2.1), an equivalent analog model describing the motion of the mass is shown in Fig. (A. 1) with operational amplifier as the basic building block, Fig. (A. 2). The relationships among the voltages are

$$e_2 = -\frac{1}{R_1C_1}\int e_1 dt \qquad \text{(A. 1)}$$

$$e_3 = -\frac{1}{R_2C_2}\int e_2 dt \qquad \text{(A. 2)}$$

$$e_1 = ae_2 - be_3 + e_o \qquad \text{(A. 3)}$$

where R_1C_1 are the values of resistance and capacitance associated

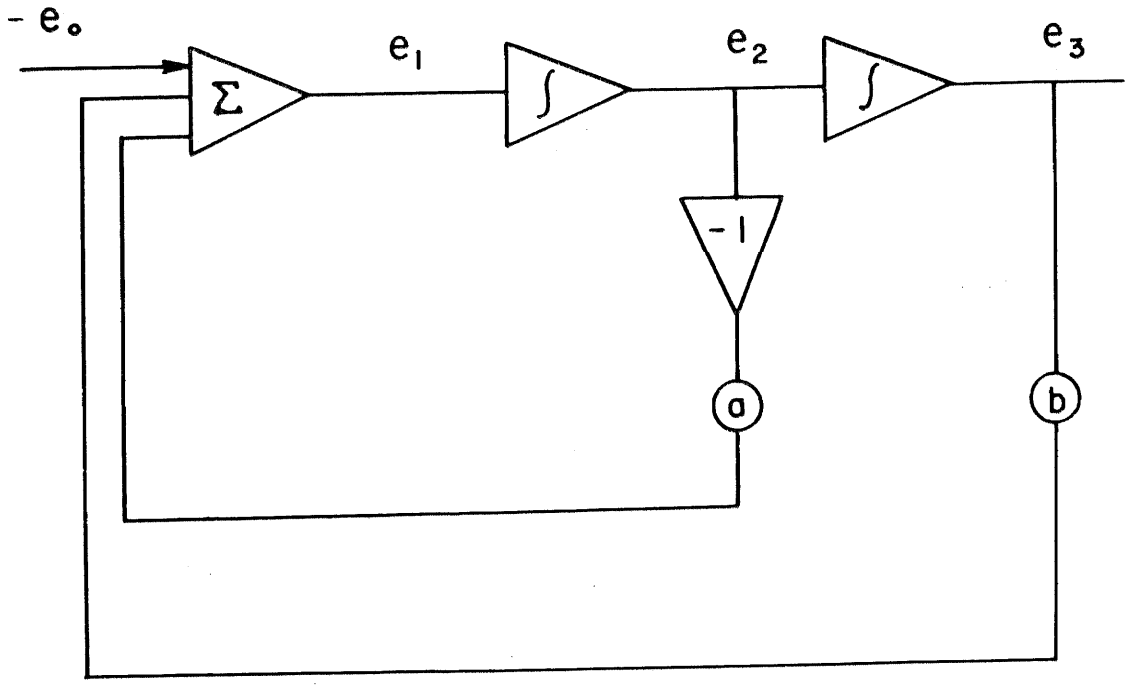

Fig. A. 1. Analog circuit diagram for a single degree of freedom system.

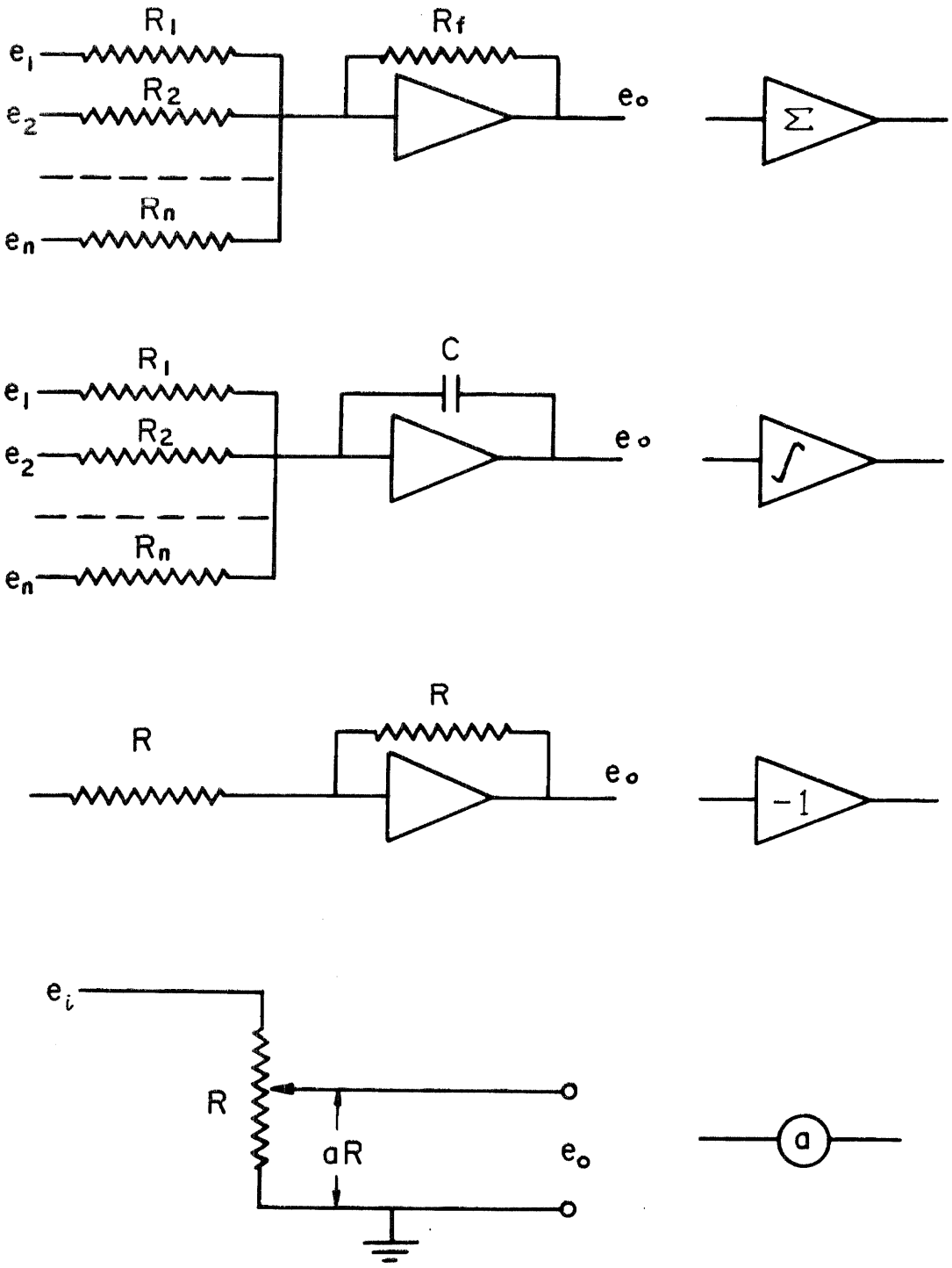

Fig. A. 2. Analog symbols.

with the first integrator, and R_2C_2 are corresponding values for the second integrator. The coefficients a, b are determined by the dial settings on the potentiometers. Combining Eqs. (A. 1) and (A. 2):

$$e_3 = \frac{1}{R_1C_1R_2C_2} \iint e_1 (dt)^2$$

Equation (A. 3) can be rewritten in terms of the voltage e_1:

$$e_1 + \frac{a}{R_1C_1} \int e_1 dt + \frac{b}{R_1C_1R_2C_2} \iint e_1 dt = e_o \qquad \text{(A. 4)}$$

The similarity between Eqs. (2. 1) and (A. 4) is clearly evident. The corresponding quantities of the mechanical system and the electronic analog system is shown in Table A. 1.

The analog voltages, representing displacement, velocity of the mechanical system, can be obtained easily from the measurable quantities e_2 and e_3. Scale factors involving the time constants will have to be taken into account while converting the corresponding quantities from the electronic analog system to the actual mechanical system. For instance, from Eq. (2. 19) the mean square displacement output of the analog system, subject to broadband Gaussian random excitation, is given by

$$\langle x^2 \rangle = \frac{s_o}{8 \zeta \omega_n^2} \qquad \text{(2. 19)}$$

Using Table A. 1 and Eq. (2. 19) the mean square displacement output of the corresponding analog system is given by

TABLE A. 1

Relation Between Corresponding Quantities of the Mechanical System and the Electrical System

Item	Mechanical system	Electrical system
Acceleration	$\ddot{x}(t)$	$e_1(t)$
Velocity	$\dot{x}(t)$	$\int e_1(t)dt$
Displacement	$x(t)$	$\iint e_1(t)(dt)^2$
Forced Acceleration	$N(t)$	$e_o(t)$
Natural frequency	$\sqrt{k/m} = \omega_n$	$\sqrt{b/R_1C_1R_2C_2}$
Damping parameter	$c/m = 2\zeta\omega_n$	$\sqrt{a/R_1C_1}$
Fraction of Critical damping	$c/c_c = \zeta$	$\frac{1}{2}a\sqrt{R_2C_2/bR_2C_2}$

$$\langle e_3^2 \rangle = \frac{1}{R_1C_1R_2C_2} \frac{s_o}{8\zeta\omega_n^3}$$

Typical values of the resistances used in the experiment are those of 500kΩ and 1meg Ω, the values of capacitances are adjusted according to the desired natural frequency and the ratio of critical damping. The potentiometers are provided to achieve a finer control on these quantities. All the resistors and capacitors are precision made within 1% tolerance limit.

APPENDIX B

A POWER SPECTRAL DENSITY ANALYZER

This section is primarily concerned with the theory and the operating principles of a power spectral density analyzer. Various calibration data which are important in the measurement of the power spectral density, are also included. Finally a brief discussion on the errors involved in the measurement is presented.

B-1. Theory

The definition for the power spectral density is commonly written as

$$S(f) = \lim_{T \to \infty} \frac{2 \left| S_T(f) \right|^2}{T} \tag{B. 1}$$

which is also known as the periodgram method and gives a frequency decomposition over the time interval $0<t<T$. The limit is found to exist always, however, the variance of S(f) does not approach zero for a large class of examples, in particular for Gaussian random processes.[19] Therefore it is not experimentally justifiable in using this method to determine the power spectral density.

The most practical method is based on the following formulation. Let the mean square value for a single sample record be

$$< x^2(t) > = \lim_{T \to \infty} \frac{1}{T} \int_0^T x^2(t) dt \tag{B. 2}$$

where T is the length of the record of the sample. Since only the power spectral densities of a stationary ergodic random process are considered, Eq. (B. 2) can be written as

$$E\left[x^2(t)\right] = \sigma_x^2 = \left\langle x^2(t) \right\rangle = \lim_{T \to \infty} \frac{1}{T} \int_0^T x^2(t)\,dt$$

From the Wiener-Khintchine relationship, the autocorrelation function for the random sample function x(t) is given by

$$R_x(\tau) = \int_0^\infty S_x(f) \cos 2\pi f\tau \, df$$

If $\tau = 0$, then $R_x(0) = \sigma_x^2$. Hence

$$\sigma_x^2 = \int_0^\infty S_x(f)\,df \qquad \text{(B. 3)}$$

Assume that the signal is sharply limited between two frequencies f_1 cps and f_2 cps which are nearby. The ideal bandwidth is given by $B = f_2 - f_1$. The mean square output within this narrow band is given by

$$\sigma_B^2(x) = \int_{f_1}^{f_2} S_x(f)\,df \cong S_x(f_o)B \qquad \text{(B. 4)}$$

where f_o is the center frequency within the narrow band B. The power spectral density at the center frequency is then given by

$$S_x(f_o) = \lim_{B \to 0} \frac{\sigma_B^2(x)}{B} = \lim_{B \to 0} \lim_{T \to \infty} \frac{1}{BT} \int_0^T x_B^2(t)\,dt \qquad \text{(B. 5)}$$

Of course, it is impossible for the record to be infinitely long,

and the bandwidth of the filter to be infinitely small in a practical sense. Invariably, there will be error in the power spectral density measurement if the limiting condition appearing in Eq. (B. 5) is not carried out. The statistical uncertainty associated with this error is conveniently written in terms of a dimensionless variance ϵ^2 with the assumption that the slope of the power spectrum is changing slowly within the bandwidth B.

$$\epsilon^2 = \frac{1}{BT} \tag{B. 6}$$

The above expression has been derived and discussed by Blackman and Turkey,[55] Bendat,[53] and Crandall.[54] Additional terms must be added to Eq. (B. 6) if the slope of the power spectrum being measured is changing more rapidly within the narrow frequency band B. It is not difficult to see that the estimation uncertainty can be reduced if the product value BT increases. The meaning of the symbol ϵ is best illustrated by an example. If BT = 10,000, the resulting estimate of $S_x(f)$ at the frequency f_o will have a standard deviation of 1% of the true power spectral density.

In real situations, it is impossible to construct a narrow band filter with very sharp cutoffs at the cutoff frequencies. An equivalent bandwidth must be calculated from the transfer characteristics of the actual filter. From Eq. (1.13) the mean square output after filtering is given by

$$\sigma_x^2 = \int_0^\infty S_x(f) \left| H(j2\pi f) \right|^2 df$$

where $|H(j2\pi f)|$ is the transfer function (the ratio of output over input) of the narrow band filter. Assuming that the $S_x(f)$ is changing slowly within the band, the mean square value could be approximated by

$$\sigma_x^2 \cong S_x(f_o)\int_0^\infty |H(j2\pi f)|^2 df$$

or

$$S_x(f_o) \cong \frac{\sigma_x^2}{\int_0^\infty |H(j2\pi f)|^2 df} \qquad \text{(B. 7)}$$

where f_o is the center frequency within the band. Equations (B. 4) and (B. 7) are similar. It follows immediately that the equivalent bandwidth can be conveniently defined by the following relation

$$B_{eq} = \int_0^\infty |H(j2\pi f)|^2 df \qquad \text{(B. 8)}$$

In general, the procedures involved in obtaining the power spectral densities are the following:

1. Select a narrow band filter having a nominal narrow bandwidth B (between half power points where it is 3 dbs down). Obtain the filter transfer function $|H(j2\pi f)|$, and then calculate the equivalent bandwidth B_{eq} according to Eq. (B. 8).

2. Square the instantaneous values of the filtered signal and then average the squared signal over a time period T.

3. Divide the averaged signal by the equivalent frequency bandwidth B_{eq}. The resulting value will be the power spectral density of the signal at the center frequency f_o of the narrow band filter.

B-2. Instrumentation and Procedure

A schematic diagram for the instrumentation setup is shown in Fig. (B.1). The types of instruments used are cataloged in the following table.

TABLE B.1

Item	Type	Manufacturer	Model Number
1	Wave Analyzer	Radiometer Denmark	FRA2
2	Random Noise Voltmeter	B&K Instruments	2417
3	Sine Wave Generator	Hewlett & Packard	202B
4	Frequency Counter	Beckman Instruments	7350
5	Visicoder	Honeywell	1508

The combination of these five instruments makes up what is known as the power spectral density analyzer. Basically it consists of a narrow band filter, a calibration unit, and a number of recording instruments. The functional relationships among them are explained as the following.

B-2a. Wave Analyzer

The type FRA2 wave analyzer is essentially a sensitive and selective VTVM which can be tuned to any frequency between 5cps and 16kc with the sensitivity from 100 mv to 1,000 volts. This is accomplished through filters with selective nominal bandwidth ranging from 2 cps, 8 cps to 25 cps. The filter transfer functions (the ratio of output over input) $|H(j2\pi f)|$ are plotted in Figs. (B.2), (B.3), (B.4).

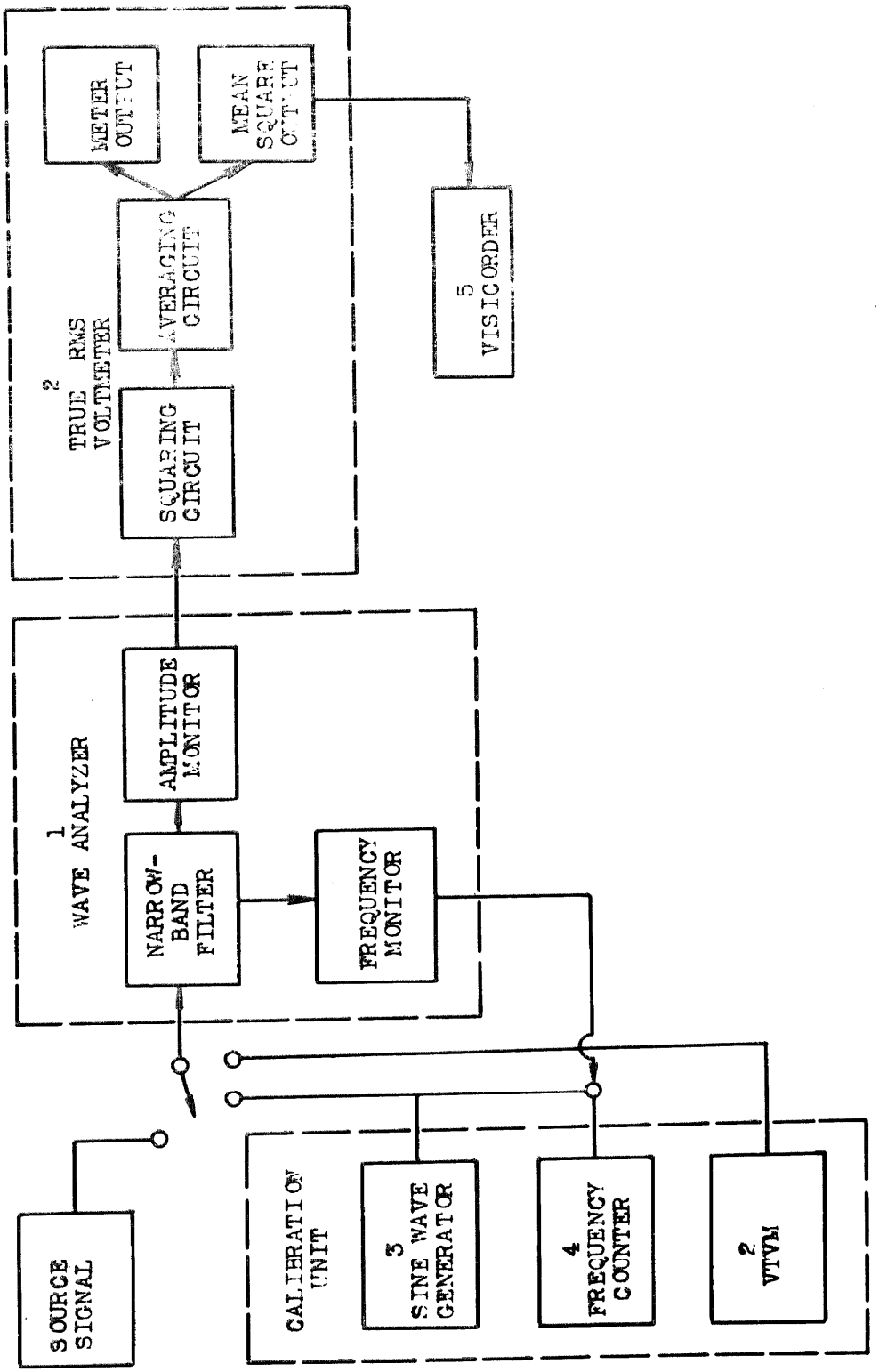

Fig. B. 1. Test set-up for the measurement of the power spectral density.

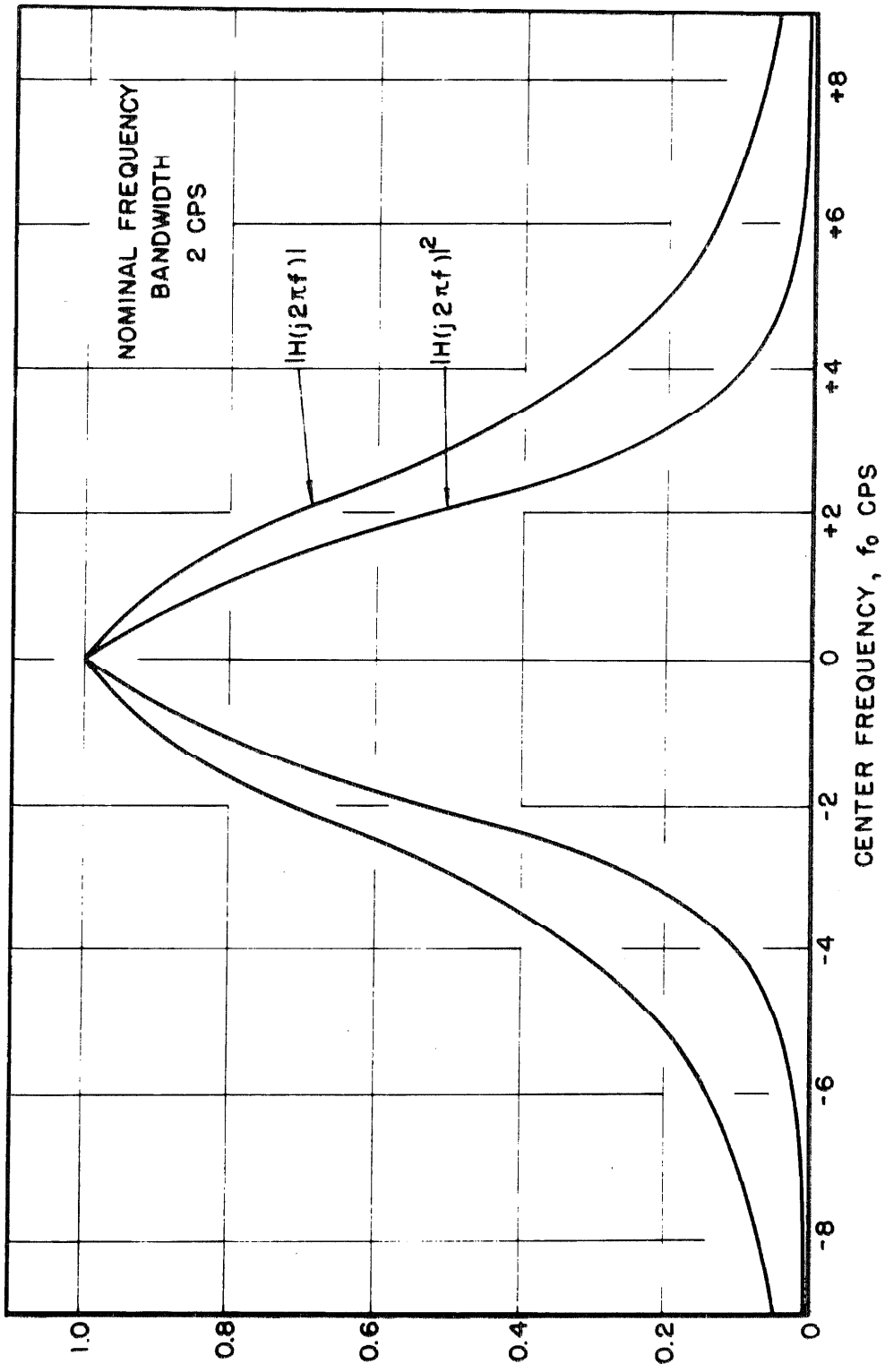

Fig. B.2. Filter transmission characteristics.

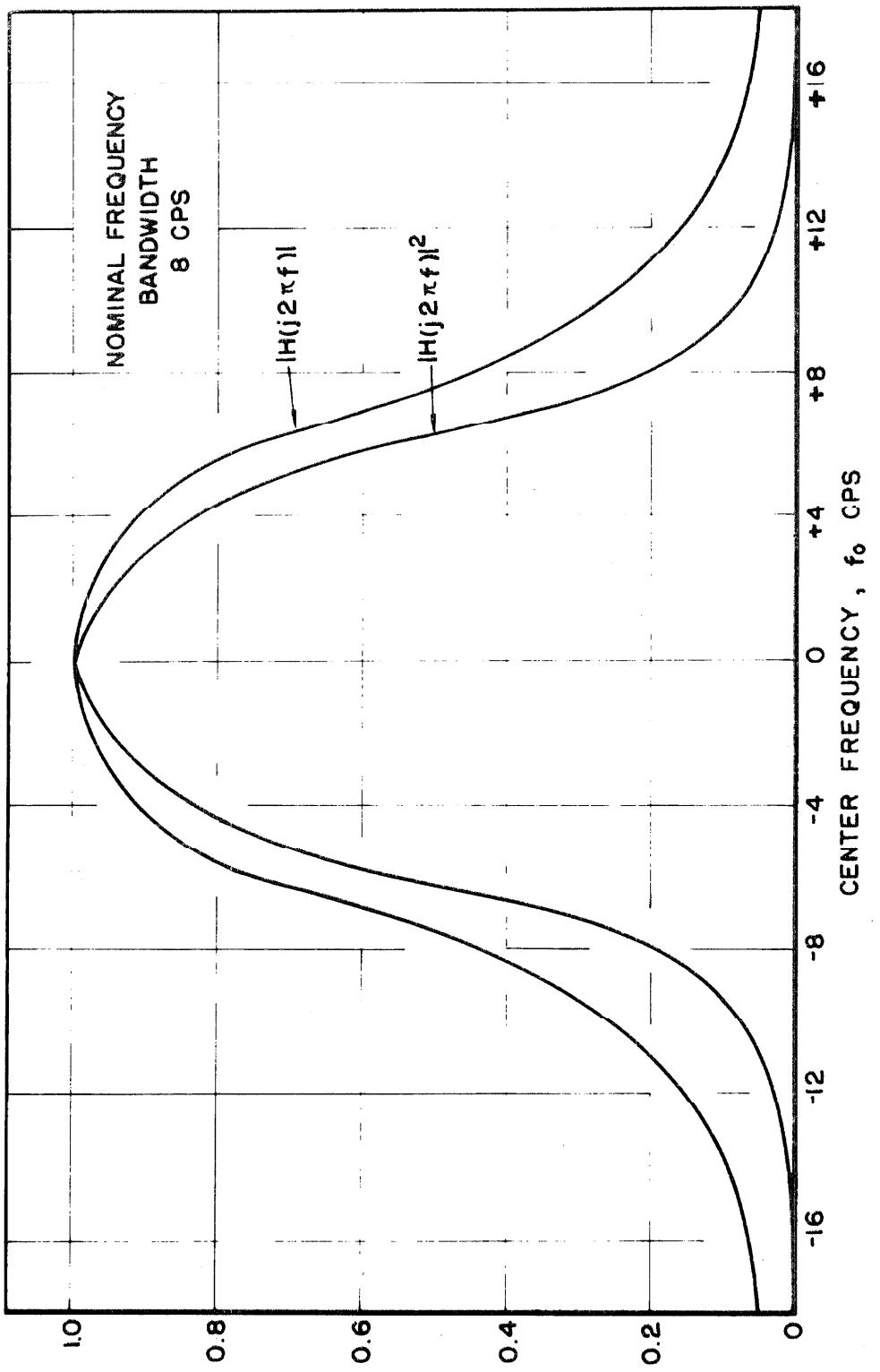

Fig. B.3. Filter transmission characteristics.

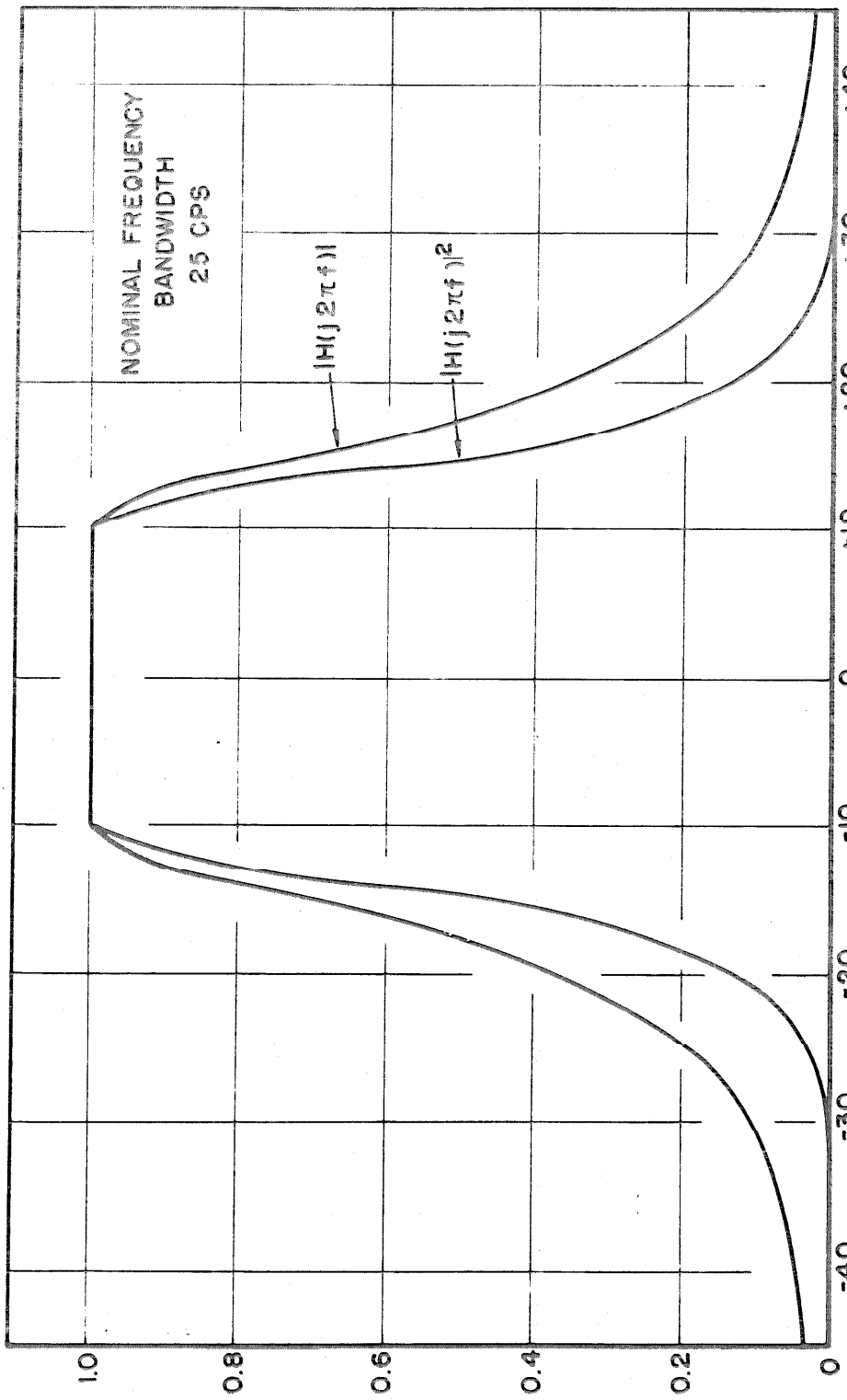

Fig. B. 4. Filter transmission characteristics.

The equivalent filter bandwidths B_{eq} are calculated according to Eq. (B. 8); the actual values B_{eq} for the respective filters are given in Table B. 2.

TABLE B. 2

Nominal Bandwidth	B	2cps	8cps	25cps
Equivalent Bandwidth	B_{eq}	4. 53cps	12. 43cps	31. 64cps

The output of the filters is displayed on a built-in voltmeter which can be monitored through an analog voltage appearing at the output terminal. This analog voltage has a fixed frequency of 1500 cps. Its magnitude is directly proportional to the meter deflection of the voltmeter. The functional relationships between them are shown in Fig. (B. 5) and (B. 6). These curves are proven to be useful since it is usually impossible to get a voltmeter reading of the filter output if the input is random. The procedure is to find an average reading of the output voltage first. The actual output of the filter is then obtained through interpolations from the curves shown in Figs. (B. 5)and (B. 6) with proper placing of the decimal points in accordance with the range switch settings of the wave analyzer.

In addition to the features already mentioned, the center frequency f_o cps of the narrow band filter can be accurately located through another output terminal which has a fixed 3 volts output and a frequency varied according to 60kc-f_o cps. This provides a convenient way to obtain the power spectral density at any desired center frequencies f_o.

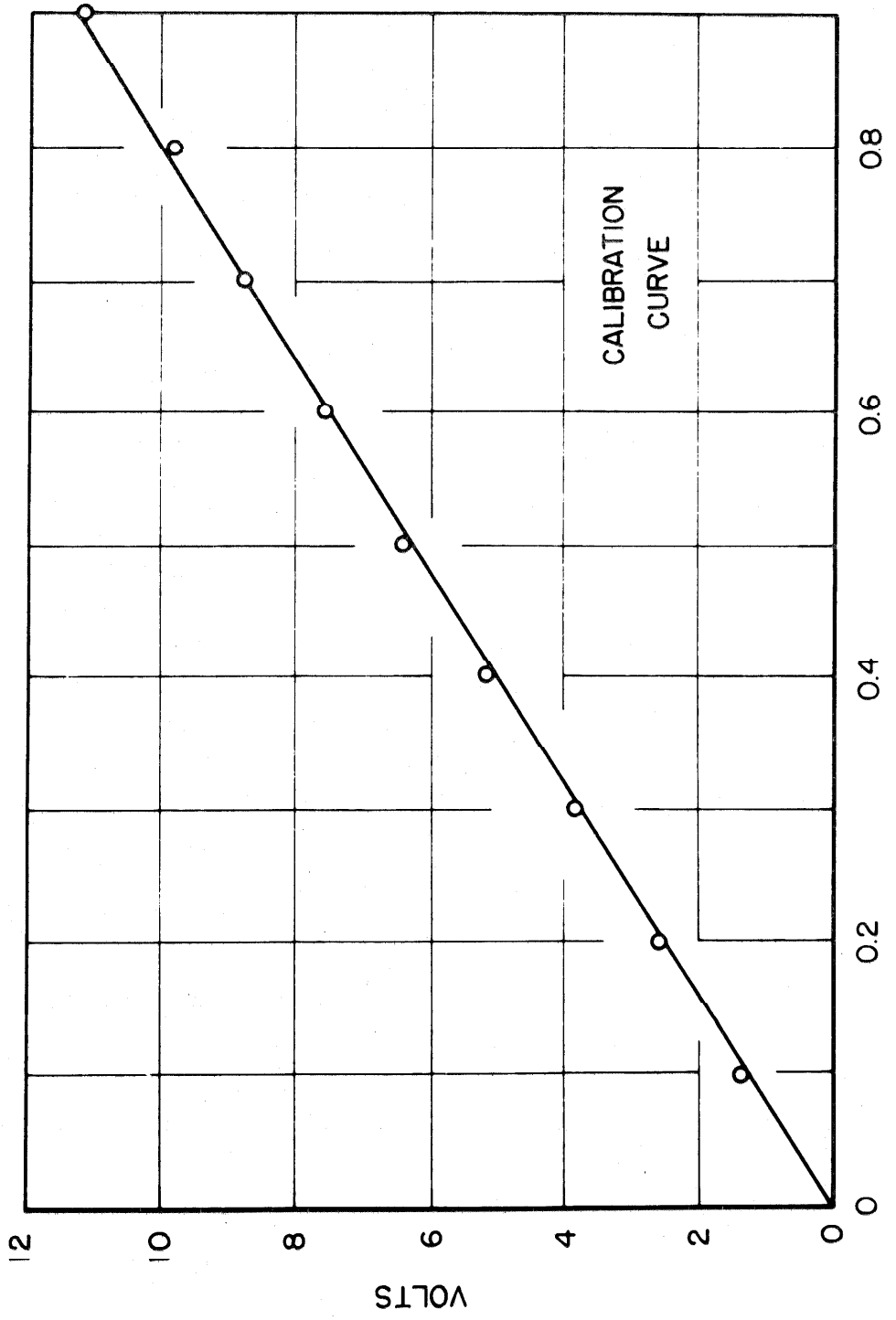

Fig. B. 5. 1500 cps voltage output (ordinate) vs. voltage appeared on the wave analyzer (abscissa).

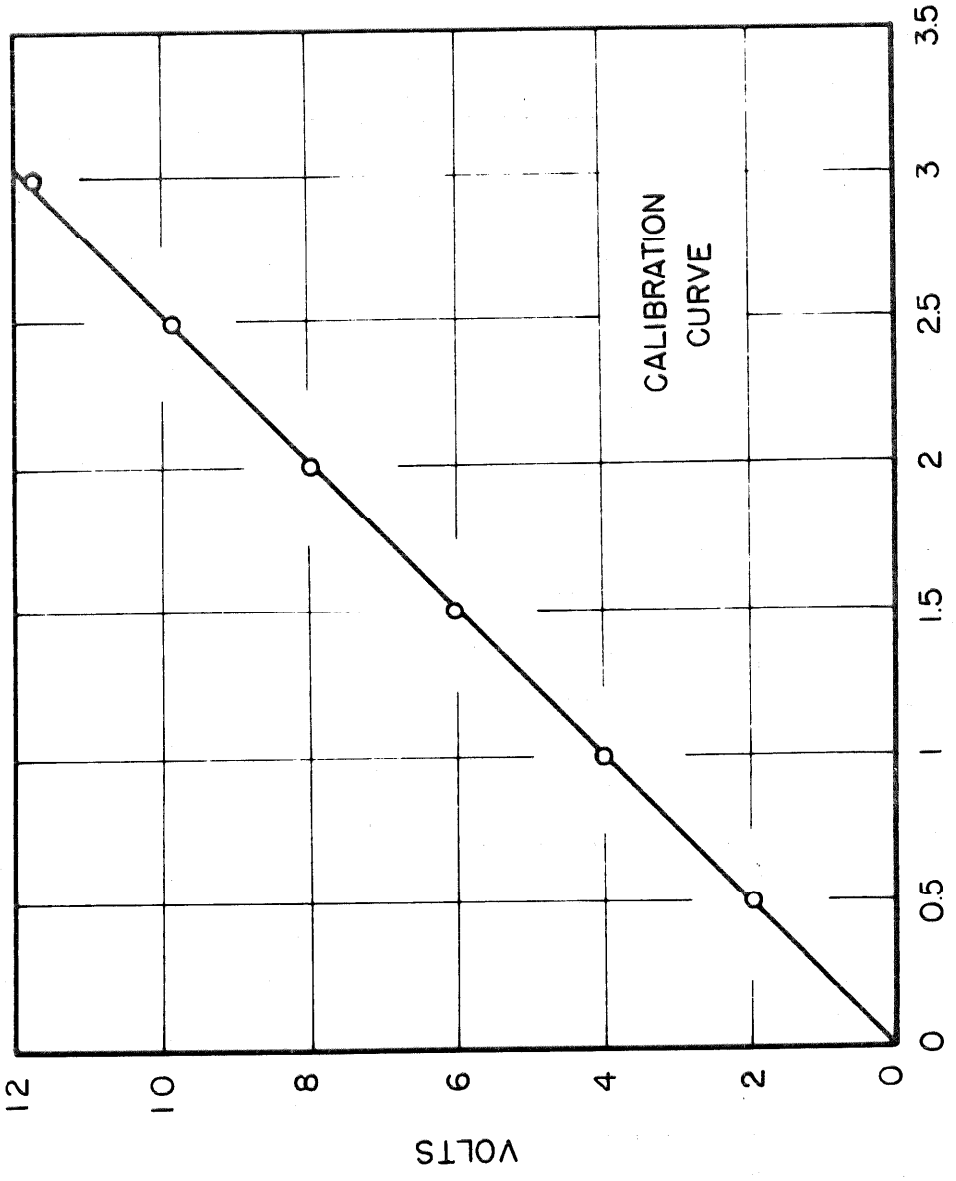

Fig. B.6. 1500 cps voltage output vs. the voltage appeared on the wave analyzer.

B-2b. Calibration Setups

The general calibration procedures are well written in the instruction manual for the wave analyzer. Improved accuracy could, however, be obtained if external calibration procedures are followed. The calibration instruments consist of a sine wave generator, a frequency counter and a VTVM.

As it was pointed out earlier, the filters within the wave analyzer need to be calibrated so that a correct value for the equivalent bandwidth B_{eq} can be determined (a unity gain at the center frequency of the narrow band filter). In addition, the curves shown in Figs. (B. 5) and (B. 6) are determined through calibration. From these curves it is possible to interpret the true output voltage values of the narrow band filter from the voltages appearing at the output terminal. External averaging is often required in the harmonic analysis of a random signal.

B-2c. Recording Instruments

The basic recording item used in measuring the power spectral densities is the B & K type 2417 random noise voltmeter, which is developed mainly to measure the rms value of the narrow band random noise or vibration signals. The built-in time averaging integrator allows a time constant up to 100 seconds. These long integration times are necessary in narrow band vibration work in order to obtain a good estimate of the mean square value of the signal. An additional D. C. output is provided for the voltmeter so that it is possible to record the mean square value on a recorder. This

recorded signal can be further processed so as to reduce the estimated error.

APPENDIX C

A PROBABILITY DISTRIBUTION ANALYZER

C-1. Theory

The basic properties of a probability function have already been discussed (Section 1.2). For a stationary continuous random signal x(t) the probability that x(t) will assume a value between the amplitude level x and x+dx at time t is p(x)dx where p(x) is the probability density function. A probability density function p(x) could also be defined as the derivative of the probability distribution function

$$p(X) = \frac{dP(x \leq X)}{dX}$$
$$P(x \leq X) = \int_{-\infty}^{X} p(x)dx \qquad \text{(C. 1)}$$

The probability distribution function $P(x \leq X)$ is defined as the probability that the random variable x(t) has a value less than a predetermined amplitude level X in the time interval $0 < t < \infty$.

To determine the probability functions experimentally, it is necessary to take measurements along the time axis. This is due to the following equivalent definitions given to the probability functions.

The probability density of a random variable x(t), which has a value falling in the interval $(X, X+\Delta X)$ during a time interval $0 < t < \infty$, may be defined by

$$p(X) = \lim_{\substack{T \to \infty \\ \Delta X \to 0}} \frac{1}{T\Delta X} \sum_{i=1}^{\infty} t_i(X, \Delta X) \qquad \text{(C. 2)}$$

where $t_i(X, \Delta X)$ is the time interval during which the random variable x(t) falls within the amplitude window $(X, X+\Delta X)$, and is dependent on the level X as well as the width of the amplitude window ΔX. In real situations, the rigorous probability density defined by Eq. (C. 2) is clearly not accessible to direct measurement. This is because:

1. It is impossible to have measurements taken over a time interval which is infinite.

2. The amplitude window ΔX should not become too small in practice.

3. The measurements can only be taken over a limited range of amplitudes, and it is impossible to obtain data when the instantaneous amplitude value is very large.

The probability density function is then estimated from

$$p(X) = \frac{1}{T\Delta X} \sum_{i=1}^{n} t_i(X, \Delta X) \qquad \text{(C. 3)}$$

where T and ΔX are finite and n is a large but fixed number. A schematic diagram for the relation given by Eq. (C. 3) is shown in Fig. (C. 1).

In many engineering applications it is often convenient to know the probability of a continuous random variable x(t) which has a value larger than the preset amplitude level X. In this case the probability distribution function may be defined as the following:

$$P(x \geq X) = \lim_{T \to \infty} \frac{1}{T} \sum_{i=1}^{\infty} \tau_i(X)$$

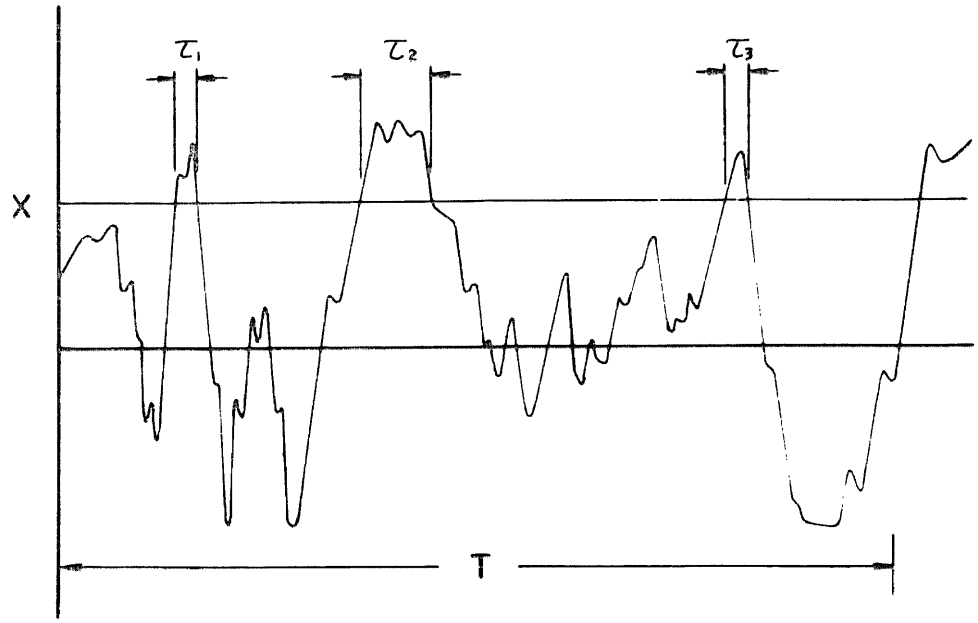

A schematic diagram for probability distribution measurement

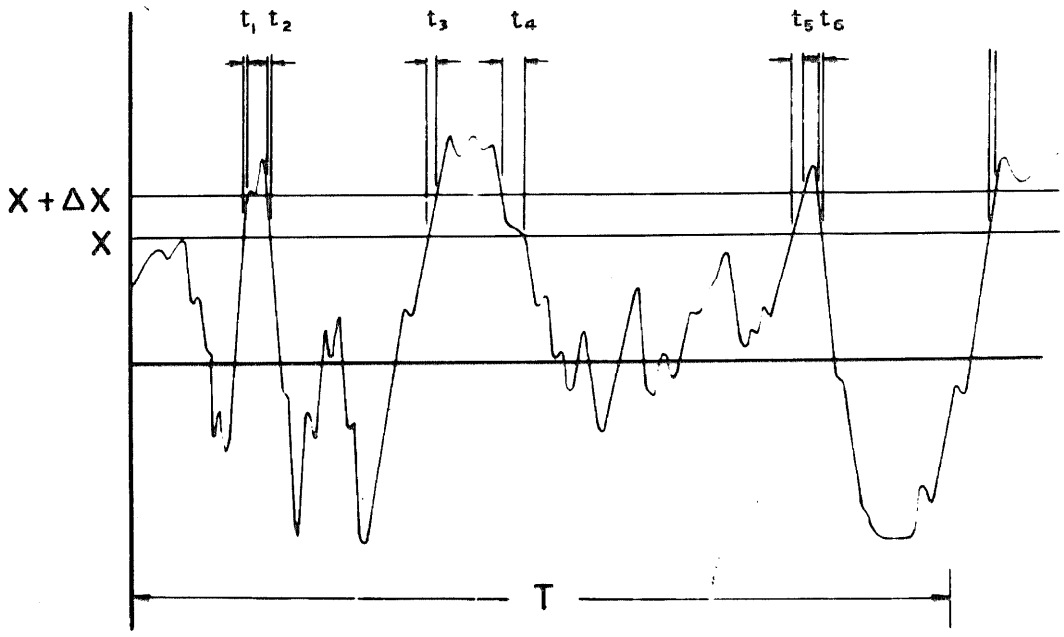

A schematic diagram for probability density measurement

Fig. C. 1

where $\tau_i(X)$ is the time interval within which the random variable $x(t)$ exceeds the level X. In real situations, the measurement time cannot be infinitely long. The probability distribution function in this case may be estimated from

$$P(x \geq X) = \frac{1}{T} \sum_{i=1}^{n} \tau_i(X) \qquad (C.4)$$

where T is a finite time interval and n is a large fixed integer. A schematic illustration for the probability distribution function given by Eq. (C.4) is shown in Fig. (C.1). Note the absence of an amplitude window in the diagram.

The experimental effort is directed toward the analysis of the probability distribution function rather than the probability density function. This is because:

1. Probability density analysis requires the setting up of a narrow amplitude window which is difficult to construct in practice (the commercial probability density analyzer made by B & K Instruments has a narrow amplitude window in the order of 0.1 volts). Probability distribution analysis, on the other hand, does not require such a setup.

2. There are two parameters, namely the total time interval T and the narrow amplitude window ΔX, involved in the statistical error estimate for the probability density function. On the other hand, in measuring the probability distribution function, only one parameter, the time interval T, need be considered in the estimation of error.

3. Probability distribution data can be readily interpreted by

an engineer who does the design work.

The relative ease in obtaining, by experiment, the probability distribution function does not mean to play down the role of the probability density analysis. The probability density function, which is very important in the analytical work of probability, can always be determined from the distribution function by simple differentiation (some pathalogical cases are excluded).

C-2. Instrumentation and Procedures

The probability distribution analyzer used in the experiment is made up of the following components:

1. Amplitude distribution analyzer.
2. Frequency counter and timer.
3. Bistable multivibrator.
4. Operational amplifiers.
5. Rectifier.

A schematic diagram for the probability distribution analyzer is presented in Fig. (C. 2). The types of instruments used are listed in Table (C. 1). Their respective performance characteristics are described in the following paragraphs.

The amplitude distribution analyzer (Quan-Tech Model 317) is used primarily to measure the amplitude distribution of a non-repetitive or random signal. It is essentially a variable amplitude Schmitt trigger which emits pulses when the input voltage signal crosses a preset amplitude level. In other words, there will be a

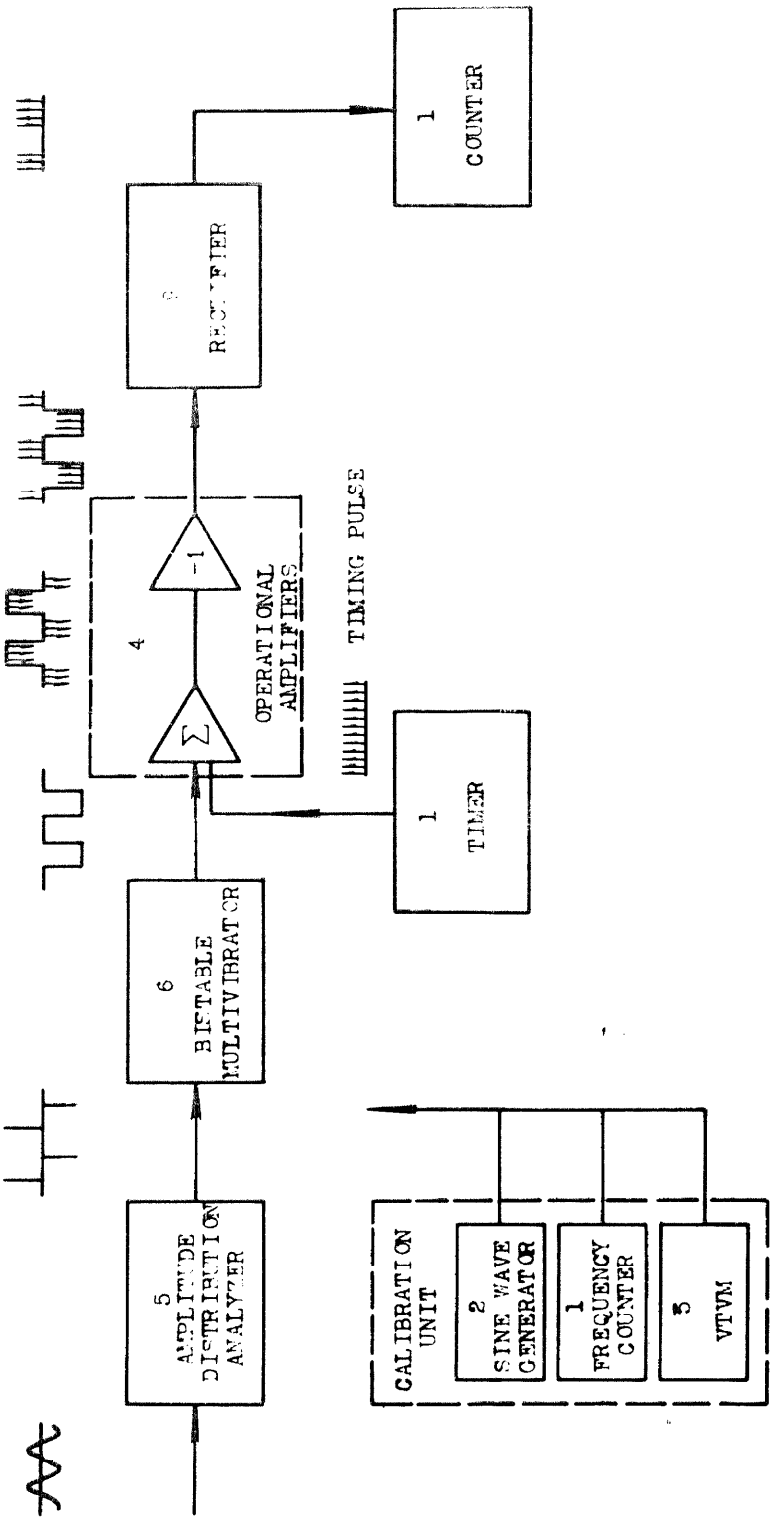

Fig. C. 2. Block diagram for the probability distribution analyzer.

TABLE C. 1

Instruments Used for the Probability Distribution Analyzer

Item	Type	Manufacturer	Model Number
1	Universal EPUT & Timer	Beckman Instruments	7350ACU 7350
2	Sine Wave Generator	Hewlett & Packard	202B
3	True RMS Voltmeter	B&K Instruments	2417
4	Operational Manifold	Philbrick	K7-A10
5	Amplitude Distribution Analyzer	Quan-Tech Laboratory	317
6	*Bistable Multivibrator	CIT Vibration Laboratory	
7	Variable D. C. Power Supply	Hewlett & Packard	721A
8	Battery	Eveready	
9	Rectifier	CIT Vibration Laboratory	
10	Oscilloscope	Tektronix	502
11	Stop Watch	Galco	80-803

* See the circuit diagram in Fig. (C. 3).

positive or negative pulse depending on whether the crossing slope of the incoming signal is positive or negative. A built-in averaging integrator accumulates the time elapsed from positive to negative pulses; the resulting sums are averaged continuously. Thus, the meter reads: the percentage of time the preset amplitude level is exceeded. This is precisely the definition given by Eq. (C. 4). Under laboratory conditions, this instrument is never used alone, since:

1. The resolution of the meter reading is poor.

2. The meter performs well only at the amplitude level where the crossings are frequent.

3. It is usually impossible to obtain a meter reading when the signals being analyzed have narrow frequency band. The meter fluctuates widely in most of these cases.

External circuits are hooked up to overcome these difficulties mentioned above. These include a bistable multi-vibrator, a timer, an EPUT counter, operational amplifiers, and a rectifier. The bistable multivibrator (Fig. C. 3) is designed to operate as a gate which can be opened by a positive pulse and closed by a negative pulse. When a timer is connected to this gate, the time $\tau_i(X)$, (Fig. C. 1), during which the gate is open, can be accumulated on an EPUT counter. The accumulated sum is denoted by $\sum_{i=1}^{n} \tau_i(X)$. If this sum is divided by the total time T elapsed during the time of measurement, the resulting quantity will represent the percentage of time the amplitude level X is exceeded. This constitutes an estimate to the probability distribution function of the given signal at this amplitude level.

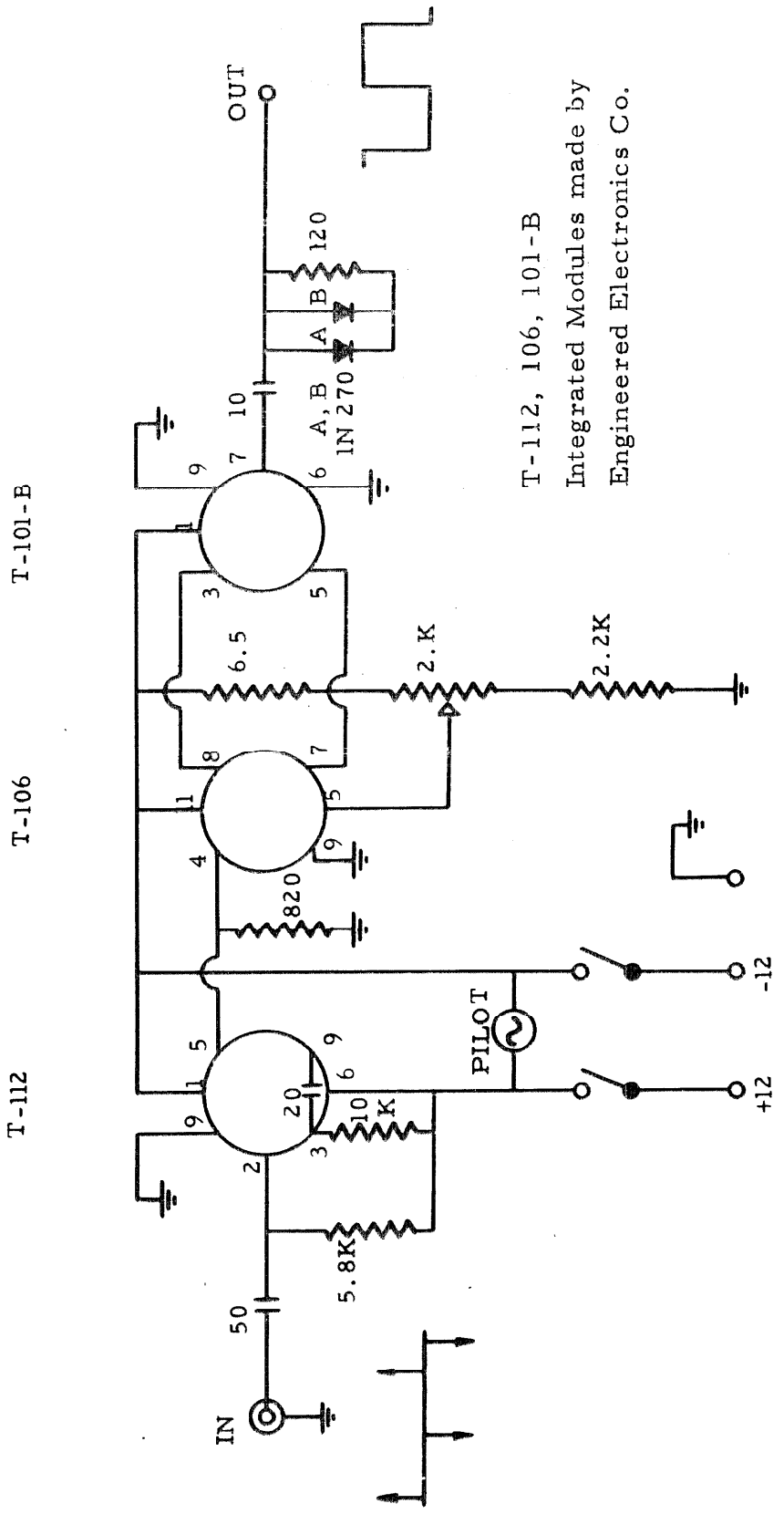

Fig. C.3. A schematic diagram for the bistable multivibrator.

The operating principle of the probability distribution analyzer is presented in Fig. (C. 2). The procedures involved are summarized as the following:

1. Set up the probability distribution analyzer as illustrated in Fig. (C. 2).

2. Connect the vibration signal to be analyzed to the amplitude distribution analyzer.

3. Select discrete amplitude levels X by adjusting the controls on the amplitude distribution analyzer so that sufficient data can be gathered for the probability distribution curves of the given signal.

4. Record the total time $\sum_{i=1}^{n} \tau_i(X)$ during which the gate is open and the total time T during which the measurements are taken. The resulting quantity $\frac{1}{T} \sum_{i=1}^{n} \tau_i(X)$ represents an estimate of the probability distribution function of the signal at the amplitude level X.

APPENDIX D

A PEAK DISTRIBUTION ANALYZER

To measure the probability distribution of peaks, several instruments are employed. The system consists of a variable amplitude rectifier, a simple differentiator, a zero crossing detector, and a frequency counter. A complete schematic diagram for the peak distribution analyzer is presented in Fig. (D. 1). The instruments used are listed in Table (D. 1).

The variable amplitude rectifier is used to eliminate the peaks located outside the amplitude range of interest. This is accomplished by connecting the circuit as that shown in Fig. (D. 1), where two diodes and a variable d. c. power supply are employed. The rectifying level is controlled by the variable d. c. power supply. The polarity of the d. c. power supply must be reversed if the rectifying level is to be extended to include the negative values as well. The circuit configuration shown in Fig. (D. 1) gives very sharp corners at the rectifying level.

Following the variable amplitude rectifier, a simple differentiator is used to convert the peaks to zero crossings, which can be easily detected by a zero crossing detector. However, the signal output of the differentiator is sometimes small, and requires further amplification in order for the signal to be detected.

The amplitude distribution analyzer is used here primarily as a zero crossing detector. A pulse, in the order of 0. 5 volts, will be

emitted whenever the input voltage crosses the d. c. level. By counting the total number of pulses, it is possible to accumulate the total number of peaks on a frequency counter.

TABLE D. 1

Instruments Used for the Peak Distribution Analyzer

Item	Type	Manufacturer	Model Number
1	Variable Amplitude Rectifier	CIT Vibration Laboratory	
2	Differentiator	CIT Vibration Laboratory	
3	Amplifier	Alinco	51-1
4	Amplitude Distribution Analyzer	Quan-Tech Laboratory	317
5	Frequency Counter	Beckman Inst.	7350
6	D. C. Power Supply	Hewlett & Packard	721A
7	Diodes	Hughes	IN 270
8	D. C. Voltmeter	Greibach	500
9	Stop Watch	Galco	80-803
10	Random Noise Voltmeter	B & K Instruments	2417

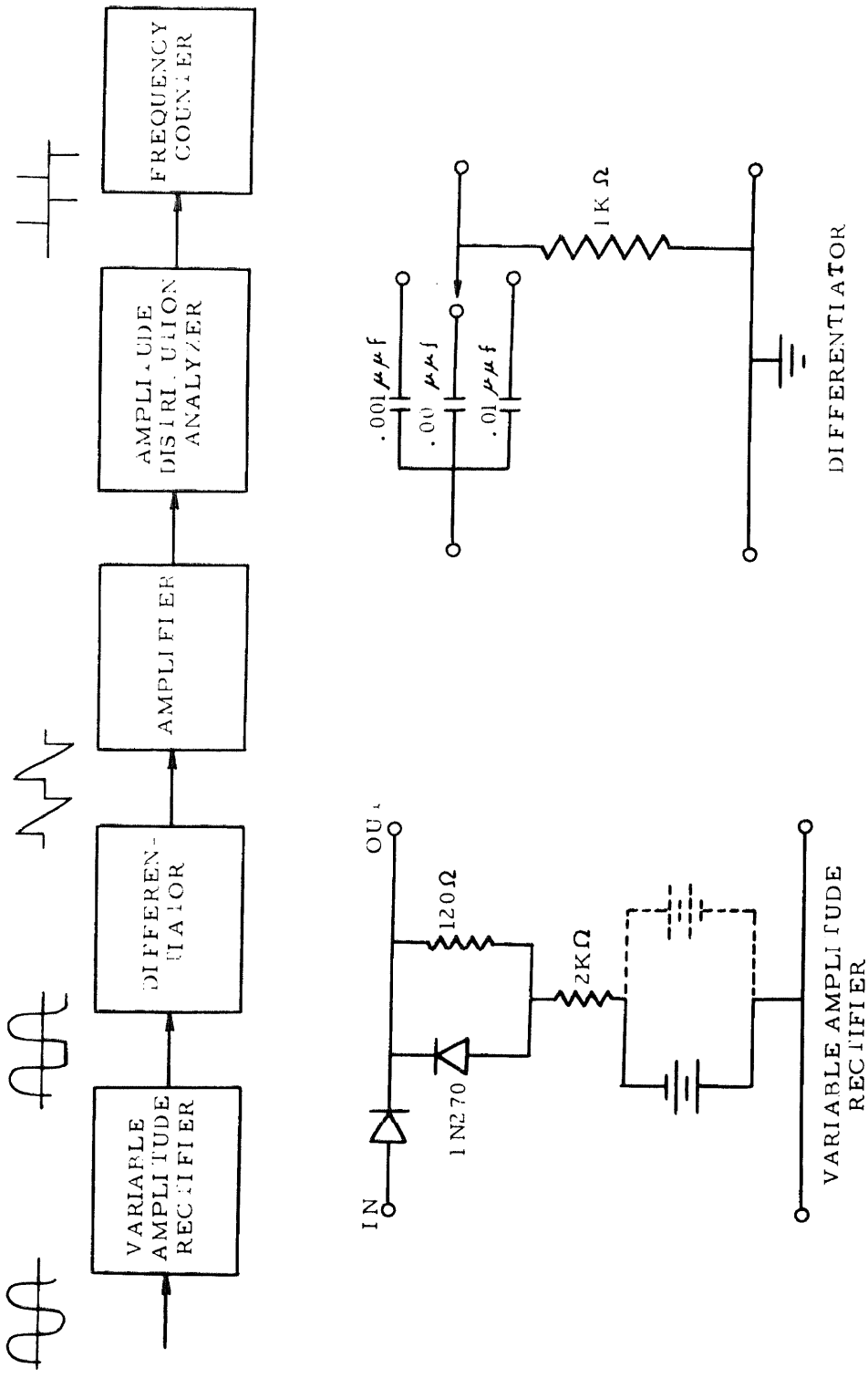

Fig. D. 1. A schematic diagram for the peak distribution analyzer.

APPENDIX E

PRICE'S THEOREM[22]

In the study of the behavior of the autocorrelation function resulting from the passage of Gaussian distributed noise through a zero-memory nonlinear device, Price's theorem appears to be very useful. Let x(t) be a Gaussian distributed random variable, and y(t) be the output random variable of a nonlinear device f(x). The autocorrelation function $R_y(\tau)$ for the random variable y(t) is now desired. Hence

$$R_y(\tau) = E\left[f(x_1)f(x_2)\right] = \int_{-\infty}^{\infty}\int_{-\infty}^{\infty} f(x_1)f(x_2)\, p(x_1, x_2)\, dx_1 dx_2$$

where $x_1 = x(t_1)$ and $x_2 = x(t_2)$.

Assume that each $f(x_j)$ can be represented by the sum of two Laplace transforms[45]

$$f(x_j) = \frac{1}{2\pi i}\int_{C_{j+}} F_{j+}(s)e^{sx_j}ds + \frac{1}{2\pi i}\int_{C_{j-}} F_{j-}(s)e^{sx_j}ds$$

where

$$F_{j+}(s) = \int_0^{\infty} f(x_j)e^{-sx_j}dx_j \qquad j=1, 2$$

$$F_{j-}(s) = \int_{-\infty}^{0} f(x_j)e^{-sx_j}dx_j$$

Thus the autocorrelation function can be written as

$$R_y(\tau) = \left(\frac{1}{2\pi i}\right)^2 \int_{C_{1\pm}}\int_{C_{2\pm}} F_{1\pm}(s_1)F_{2\pm}(s_2)M_{x_1x_2}(s_1, s_2)ds_1 ds_2$$

where

$$M_{x_1x_2}(s_1, s_2) = \exp\left[m_x(s_1+s_2) + \frac{1}{2}\sigma_x^2(s_1^2+2\rho s_1 s_2+s_2^2)\right]$$

where m_x and σ_x^2 denote the mean and the variance of the random variable x(t). Let us now take derivatives of $M_{x_1x_2}(s_1, s_2)$ with respect to the autocorrelation coefficient, we have

$$\frac{d^k M_{x_1x_2}}{d\rho^k} = s_1^k s_2^k \sigma_x^{2k} M_{x_1x_2}(s_1, s_2)$$

therefore

$$\frac{d^k R_y(t)}{d\rho^k} = \left(\frac{\sigma_x^k}{2\pi i}\right)^2 \int_{C_{1\pm}} \int_{C_{2\pm}} s_1^k s_2^k F_{1\pm}(s_1) F_{2\pm}(s_2) M_{x_1x_2}(s_1, s_2) ds_1 ds_2$$

Since

$$f(x_j) = \int_C F_j(s)\, e^{sx_j} ds$$

then

$$\frac{d^k f(x_j)}{dx_j^k} = \int_C s^k F_j(s)\, e^{sx_j} ds$$

Finally we arrive at Price's theorem

$$\frac{d^k R_y(\tau)}{d\rho^k} = \sigma_x^{2k} E\left[\frac{d^k f(x_1)}{dx_1^k}, \frac{d^k f(x_2)}{dx_2^k}\right].$$